



The  
University  
Of  
Sheffield.

# Simulation and Performance Assessment of Post-Combustion Carbon Capture based on Chemical Absorption at Commercial Scale

By:

Saja Albdairat

Supervisor: Prof. Meihong Wang

A thesis submitted in partial fulfilment of the requirements for the degree of  
Doctor of Philosophy

Department of Chemical and Biological Engineering

Faculty of Engineering

The University of Sheffield

November 2022

## Acknowledgment

I would like to express my deepest gratitude to God for offering me the continuous support and patience I needed to finalise my PhD thesis. May his name be praised. I would like to thank my supervisor, Professor Meihong Wang, for his valuable guidance and advice throughout my PhD journey. I could not have undertaken my research without his expertise, which enhances my critical thinking. Also, without his strict feedback, my PhD thesis would not be of superior quality. Moreover, I am so grateful to our postdoctoral fellow, Dr. Toluleke Akinola, for his immense knowledge and support since I started my PhD. He did not hesitate to answer any questions. Many thanks go to other members of the Process and Energy System Engineering Research Group for their support and discussion throughout my journey. Their friendships are really appreciated, which strengthens moral support.

I would like to acknowledge Mutah University for their financial support to complete my PhD research. It is a great honor when it is impossible to complete the thesis without their support. I am so grateful as they provided me with the full scholarship, which is an enormous privilege.

Lastly, I would be remiss in not mentioning my greatest family, especially my parents, my sisters, and my brothers, for their continuous support, their prayers, and their belief, which kept me motivated and confident during my journey. Additionally, I would like to recognise my mother for her calling and emotional support from the first day of my journey until the last minute. She kept me up, especially with the PhD challenges in the COVID period.

## Abstract

The most dominant energy source is fossil fuels, such as coal-fired and combined-cycle gas turbine (CCGT) power plants. However, it has a significant negative impact on the environment due to the massive amount of CO<sub>2</sub> emissions released from these sources. To combat this issue, researchers identified the most mature technology known as carbon capture, utilisation, and storage (CCUS). The solvent-based post-combustion CO<sub>2</sub> capture process (PCC) is the most commonly used among other approaches. This approach is deployed using solvents such as monoethanolamine (MEA), which is the most widely used viable solvent in chemical absorption. However, this solvent has a negative impact on energy consumption. Thereby, the researchers investigated other solvents such as single solvents (e.g., piperazine (PZ) and 2-amino-2-methyl-1-propanol (AMP)). Also, mixed solvents such as a blend of PZ and AMP.

In this study, a steady-state rate-based PCC process model was developed using MEA, PZ, and mixed solvents (PZ with AMP). At the pilot scale, the three models were validated against experimental data using Aspen Plus<sup>®</sup>. The results of the model validation confirmed that the rate-based model for the three solvents predicted the experimental data with a lower than 10% deviation. When scaled up to a 250 MWe combined-cycle gas turbine power plant (CCGT), the packed column size for MEA solvent has the highest diameter and height, followed by PZ solvent and mixed solvents.

Sensitivity analysis and technical evaluation were performed to obtain the optimal CO<sub>2</sub> lean loading, which affects the liquid to gas ratio (L/G ratio) and specific re-boiler duty. Based on the L/G ratio, the values were 1.49 kg/kg, 0.76 kg/kg, and 1.55 kg/kg for MEA, PZ, and mixed solvents (PZ with AMP), respectively. On the other hand, specific re-boiler duties were 4.14 GJ/tonne CO<sub>2</sub>, 3.92 GJ/tonne CO<sub>2</sub>, and 2.95 kg/kg for MEA, PZ, and mixed solvents (PZ with AMP). Furthermore, economic evaluations were assessed for the three models at different solvents. The economic findings show that the lowest total annualised cost per tonne CO<sub>2</sub> was estimated in the case of 40 %wt. PZ, which equals 21£ per tonne CO<sub>2</sub>.

Control structure and design dynamics demonstrate that the performance of PZ was faster in terms of reaching the steady-state when compared to other solvents.

**Keywords:** Post-combustion CO<sub>2</sub> capture, Chemical absorption, MEA, PZ, Mixed solvents (PZ with AMP), Process simulation, Scale-up, Technical evaluation, Economic evaluation, Combined Cycle Gas Turbine (CCGT), Control structure design, Process dynamics.

## List of peer Publications (in preparation) and presentation

From PhD thesis, two publications are in preparation:

- **Albdairat, S.**, Akinola, T.E., Wang, M. (2023). Techno-economical assessment of solvent-based post-combustion CO<sub>2</sub> capture through process modification (multi absorber feed with Inter-heating stripper) for commercial scale CCGT power plants *Applied energy*.
- **Albdairat, S.**, Akinola, T.E., Wang, M. (2023). Comparative analysis of commercial scale solvent-based PCC through dynamic simulation using MEA, PZ, PZ with AMP. *International Greenhouse Gas Control*.

### Conference presentation:

- **Albdairat, S.**, Akinola, T.E., Wang, M. (2022). Techno-economical Assessment of Solvent-based Post-Combustion CO<sub>2</sub> Capture through Process Modification (Multi absorber feed with Inter-heating stripper) for Commercial Scale CCGT Power Plants. 16<sup>th</sup> international conference on the Greenhouse Gas Control Technology GHGT-16, Lyon, France, 23-27<sup>th</sup> October 2022.

# Table of Contents

Acknowledgment .....	iii
Abstract .....	v
List of peer Publications (in preparation) and presentation .....	vii
Table of Contents .....	viii
List of Tables .....	xiii
List of Figures .....	xvii
Nomenclature .....	xxi
Greek Symbol .....	xxii
Abbreviation .....	xxiii
Chapter 1: Introduction .....	24
1.1 Overview .....	24
1.2 Background .....	24
1.2.1 Electricity Generation and climate Change .....	24
1.2.2 Technologies for Carbon Capture .....	26
1.2.3 Introduction to solvent-based PCC based on Chemical Absorption .....	28
1.3 Motivation for the study .....	30
1.4 Aim and objectives .....	31
1.5 Novel contributions of this study .....	32
1.6 Scope of this study .....	33
1.7 Research Methodology .....	34
1.8 Software used in this study .....	34
1.8.1 Aspen Plus® .....	34
1.8.2 Aspen Process Economic Analyser .....	35
1.8.3 Aspen Dynamics® .....	35
1.9 Outline of PhD Thesis .....	35
Chapter 2: Literature Review .....	37
2.1 Overview .....	37
2.2 Pilot plants of solvent-based PCC with PB using solvents .....	37
2.3 Scale-up of solvent-based PCC process using packed bed column .....	38
2.4 Different solvents for solvent-based PCC .....	40
2.4.1 Different solvents for PCC process .....	42

---

2.4.2	Sterically hindered amine .....	44
2.4.3	Ionic Liquid .....	44
2.4.4	Solvents blend .....	44
2.4.5	Water-free solvents .....	45
2.5	Steady-state simulation of solvent-based PCC .....	46
2.6	Control design of solvent-based PCC plant using packed bed with solvents ....	48
2.7	Dynamic simulation and validation of solvent-based PCC using packed bed with solvents .....	50
2.8	Solvent-based PCC using Rotating packed bed for Process Intensification .....	56
2.9	Summary.....	57
Chapter 3: Process Simulation PCC using MEA .....		59
3.1	Overview .....	59
3.2	Steady-state model development of PCC using MEA at pilot scale .....	59
3.2.1	Correlations and reactions used .....	61
3.2.2	Transport phenomena properties .....	64
3.3	Steady-state model validation of PCC using MEA at pilot scale.....	65
3.3.1	Pilot plant data.....	65
3.3.2	Steady-state model validation of PCC using MEA at pilot scale .....	66
3.4	Scale-up of solvent-based PCC using MEA to commercial scale .....	69
3.4.1	Packing type .....	69
3.4.2	Packed column size.....	70
3.5	Simulation of solvent-based PCC model at commercial scale and technical evaluation .....	74
3.5.1	Commercial scale PCC simulation .....	74
3.5.2	Technical evaluation .....	74
3.6	Economic evaluation of commercial solvent-based PCC model using MEA .....	77
3.7	Dynamic modelling of commercial scale solvent-based PCC model using MEA 82	
3.7.1	Dynamic considerations.....	85
3.7.2	Open loop analysis .....	88
3.7.3	Control structure and design.....	96
3.7.4	Process control evaluation.....	97
3.8	Conclusion .....	101

---

Chapter 4: Process Simulation of PCC using PZ.....	103
4.1 Overview .....	103
4.2 Steady-state model development of PCC using PZ at pilot scale.....	103
4.2.1 Thermodynamic properties .....	104
4.2.2 Chemical reactions used in this model.....	104
4.2.3 Model development of PCC using PZ at pilot scale .....	106
4.2.4 Mass transfer heat transfer correlations.....	108
4.2.5 Transport properties.....	108
4.3 Steady-state model validation of PCC using PZ at pilot scale .....	109
4.3.1 Pilot plant data .....	109
4.3.2 Model validation of PCC using PZ at pilot scale.....	112
4.4 Scale-up of solvent-based PCC using PZ to commercial scale .....	113
4.4.1 Flue gas specifications.....	114
4.4.2 Lean solvent flowrate estimation.....	114
4.4.3 Packed column sizing .....	114
4.5 Technical evaluation of commercial solvent-based PCC using PZ.....	116
4.5.1 Technical evaluation of solvent-based PCC process of 30 and 40% wt. PZ 116	
4.5.2 PCC process comparison of 30%wt. MEA versus 30,40%wt.PZ .....	120
4.6 Economic evaluation of commercial PCC model.....	121
4.7 Dynamic performance analysis of PCC using PZ.....	125
4.7.1 Base case operating conditions .....	125
4.7.2 Control structure and design .....	127
4.7.3 Process control evaluation.....	128
4.8 Conclusion.....	132
Chapter 5: Process simulation using a blend of PZ with AMP .....	134
5.1 Overview .....	134
5.2 Steady-state model development of PCC at pilot scale using PZ with AMP solvent.....	134
5.2.1 Thermodynamic properties .....	135
5.2.2 Chemical reactions used in this model.....	135
5.2.3 Model development of PCC using PZ with AMP .....	137
5.3 Steady-state Model validation of PCC at pilot scale using PZ with AMP .....	139
5.3.1 Pilot Plant data.....	139
5.3.2 Model validation of PCC at pilot scale using PZ with AMP .....	139



---

5.4	Scale-up of solvent-based PCC to commercial scale.....	141
5.5	Technical evaluation of commercial scale PCC using PZ with AMP .....	143
5.6	Economic evaluation of commercial scale solvent-based PCC.....	144
5.7	Dynamic performance analysis of PCC using PZ with AMP .....	145
5.8	Base case operating condition for PCC model.....	146
5.8.1	Control structure and design.....	148
5.8.2	Process control evaluation.....	149
5.9	Conclusion .....	153
Chapter 6: Comparative analysis of PCC using MEA, PZ, and (PZ with AMP) .....		155
6.1	Comparative analysis of scale-up .....	155
6.2	Comparative results of technical and economic evaluations .....	156
6.3	Dynamic performance comparison.....	158
6.4	Conclusion .....	160
Chapter 7: Conclusion and recommendation for future research .....		162
7.1	Conclusion .....	162
7.2	Recommendation for future research.....	164
References.....		165

## List of Tables

Table 2.1: A summary of successful pilot plants in CO <sub>2</sub> capture process.....	38
Table 2.2:A Summary of commercial scale for solvent-based PCC process.....	38
Table 2.3:Solvents properties for some single solvents and a blend of solvents(Papadopoulos, 2017).....	42
Table 2.4: summary of some amine solvents used in CO <sub>2</sub> capture process .....	43
Table 2.5: Solvent blends of solvent-based PCC process.....	45
Table 2.6: Summary of some project conducted dynamic modelling of solvent-based PCC using different solvents .....	54
Table 3.1: Components and ions in gas and liquid phase .....	60
Table 3.2: Absorber and stripper packing material characteristics (Canepa et al., 2013) .....	60
Table 3.3: Absorber and stripper specification at pilot scale .....	61
Table 3.4: Coefficients for equilibrium constant and kinetic reactions(Canepa et al., 2013) .....	63
Table 3.5: Correlation models used for transport phenomena properties(AspenTech, 2010) .....	64
Table 3.6: Water and MEA make-up input and output specifications .....	65
Table 3.7: Pilot plant data specifications for case 28 from SRP(Canepa et al., 2013) ...	66
Table 3.8: Model predictions validation against SRP pilot plant data .....	66
Table 3.9: Input parameter and scale-up calculation results .....	73
Table 3.10: Absorber and stripper input specification at commercial scale .....	74
Table 3.11: Flue gas and lean solvents specifications at commercial scale.....	74
Table 3.12: Technical evaluation results of commercial PCC model using MEA .....	75
Table 3.13: Total capital cost breakdown for economic evaluation of PCC model using MEA .....	77
Table 3.14: Base case operating conditions of absorber for commercial PCC model using MEA.....	83
Table 3.15: Base case operating conditions of stripper for commercial PCC model using MEA .....	84
Table 3.16: Sump input value for absorber and stripper.....	88
Table 3.17: Open loop characteristics for CO <sub>2</sub> capture level and re-boiler temperature	91
Table 3.18: Open loop characteristics of CO <sub>2</sub> capture level and re-boiler temperature on changing lean solvent flowrate .....	93
Table 3.19: Open loop characteristic for CO <sub>2</sub> capture level and re-boiler temperature on changing re-boiler duty.....	95
Table 3.20: Tuning parameter for conventional controllers .....	97

Table 4.1: Pre-exponential factor and activation energy parameters used in the kinetic reactions.....	106
Table 4.2: Absorber specifications for model development of PCC at pilot scale(Plaza and Rochelle, 2011; Van Wagener, 2011).....	107
Table 4.3: Stripper specifications for model development of PCC at pilot scale( Plaza and Rochelle, 2011; Van Wagener, 2011).....	107
Table 4.4: Correlations used in model development of PCC process.....	108
Table 4.5: The models used for transport properties for PCC process (AspenTech, 2010) .....	109
Table 4.6: pilot plant data for 14 runs of model validation (Van Wagener, 2011) .....	110
Table 4.7: model predictions for rate-based model against pilot plant data .....	112
Table 4.8: Flue gas specifications and its composition(Canepa et al., 2013) .....	114
Table 4.9: Scale-up calculation for packed columns (absorber and stripper) .....	115
Table 4.10: Scale-up results for packed columns .....	115
Table 4.11: Operating conditions of PCC scaled model .....	116
Table 4.12: Technical evaluation results of PCC model using 40%wt. PZ .....	117
Table 4.13: Technical evaluation results of PCC model using 30%wt. PZ .....	119
Table 4.14: Base case operating conditions of absorber for commercial PCC model using PZ .....	126
Table 4.15: Base case operating conditions of stripper for commercial PCC model using PZ.....	126
Table 4.16: Tuning parameter of controller in PCC model using PZ.....	128
Table 5.1: Kinetics parameters for kinetic-rate reactions.....	137
Table 5.2: Flue gas and lean solvent specifications (Zhang et al., 2017) .....	138
Table 5.3: Absorber and stripper specifications for PCC model development (Zhang et al., 2017).....	138
Table 5.4: Pilot plant data specifications Mangalapally and Hasse, 2011) .....	139
Table 5.5: Model predictions validation of PCC against CESAR 1 pilot plant data .....	140
Table 5.6: Initial inputs for scale-up calculations for absorber and stripper .....	142
Table 5.7: The operating condition for scaled model using 17wt.% PZ and 28 wt.% AMP .....	142
Table 5.8: blend solvent composition ratio .....	143
Table 5.9: Base case operating conditions of absorber for commercial PCC model using PZ with AMP.....	146
Table 5.10: Base case operating conditions of stripper for commercial PCC model using PZ with AMP .....	147
Table 5.11: Tuning parameter for control structure.....	149
Table 6.1: Packed bed column sizes resulting from scale-up calculations .....	156
Table 6.2: Economic evaluation comparison for three solvents.....	157

Table 6.3: Integral square error results for solvent-based PCC using the three solvents .....158

Table 6.4: Settling time of dynamic performance for the three solvents .....159

## List of Figures

Figure 1.1: Electricity generated by different fuels by 2020 (Global, 2020) .....	25
Figure 1.2: CO <sub>2</sub> emissions trend from 1750 to 2020 (Global, 2020).....	26
Figure 1.3: CO <sub>2</sub> capture technologies(Madeddu et al., 2019) .....	27
Figure 1.4: A schematic of the solvent-based PCC process (Wang et al,2011) .....	30
Figure 1.5: A schematic of process methodology of PCC process.....	34
Figure 2.1: Solvent properties influence on process design, operating and capital cost, energy performance and avoided cost of CO <sub>2</sub> (Papadopoulos, 2017) .....	41
Figure 2.2: A schematic of model level complexity for equilibrium -based model and rate-based model (Wang et al., 2011) .....	47
Figure 3.1: A schematic of flowsheet of solvent-based PCC,showing closed loop.....	65
Figure 3.2: Temperature profile for both packed columns: absorber and stripper .....	68
Figure 3.3: Generalized pressure drop correlation (Towler and Sinnott,1969) .....	72
Figure 3.4: Technical evaluation plot showing the correlation between L/G ratio with specific re-boiler duty and CO <sub>2</sub> lean loading .....	76
Figure 3.5: Annualised capital cost correlation with changing CO <sub>2</sub> lean loading .....	80
Figure 3.6: Annualised total cost correlation with changing CO <sub>2</sub> lean loading .....	81
Figure 3.7: Annualised total cost per tonne CO <sub>2</sub> correlation with changing CO <sub>2</sub> lean loading.....	82
Figure 3.8: PCC commercial model flowsheet with valves and external condenser using MEA .....	83
Figure 3.9: Flue gas flowrate step change .....	89
Figure 3.10: (A) CO <sub>2</sub> capture level correlation on changing flue gas flowrate. (B) Re-boiler temperature correlation on changing flue gas flowrate .....	90
Figure 3.11: Lean solvent flowrate step change.....	92
Figure 3.12: (A) CO <sub>2</sub> capture level correlation on changing lean solvent flowrate. (B) Re-boiler temperature correlation on changing lean solvent flowrate .....	93
Figure 3.13: Re-boiler duty step change .....	94
Figure 3.14: CO <sub>2</sub> capture level correlation on changing re-boiler duty .....	94
Figure 3.15: Re-boiler temperature correlation on changing re-boiler duty .....	95
Figure 3.16: Flowsheet of PCC process with control structure.....	96
Figure 3.17: Flue gas step change for PCC process using 30wt.% MEA.....	98
Figure 3.18: CO <sub>2</sub> capture level performance with 10% flue gas step change.....	99
Figure 3.19: Re-boiler temperature performance with 10% flue gas step change.....	99
Figure 3.20: CO <sub>2</sub> capture level step change of -5.5% .....	100

Figure 3.21: Re-boiler duty performance with steppoint reduction in CO <sub>2</sub> capture level - 5.5% .....	100
Figure 4.1: Vapour and liquid phase with interface accounted in model development(A. Lawal et al., 2009) .....	104
Figure 4.2: Absorber temperature profile for PCC model using PZ .....	113
Figure 4.3: Technical evaluation results of PCC model using 40%wt. PZ .....	118
Figure 4.4: Technical evaluation results of commercial PCC model using 30%wt. PZ .....	120
Figure 4.5: The Key parameters of PCC model using MEA, PZ solvents .....	121
Figure 4.6: Annualised capital cost correlation using 30%wt. PZ with changing CO <sub>2</sub> lean loading .....	122
Figure 4.7: Annualised total cost per tonne CO <sub>2</sub> correlation using 30%wt. PZ with changing CO <sub>2</sub> lean loading .....	122
Figure 4.8: Annualised total cost correlation using 30%wt. PZ with changing CO <sub>2</sub> lean loading .....	123
Figure 4.9: Annualised capital cost correlation using 40wt.% PZ with changing CO <sub>2</sub> lean loading .....	124
Figure 4.10: Annualised total cost per tonne CO <sub>2</sub> using 40wt.% PZ with changing CO <sub>2</sub> lean loading .....	124
Figure 4.11: Annualised total cost correlation using 40wt.% PZ with changing CO <sub>2</sub> lean loading .....	125
Figure 4.12: A schematic of PCC using PZ solvent with control structure .....	127
Figure 4.13: Flue gas 10% step change using 40%wt.PZ .....	129
Figure 4.14: CO <sub>2</sub> capture level performance with 10% flue gas step change using 40%wt.PZ .....	130
Figure 4.15: Re-boiler temperature performance with 10% flue gas step change .....	130
Figure 4.16: CO <sub>2</sub> capture level setpoint step change -5.5% using PZ .....	131
Figure 4.17: Re-boiler duty performance with CO <sub>2</sub> capture level step -5.5% change ..	131
Figure 5.1: Absorber temperature profile of rate-based model against CESAR 1 pilot plant data .....	141
Figure 5.2: Stripper temperature profile of rate-based model against CESAR1 pilot plant data .....	141
Figure 5.3: Specific re-boiler duty correlation with changing L/G ratio at different blend ratios .....	144
Figure 5.4: Annualised total cost with changing CO <sub>2</sub> lean loading using 7 wt.% PZ and 38 wt.% AMP .....	145
Figure 5.5: Annualised total cost per tonne CO <sub>2</sub> with changing CO <sub>2</sub> lean loading using 7 wt.% PZ and 38 wt.% AMP .....	145
Figure 5.6: A schematic of PCC model with control structure using PZ with AMP .....	148
Figure 5.7: 10% flue gas step change using PZ with AMP .....	150

---

Figure 5.8: CO <sub>2</sub> capture level performance with flue gas step change using PZ with AMP .....	151
Figure 5.9: Re-boiler temperature performance with flue gas step change using PZ with AMP .....	151
Figure 5.10: CO <sub>2</sub> capture level change -5.5% using PZ with AMP .....	152
Figure 5.11: Re-boiler duty performance with -5.5% CO <sub>2</sub> capture level .....	152
Figure 6.1: Comparative results of technical evaluation for the three solvents.....	157

## Nomenclature

$a$	Actual area of packing ( $\text{m}^2/\text{m}^3$ )
$a_w$	Effective interfacial area per volume ( $\text{m}^2/\text{m}^3$ )
$C_t$	Total concentration ( $\text{kmol}/\text{m}^3$ ) while equal $\rho_L$ /molecular solvent weight
$D$	Diameter (m)
$D_L$	Liquid diffusivity ( $\text{m}^2/\text{s}$ )
$d_p$	Packing size (m)
$d_p$	Particle diameter (m)
$D_V$	Gas diffusivity ( $\text{m}^2/\text{s}$ )
$E$	Activation energy (kJ/kmol)
$F_{LV}$	Flow parameter
$F_p$	Packing factor ( $\text{m}^{-1}$ )
$G_m$	Molar gas flowrate per cross sectional area ( $\text{kmol}/\text{m}^2 \cdot \text{s}$ )
$H_G$	Height of gas phase transfer unit (m)
$H_L$	Height of liquid phase transfer unit (m)
$K_5$	Constant 5.23 for packing size above 15 mm, and 2 if it is below 15mm
$k_G$	Gas mass transfer coefficient ( $\text{kmol}/\text{m}^2 \cdot \text{s}$ )
$k_L$	liquid mass transfer coefficient ( $\text{kmol}/\text{m}^2 \cdot \text{s}$ )
$L_m$	Molar liquid flowrate per cross sectional area ( $\text{kmol}/\text{m}^2 \cdot \text{s}$ )
$n$	Project Interest (%)
$P$	Pressure (bar)
$R$	Gas constant ( $\text{atm} \cdot \text{m}^3/\text{kmol} \cdot \text{K}$ )
$r$	Project Lifetime (year)
$T$	Temperature ( $^{\circ}\text{C}$ )
$V_w$	Gas mass flowrate per cross sectional area ( $\text{kg}/\text{m}^2 \cdot \text{s}$ )
$X_{\text{CO}_2}$	Mole fraction of $\text{CO}_2$ in flue gas
$\check{z}$	Number of equivalents/moles of amine
$dp$	Effective diameter of packing (m)



## Greek Symbol

$\sigma_c$	Critical surface tension for packing (mN/m)
$\rho_G$	Gas density (kg/m <sup>3</sup> )
$\mu_g$	Gas viscosity (Ns/m <sup>2</sup> )
$\nu$	Kinematic viscosity (m <sup>2</sup> /s)
$\alpha_{Lean}$	Lean loading (mol <sub>CO2</sub> /mol <sub>MEA</sub> )
$\rho_l$	Liquid density (kg/m <sup>3</sup> )
$\varphi_{CO2}$	Percentage of CO <sub>2</sub> capture (%)
$\alpha_{Rich}$	Rich loading (mol <sub>CO2</sub> /mol <sub>MEA</sub> )
$\alpha_{ij}$	Specie i reaction order in reaction j
$\sigma_L$	Surface tension for liquid (N/m)
$\omega_{amine}$	Weight of amine (%)

## Abbreviation

AMP	Aminomethyl propanol
ENRTL	Electrolyte Non-Random Two Liquid
ACC	Annualised capital cost
ATC	Annualised total cost
CCGT	Combined cycle gas turbine
CCUS	CO <sub>2</sub> capture, utilisation, and storage
DCC	Direct contact cooler
DEA	Diethanolamine
DETA	Diethylenetriamine
DGA	Diglycolamine
DIPA	Diisopropanolamine
FGD	Flue gas desulphurisation
GHG	Greenhouse gas
GHGT	Greenhouse gas control technology
HETP	Height equivalent to a theoretical plate
MDEA	Methyldiethanolamine
MEA	Monoethanolamine
MIMO	Multiple input-multiple output
OC	Operating cost
PB	Packed bed
PCC	Post-combustion CO <sub>2</sub> capture
PSA	Pressure swing adsorption
PZ	Piperazine
RPB	Rotating Packed bed
SCR	Selective catalytic reduction
SISO	Single input single output
SRP	Separation research program
TCC	Total Capital Cost
TSA	Temperature swing adsorption
VOCC	Validation of Carbon Capture

# Chapter 1: Introduction

## 1.1 Overview

This chapter discusses the research framework, including power generation, climate change, and carbon capture, specifically solvent-based post-combustion carbon capture (PCC) in Section 1.2. In Section 1.3, the motivations for this research are discussed. Section 1.4 describes the purpose and objectives of the research. Novel contributions are detailed in Section 1.5. In addition, Section 1.6 addresses the scope of this study, while Section 1.7 focuses on the research methodology. In Section 1.8, software tools used in this research are covered in detail. Finally, the research outline is defined in Section 1.9.

## 1.2 Background

### 1.2.1 Electricity Generation and climate Change

Electricity plays a vital role as it is used as a high-grade energy source and enables the use of different advanced facilities that enhance the quality of life, increasing the economy. Electricity is considered a part of the driving force behind the world economy. It can be produced from thermal power generation such as coal, oil, natural gas, renewable energy, and others, as shown in Figure 1.1, which presents the regional electricity generation by fuel type in 2020, which keeps becoming dominant in the worldwide market to provide the energy required, especially with population growth.

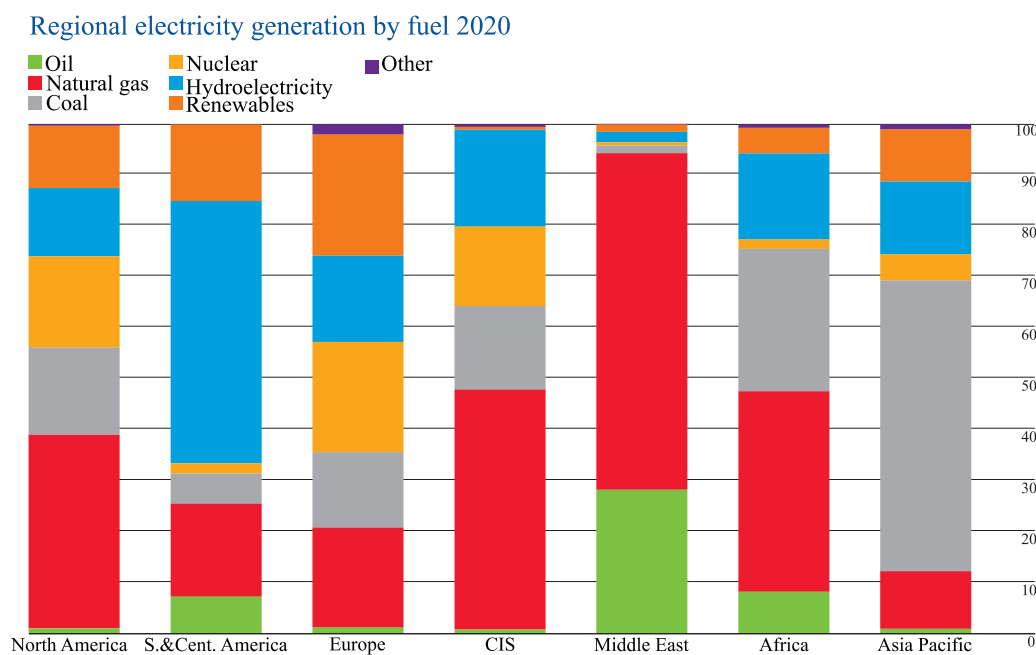


**Figure 1.1: Electricity generated by different fuels by 2020 (Global, 2020)**

By 2035, it is noted that the population would be approximately 8.7 billion; by default, an additional 1.6 billion people would need energy. As a result, the use of fossil fuels for electricity, such as coal, oil, and natural gas, will increase. By 2035, the fossil fuel share is expected to be between 26-28%, with renewable energy possibly accounting for 8%; as a result, fossil fuel is the most dominant in the electricity share (Hasanuzzaman et al., 2017). However, fossil fuels contribute directly to CO<sub>2</sub> emissions in the atmosphere, which are rising gradually with time. Although, in 2020, the trend decreases due to COVID-19, as shown in Figure 1.2, which leads to global warming and, hence, rising sea levels and more acidity in the oceans.

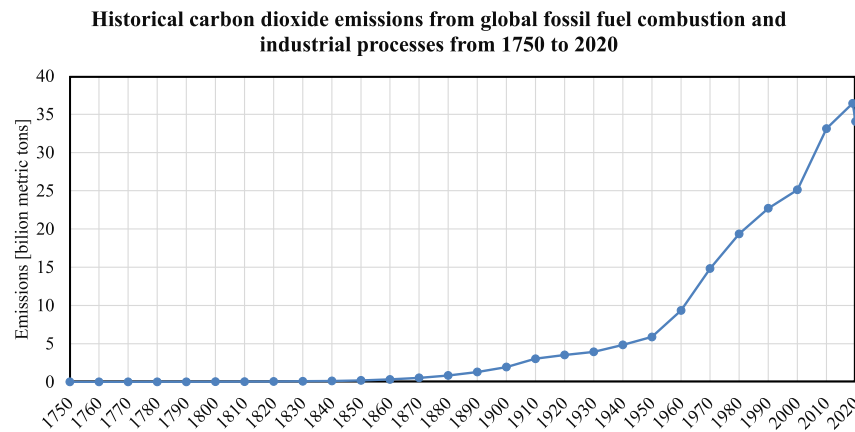


**Figure 1.2: CO<sub>2</sub> emissions trend from 1750 to 2020 (Global, 2020)**

According to this trend, CO<sub>2</sub> emissions are gradually increasing from 1750-2019, indicating the need for practical policy to address this quandary. The EU's decarbonization is aimed at reaching its target by 2050 to reach the target by reducing greenhouse gas (GHG) emissions from fossil fuels from 93-99% (Deiana et al., 2017). Hence, the EU promotes carbon capture, utilization, and storage. This support is associated with practical policy and framework that could innovate the research towards a shift of lower CO<sub>2</sub> than the current situation.

## 1.2.2 Technologies for Carbon Capture

CO<sub>2</sub> separation, utilization, and storage (CCUS) have been identified as a feasible method for reducing CO<sub>2</sub> emissions from the atmosphere. CO<sub>2</sub> separation, refers to the capture of CO<sub>2</sub> from energy-related sources, followed by a utilisation procedure in which it may be used in industries such as enhanced oil recovery (EOR) or transported to a long-term location where it is safely isolated from the atmosphere (Wang et al., 2011).

There are three fundamental CCUS processes as presented in Figure 1.3:

### 1.2.2.1 Pre-combustion CO<sub>2</sub> capture

Pre-combustion is defined as a process to eliminate the majority of CO<sub>2</sub> content from fossil fuels before their combustion. It is expressed as the reaction between fossil fuels and air with steam to generate the product (syngas), which is mostly comprised of CO<sub>2</sub> and H<sub>2</sub>. The fuel is first processed to a mixture of CO<sub>2</sub> and H<sub>2</sub> through a reforming process or to a mixture of CO and H<sub>2</sub> through a coal gasification process, and is then fed to a shift reaction

section (Maroto-Valer, 2010). By the final stage, it will be easier to separate it for energy generation, utilization, or storage of  $\text{CO}_2$ .

### 1.2.2.2 Oxyfuel $\text{CO}_2$ Capture

Oxyfuel is known as a process of burning the fuel with an  $\text{O}_2$  stream, which is classified as an oxidising agent. The fuel is burned in an  $\text{O}_2$  stream with no (or very little) nitrogen. Instead of air. In these plants, the primary stage in separating  $\text{O}_2$  from  $\text{N}_2$  is the separation of pure  $\text{O}_2$  from air, which is subsequently transferred to the energy conversion unit (Maroto-Valer, 2010). However, it is not viable for pulverised hard coal in the foreseeable future.

### 1.2.2.3 Post-combustion $\text{CO}_2$ capture

This process aims to remove the  $\text{CO}_2$  from flue gas released from power plants such as coal-fired power plants and combined cycle gas turbines (CCGT). It is considered the most viable and applicable among the above processes. It has several methods, such as physical absorption, adsorption, cryogenics, membrane, and chemical absorption.

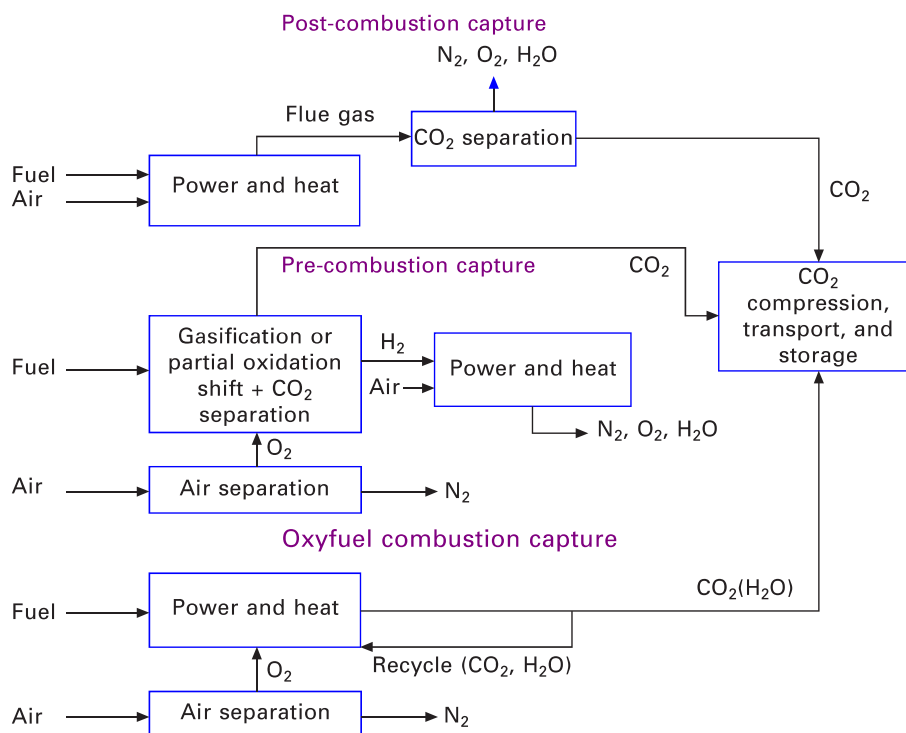


Figure 1.3:  $\text{CO}_2$  capture technologies (Madeddu et al., 2019)

#### ❖ Physical absorption

This separation method relies on Henry's law for CO<sub>2</sub> absorption into solvents such as Selexol (dimethyl ethers of polyethylene glycol) and Rectisol (methanol). CO<sub>2</sub> absorption occurs at high pressure, where the high energy penalty originates. Hence, it is not economical to CO<sub>2</sub> content lower than 15 vol%.

#### ❖ Adsorption

This separation takes place where there is contact between a gas or liquid and solid surface. In the regeneration case, the adsorbent is regenerated, whether at temperature swing adsorption (TSA) or pressure swing adsorption (PSA). The adsorbent could be used in activated carbon and zeolites.

#### ❖ Cryogenics

Cryogenics is a separation procedure using condensation, where CO<sub>2</sub> condenses at -56.6 °C and atmospheric pressure. It is adapted to the high CO<sub>2</sub> content in the flue gas. Consequently, it is applicable more for oxyfuel CO<sub>2</sub> capture.

#### ❖ Membrane

Membrane execution is based on selectivity. It includes thin polymeric films to separate the mixture of permeation rates. This rate is different for each molecule. It is identified based on the relative size of molecules or the diffusion coefficient in the membrane. The drawback of this separation is that the selectivity is low. Hence, the low CO<sub>2</sub> capture level.

#### ❖ Chemical absorption

This separation method includes the reactivity between CO<sub>2</sub> and the specified solvent to produce a weakly bonded intermediate compound, where it is regenerated in the stripping process at elevated temperature to produce the original solvent and pure CO<sub>2</sub>. This method is preferable and more mature than other separation methods for several reasons, such as its high selectivity, which means a higher CO<sub>2</sub> capture level. In addition, it applies to existing power plants.

### **1.2.3 Introduction to solvent-based PCC based on Chemical Absorption.**

Post-combustion CO<sub>2</sub> capture is achieved by removing the CO<sub>2</sub> from the flue gas after combustion. This process utilises different solvents such as monoethanolamine (MEA),

methyldiethanolamine (MDEA), piperazine (PZ), and blends such as a mixture of PZ with 2-amino-2-methyl-1-propanol (AMP). The process description consists of pre-treating flue gas and post-combustion CO<sub>2</sub> capture (PCC) using chemical solvents.

Flue gas should be pre-treated from acid gases such as NO<sub>x</sub> in the case of CCGT and SO<sub>x</sub> in the case of coal-fired power plants before the solvent-based PCC process. Generally, these acid gases enhance the generation of heat-stable salts, particularly with MEA. Hence, the recommended concentration of SO<sub>x</sub> should be lower than 10 ppm by using a flue gas desulfurization (FGD) unit, while NO<sub>x</sub> should be eliminated by using a selective catalytic reduction (SCR) unit. On the contrary, oxygen concentration must be lower than acid gases, which are lower than 1 ppm, because it increases the likelihood of corrosion for the equipment, such as carbon steel. Consequently, inhibitors might be deployed when the oxygen percentage is higher than the recommended concentration. The recommended temperature for the solvent-based PCC process should be between 45 and 50 °C to reduce solvent degradation by evaporation at elevated temperatures in the absorption process. To cool down the flue gas, a Direct contact cooler (DCC) should be utilised before entering the CO<sub>2</sub> capture process. This cooling process is achieved by using water in counter-current contact with flue gas, which will enhance the water balance of the entire process. The CO<sub>2</sub> capture process has two main columns, i.e., the absorber and stripper, which are attached to the heat exchanger as shown in Figure 1.4

The flue gas enters the absorber at a temperature of 45 to 50 °C, where a counter-current flow of lean amine solution is present. Lean amine solutions can react chemically with CO<sub>2</sub> in the flue gas to produce an intermediate, weakly bonded compound. This reaction is defined as exothermic, where the lean amine solution is heated up. From the top of the absorber, the treated gas is washed before being vented into the atmosphere. The lean amine solution becomes rich in CO<sub>2</sub> at the bottom of the absorber. It has a higher temperature than lean amine solution, which is up to 60 °C. From the bottom of the absorber, the rich amine solution is pumped to the heat exchanger, where there is heat transfer between the rich amine solution and the lean amine solution coming back from the stripper. After that, the rich amine solution heats up to 100 °C before entering the stripper at a higher pressure than the atmospheric pressure in the absorber, which is between 1.5 and 2 atm. The regeneration process occurs in the stripper to generate CO<sub>2</sub> of specified purity, which leaves the top of the stripper, while lean amine solution leaves



the bottom of the stripper with low CO<sub>2</sub> content to pass through the heat exchanger before being recycled back

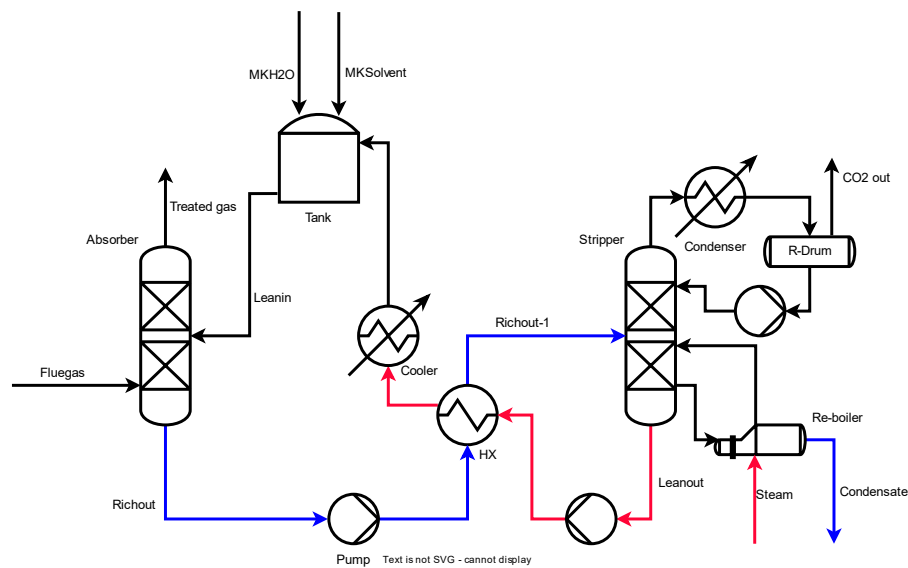


Figure 1.4: A schematic of the solvent-based PCC process (Wang et al,2011)

### 1.3 Motivation for the study

Concerns about the effects of global warming and GHG emissions have prompted the global search for a more environmentally friendly energy source. Renewable energy is classified as the "cleaner" energy among other energy resources and might become a substitute for fossil fuel energy. However, it is intermittent energy. With the high rate of continuous increase and development of human life, it cannot be sufficient. Hence, fossil fuel energy remains predominant and an essential contributor to the energy mix. In 2015, the United Nations climate change conference agreement in Paris promised to reduce GHG emissions to keep temperature rises below 2 °C (Hasanuzzaman et al., 2017). Using Fossil fuel-fired power plants such as coal-fired and CCGT is classified as the main source for CO<sub>2</sub> release to the atmosphere. To combat this dilemma, an efficient process is suitable to reduce GHG emissions. This process has already been proven to be matured among other process which is known as CCUS.

Although coal-fired and CCGT power plants emit CO<sub>2</sub> into the atmosphere, to combat this dilemma, an efficient process is needed to reduce GHG emissions. This process has already been proven to be mature among other processes, which are known as CCUS.

The PCC process is the most suitable among other methods because CCGT power plants have lower partial pressures of CO<sub>2</sub> than IGCC processes. The following highlights are provided for the study's motivations:

- High energy consumption, which is connected to the stripping process, is needed to supply the target CO<sub>2</sub> capture level. This energy is related to the amount of steam needed in the re-boiler.
- High CO<sub>2</sub> capture costs: It is connected to MEA solvent, which is defined by high operating and capital costs for the entire solvent-based PCC process.
- The requirement to implement flexible solvent-based PCC operation to meet power demand during transient conditions, such as start-up and shut-down, and to track CO<sub>2</sub> capture level in the presence of disturbances. Furthermore, control design and structure are needed for analysing the dynamic characteristics of solvent-based PCC using different solvents.

## 1.4 Aim and objectives

The aim of this research is to assess the steady-state and dynamic performance of post-combustion CO<sub>2</sub> capture using different solvents such as MEA, PZ, and a blend of PZ and AMP through process simulation and control.

The research objectives:

- To carry out a literature review on process simulation and the control design of the PCC process.
- To perform a steady-state simulation in Aspen Plus® for the PCC process using MEA, followed by validation against experimental data at pilot scale.
- To carry out steady-state simulation in Aspen Plus® for the PCC process using PZ, followed by validation against experimental data at pilot scale.
- To develop steady-state simulation in Aspen Plus® for PCC process using a blend of PZ and AMP, followed by validation against experimental data at pilot scale.
- To implement scale-up of the PCC process to a 250 MWe CCGT power plant for three different solvents (e.g., MEA, PZ, and a blend of PZ and AMP).

- To perform a technical evaluation of solvent-based PCC at commercial scale (a 250 MWe CCGT power plant) for three different solvents (e.g., MEA, PZ, and a blend of PZ and AMP).
- To assess the economic performance of commercial-scale solvent-based PCC for three different solvents (e.g., MEA, PZ, and a blend of PZ and AMP),
- To perform the control design for the PCC process using three different solvents (e.g., MEA, PZ, and a blend of PZ and AMP).
- To simulate the PCC process in Aspen Dynamics<sup>®</sup> using three different solvents (e.g., MEA, PZ, and a blend of PZ and AMP) for dynamic performance assessment

## 1.5 Novel contributions of this study

The majority of previous studies focused on alkanolamine, particularly MEA, as a mature organic solvent in a solvent-based PCC process due to its fast reaction kinetics, high mass transfer, and low cost. It is classified as a primary amine (Kittel et al., 2009; Mangalapally et al., 2012; Huertas et al., 2015; Li et al., 2016; Feron et al., 2020; Karunarathne et al., 2020). However, using MEA as a benchmark for solvent-based PCC process has a high energy penalty, especially for solvent regeneration, due to its high desorption enthalpy.

The researchers have paid attention to a continuous investigation of other solvents such as piperazine, which is known as cyclic diamine. It has been developed and utilised as an activator and sole absorbent (Luyben et al., 1997; Fredriksen et al., 2013; Artanto et al., 2014; Li et al., 2016; Krótki et al., 2017; Stec et al., 2017; H. Liu et al., 2019; Oh et al., 2020; Romeo et al., 2020). Both specifications work better than MEA because they have a higher rate of absorption and a lower rate of degradation. Nevertheless, it has a drawback, which has low solubility in water. Hence, high PZ content is required for proving high CO<sub>2</sub> capture level.

The solvent blend is conducted in the PCC process in order to identify which solvents are most promising for reducing the energy penalty. The sole solvents have limitations on reducing the energy penalty, including solvent regeneration and degradation, especially in the stripper. (Idem et al., 2006; Adeosun et al., 2013; van der Spek et al., 2016; Zhang et al., 2018; J. Liu et al., 2019; Perumal et al., 2021). A variety of solvents blend has been proposed in PCC process for example Methyl-diethanolamine (MDEA) was the first solvent

blended with other amines such as MEA, diethanolamine (DEA), and PZ. These amines were defined as a promoter for MDEA. In addition, PZ was combined with AMP as blended solvents. All the aforementioned studies highlighted PCC process at steady-state. This study gives highlight on the commercial scale of PCC by investigating the techno-economical evaluation, control structure and design, and dynamic performance, where dynamic simulation will be investigated for single amine such as MEA, PZ, and solvents blend (PZ with AMP) to investigate how fast the PCC respond in case of disturbance rejection and setpoint tracking.

## 1.6 Scope of this study

This study is focused on the steady- state and dynamic performance of solvent-based post combustion CO<sub>2</sub> capture process using solvents such as MEA, PZ, and a blend of PZ and AMP through process simulation.

This study is limited to a solvent-based PCC process using MEA, PZ, and a blend of PZ and AMP.

- The effects of physical and chemical properties for the specified solvents, such as viscosity and the possibility of solid precipitation production, are not studied.
- This study is conducted at the steady-state and dynamic simulation of solvent-based PCC at pilot scale and commercial scale.
- The investigation analysis in chapters 3, 4, and 5 includes: model development and validation at pilot scale and commercial scale, techno-economical evaluation, control structure and design, and dynamic simulation of solvent-based PCC using the specified solvents in Aspen Plus<sup>®</sup>, Aspen Dynamics<sup>®</sup>.
- The study is limited to packed bed columns, where scale-up calculations estimate only the packed bed column diameter while height estimation was considered from Aspen Plus<sup>®</sup> based on the flow rate in the entire process.
- This study deals with a single input, single output control structure.

## 1.7 Research Methodology

In this section, the research methodology is depicted as follows, providing all the steps implemented to achieve the aim of this study, starting by collecting literature reviews on solvent-based PCC process using different solvents, to be followed by a performance evaluation of the process.

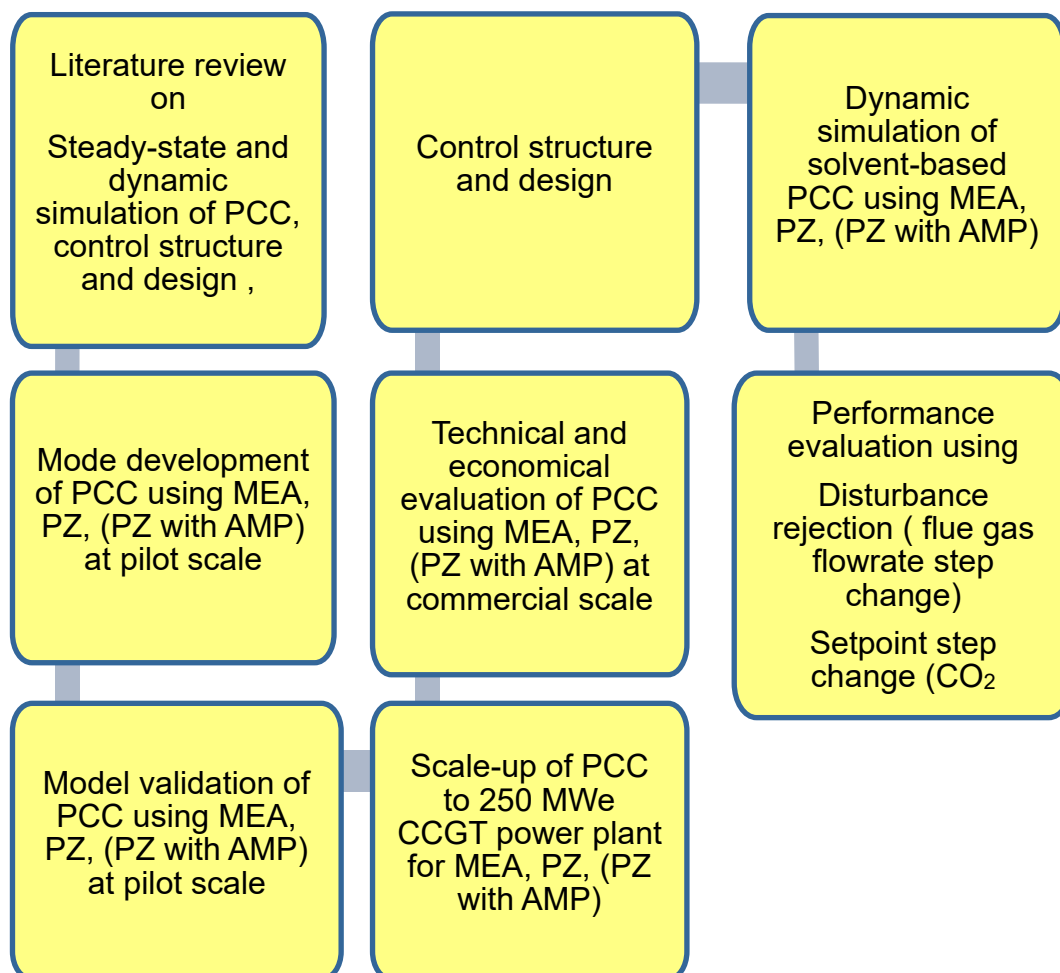


Figure 1.5: A schematic of process methodology of PCC process

## 1.8 Software used in this study

### 1.8.1 Aspen Plus®

Aspen is generally the abbreviation for "Advanced System for Process Engineering." This software is based on flowsheet simulation, where it is used to express the process statistically. This is very beneficial because of different advantages such as modelling,

simulation, design specification, data regression, optimisation, and sensitivity analysis. Aspen Plus® v.11 offers mass and energy balance. The thermodynamic relationship between reacting and non-reacting medium was utilised. This software was used to develop the process simulation of a solvent-based PCC process using different solvents (i.e., MEA, PZ, and PZ+AMP) at pilot scale. In addition, the validated model will be scaled up to 250 MWe CCGT power plants, followed by technical evaluation.

### 1.8.2 Aspen Process Economic Analyser

This software is used to perform economic evaluations for solvent-based PCC process. By selecting the basis cost, feed stream basis price, and product stream basis price, this software provides the cost of each equipment for the entire process. Furthermore, the utility prices should be added to the entire process where each utility is connected to each piece of equipment. In this research, an economic evaluation was performed for a solvent-based PCC process using different solvents after scaling-up the validated model to 250 MWe CCGT power plants. By following this procedure, it will be easy to select the optimal value for lean loading, L/G ratio, and specific re-boiler duty after a technical evaluation approach.

### 1.8.3 Aspen Dynamics®

This tool is deployed to implement the dynamic analysis of chemical process by applying different controllers that connect the dependent variables with independent variables. The dependent variable's structure is selected based on the effect of the latter on the former. It is known how the dependent variables will respond within time to modify the controller output, disturbance, or both. With Aspen Dynamics®, it is easy to keep track of blocks and controller characteristics over time. In this research, Aspen Dynamics® was used to understand the dynamic simulation of a solvent-based PCC process using three different solvents (i.e., MEA, PZ, and PZ+AMP). Hence, it helps to figure out the appropriate controllers used in the entire process.

## 1.9 Outline of PhD Thesis

The outlines of this research are as follows:

**Chapter 2: Literature Review.** In this chapter, an overview of post-combustion carbon capture has been discussed using different solvents, whether it is experimental or

simulated. Moreover, scaling up post-combustion carbon capture (PCC) is presented. Control structure and design followed by dynamic simulation. By the end of this chapter, the thesis will highlight the gaps in previous studies on research theory.

**Chapter 3 Process Simulation PCC using MEA.** This chapter illustrates in detail the simulation and validation of a solvent-based PCC process using the MEA benchmark as a solvent. This chapter includes four sections: Firstly, simulation and validation of solvent-based PCC at pilot scale using Aspen Plus®. Second, the validated model is scaled up to 250 MWe CCGT power plants, followed by technical evaluation to achieve the specified CO<sub>2</sub> capture level. Thirdly, economic evaluation will be discussed to obtain the base case needed for dynamic simulation. Finally, the solvent-based PCC's control structure and design are completed to prepare the model for dynamic performance analysis using Aspen Dynamics®.

**Chapter 4 Process Simulation of PCC using PZ.** The simulation and validation of a solvent-based PCC process using PZ at pilot scale using Aspen Plus® is detailed in this chapter. The validated model was converted from pilot scale to commercial scale to meet the needs of 250 MWe CCGT power plants using the same procedure as in Chapter 3. followed by a technical and economic evaluation that will be ready for control structure and design. After that, dynamic simulation was deployed based on setpoint change and disturbance rejection.

**Chapter 5 Process simulation using a blend of PZ with AMP.** This chapter represents the simulation and validation of solvent-based PCC using a blend of PZ and AMP. Model development and validation are implemented using Aspen Plus® at pilot scale. The validated model is scaled-up to 250 MWe of CCGT power plants. Furthermore, technical evaluation and economic evaluation are estimated to obtain the optimised target for dynamic simulation analysis through setpoint change and disturbance rejection.

**Chapter 6 Comparative analysis of PCC using MEA, PZ, and (PZ with AMP).** This chapter describes the comparative analysis of solvent-based PCC process using MEA, PZ, and PZ with AMP for scale-up results, technical evaluation, control structure and design, and dynamic simulation.

**Chapter 7: Conclusion and recommendation for future work.** This chapter recaps the PhD thesis briefly with recommendations for future research.

## Chapter 2: Literature Review

### 2.1 Overview

This chapter presents the previous studies on the solvent-based PCC process, including the pilot plant deployment, commercial scale implementation, steady-state simulation and validation of the solvent-based PCC process, different solvents used for solvent-based PCC, control structure and design, dynamic simulation and validation of solvent-based PCC, and solvent-based PCC using a rotating packed bed. Section 2.2 presents the pilot plant deployments of solvent-based PCC. In Section 2.3 the scale-up of solvent-based PCC with a summary of commercial-scale deployments is discussed. The different solvents used in solvent-based PCC are highlighted in Section 2.4. In Section 2.5, a steady-state simulation of solvent-based PCC is presented. Control structure and design are demonstrated in detail in Section 2.6, dynamic simulation and validation of solvent-based PCC is presented in Section 2.7 using packed bed (PB). Finally, Section 2.8 highlights the previous studies on solvent-based PCC using rotating packed bed column

### 2.2 Pilot plants of solvent-based PCC with PB using solvents

Solvent-based PCC facilities at pilot plant deployment were reviewed by Wang et al., (2011). The motivation of pilot plant deployment was to bridge the gap between experimental and commercial plants. Each pilot plant had specific activities including utilising several solvents, solvent resistance to elevated temperature, efficiency improvement including reducing energy penalty, and process modification. Some of these activities were reviewed by (Idem et al., 2006; Hari Prasad Mangalapally et al., 2011; Mangalapally et al., 2012; von Harbou et al., 2013; Artanto et al., 2014; Stec et al., 2015). Some of the successful pilot plants are shown in Table 2.1.



**Table 2.1: A summary of successful pilot plants in CO<sub>2</sub> capture process**

Project	Location	Operational date	Reference
Zama field validation test	Canada	2005	Smith et al. (2011)
Bell Creek	USA	2010	Jin et al. (2017)
CNPC Jilin Field EOR	China	2008	Hill et al. (2020)
CO <sub>2</sub> CRC Otway	Australia	2008	Ingram (2007)
Michigan Basin Geologic CO <sub>2</sub> sequestration field test	USA	2008	Gupta et al. (2014)

### 2.3 Scale-up of solvent-based PCC process using packed bed column

In terms of a pilot plant, there are limitations in accommodating the flue gas coming from a coal-fired power plant or a combined cycle gas turbine (CCGT) power plant. Hence, a variety of commercial plants have been established. This means that understanding the performance of solvent-based PCC at a targeted flowrate will improve the knowledge behind dynamic performance. For example, Abu Dhabi Phase 2 connected to the natural gas process will be established in 2025. Table 2.2 represents the most relevant commercial solvent-based PCC.

**Table 2.2: A Summary of commercial scale for solvent-based PCC process**

Plant name	Status	Date	Country	Process industry
Century plant	Operational	2010	USA	Natural gas
Uthmaniyah CO <sub>2</sub> -EOR	Operational	2015	Saudi Arabia	Natural gas
Terrell Natural Gas plant	Operational	1972	USA	Natural gas
Steamboat Rock Biorefinery Carbon Capture and storage	Non- operational	2024	USA	Ethanol Production
Sinopec Qilu Petrochemical CCS	Non- operational	2021	China	Chemical Production

A few previous studies investigated the scale-up of solvent-based PCC process. Lawal *et al.* (2012) performed a scale-up calculation to determine the lean solvent flowrate as well as the sizes of the unit operations (absorber and stripper column) in the solvent-based PCC process required to process flue gas from a 500 MWe subcritical coal-fired power plant based on insights gained from pilot plant studies and chemical engineering principles. The process was designed to capture 90% of CO<sub>2</sub> from 600 kg/s flue gas extracted from the power plant. MEA (30% wt.) was used as the solvent. It was reported that the required solvent flow rate was 2900 kg/s. Moreover, columns size includes a diameter of 9 m for absorber, and 9 m for the stripper. The height was 27 m for two absorbers and one stripper. On the other hand, Nittaya *et al.* (2014) deployed a scale-up to 750 MWe supercritical coal-fired power plant in gPROMS using the same procedure as with Lawal *et al.* (2012). The capture rate was designed to approach 87% or higher. However, different results were obtained because further correlations were utilised such as generalised pressure drop correlation (GPDC) depending on packing factor and correlations to calculate the height required for absorber and stripper which was conducted by assumption in Lawal *et al.* (2012). The calculated results of absorber were to design three absorbers with a diameter of 11.8 m and height of 34 m, while two strippers were estimated, each with a diameter of 10.4 m and height of 16 m.

Agbonghae *et al.* (2014) performed a scale-up of a validated model to capture 90% of CO<sub>2</sub> from flue gas from a 400 MWe CCGT power plant using Aspen Plus<sup>®</sup>. The findings were to design two absorbers with a diameter of 11.93 m and a height of 19.06 m, whereas a stripper was developed with a diameter of 11.93 m and height of 28.15 m. The scale-up procedure was extended to be utilised with different solvents such as PZ as a solvent. Otitoju *et al.* (2021) conducted a scale-up of the validated model to a 250 MWe CCGT power plant in Aspen Plus<sup>®</sup>. The capture rate was supposed to be 90%. The procedure is similar to Agbonghae *et al.* (2014). However, the diameter for both columns was determined based on the flooding velocity. The scale-up results for the absorber were a diameter of 12.5 m and a height of 20 m, while the stripper had a diameter of 8 m and a height of 20 m.

The extension of scale-up was performed using other solvents such as PZ, as mentioned by Otitoju *et al.* (2021). It was conducted to capture 90% CO<sub>2</sub> from flue gas extracted from a 250 MWe CCGT power Plant, where solvent flow rate estimation was calculated using

a similar approach in Agbonghae *et al.* (2014) whereas the column size, including diameter and height, was calculated and provided by Otitoju *et al.* (2019). The calculation results were one absorber column with a diameter of 12.5 m and one stripper with a lower diameter, which was 8 m, with a similar height of absorber. Moreover, the scale-up was also performed using a mixed solvent, such as PZ and AMP, as explained in van der Spek *et al.* (2016). In this study, the scale-up calculation was constrained by height. The absorber height was 20 m, which is higher compared to the stripper height, which was 10 m to accommodate the flue gas flow rate. The CO<sub>2</sub> capture rate was 90%.

## 2.4 Different solvents for solvent-based PCC

In the case of solvent characterization, there are several criteria for selecting the appropriate solvents in a solvent-based PCC process some of these criteria are as follows (Wang *et al.*, 2011):

- The ability to react fast with CO<sub>2</sub>, which reduces the absorber size and solvent flow rate circulation.
- Low regeneration cost, based on the low heat generated when reacting with CO<sub>2</sub>
- Low solvent cost which will affect the entire process cost.
- Environmentally friendly.
- High absorption capacity, which has a profound effect on solvent circulation rate.
- Low solvent degradation and low corrosivity.

Solvent properties play an important role in process design and operation at many levels, resulting in improved energy performance and reduced CO<sub>2</sub> emissions, as illustrated in Figure 2.1.

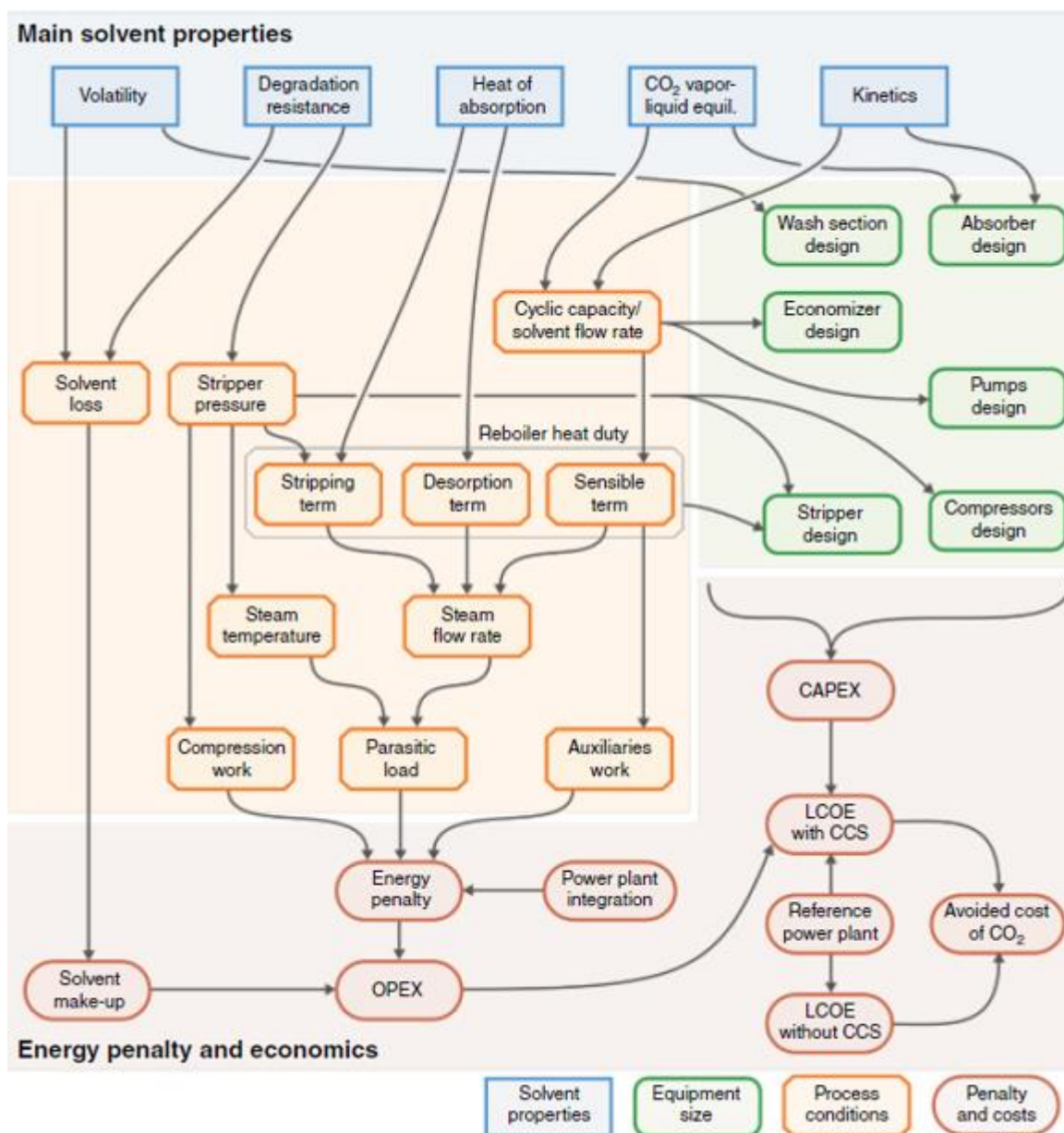


Figure 2.1: Solvent properties influence on process design, operating and capital cost, energy performance and avoided cost of CO<sub>2</sub> (Papadopoulos, 2017)

It was evident during European projects (i.e., CASTOR, CESAR) where different solvents have been investigated through different process modifications (Knudsen et al., 2011) as depicted in Figure 2.1. The reaction kinetics, CO<sub>2</sub> solubility, and heat of absorption rate are the most important solvent properties. These properties have a profound impact directly on energy and operating and capital costs (i.e., re-boiler heat duty, lean solvent flowrate, and equipment size). On the other hand, solvent volatility and resistance to degradation are limitations that put constraints on process operation. For example, the

maximum stripper pressure contributes to the lower temperature, (Freeman et al., 2012), and the constraint on equipment to adjust the solvent losses. Table 2.3 depicts a few solvent properties published in the literature, such as physicochemical properties, with a sign indicating a positive (+), negative (-), or median (=) impact on the overall process.

**Table 2.3: Solvents properties for some single solvents and a blend of solvents (Papadopoulos, 2017)**

Solvent property	MEA 30wt.%	PZ 30wt.%	AMP 30wt.%	AMP+PZ 15+15wt.%
Thermal degradation at 140°C (%per week)	5.3(-)	0.07(+)	0(+)	0(+), 0.25(+)
Cyclic capacity (mol <sub>CO<sub>2</sub></sub> /mol <sub>amine</sub> )	0.25(=)	-	0.5(+)	0.4(+)
Kinetic constant log(k <sub>app</sub> )(s <sup>-1</sup> )	4.6(+)	-	3.3(=)	5.1(+)
Heat of absorption(kJ/mol) at 40 °C	80-85(- )	84-87	50- 90(=)	60-90(=)

Thermal degradation resistance measures the solvent loss in the entire process, which affects the operating cost and environmental emissions. Furthermore, when using thermally resistant amine, this property is advantageous for the CO<sub>2</sub> compression step. On the other hand, cyclic capacity, which is the difference between rich and lean loadings, determines the required solvent flow rate, affecting indirectly the re-boiler duty, pumping work, and operating cost. The reaction kinetics have a profound effect on the absorber packed column height that is needed to provide the target CO<sub>2</sub> capture level, hence affecting investment costs. The heat of absorption has a direct impact on re-boiler duty needed to regenerate the solvent. Furthermore, sensible heat (to raise the solvent heat) and stripping heat, which is required for solvent steam generation.

#### 2.4.1 Different solvents for PCC process

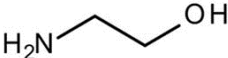
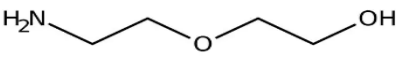
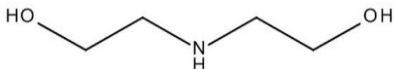
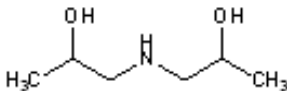
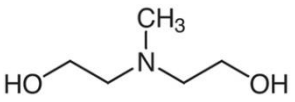
Amine solvents have been widely used for 75 years in industrial gas treatment, particularly alkanolamine. It can be classified into three types based on the nitrogen degree of substitution: primary, secondary, and tertiary, as shown in Table 2.4. These amines contain at least one amino group and one hydroxyl group, which reduces vapour pressure and promotes alkalinity in the solution. For example, monoethanolamine (MEA) and diglycolamine (DGA) are classified as primary amines. These are defined as the most mature solvents because they provide a high reaction rate, medium absorption capacity,

and stability within acceptable limits. Nonetheless, because DGA has a low vapour pressure, it can be used at higher concentrations ranging from 40 to 60% wt.

Secondary amines such as diethanolamine (DEA) and diisopropanolamine (DIPA) in which the hydrogen is bonded directly to nitrogen, are known as alternative solvents to primary amines. On the other hand, in terms of corrosion and degradation, DEA is better than MEA. DIPA, on the other hand, has a lower energy penalty than MEA.

Tertiary amines, which have the highest molecular weight among other amines, have disadvantages in terms of absorption capacity and stability, which are lower than those of primary and secondary amines. In the chemical structure of this amine, there is no hydrogen bonded with a nitrogen atom, meaning that the CO<sub>2</sub> hydrolysis facilitates bicarbonate formation, which has a lower heat of reaction compared to carbamate formation. As a result, tertiary amines are always combined with primary or secondary amines to increase the heat of reaction.

**Table 2.4: summary of some amine solvents used in CO<sub>2</sub> capture process**

Abbr.	Name	Process	Chemical Structure	CO <sub>2</sub> loading
MEA	Monoethanolamine	Natural and syngas		0.5
DGA	Diglycolamine	Syngas		0.25-0.35
DEA	Diethanolamine	Natural gas		0.7-1
DIPA	Diisopropanolamine	Refinery gas treatment		0.43-0.22
MDEA	Methyldiethanolamine	Gas washing in Claus's Plants		0.1-0.3

### 2.4.2 Sterically hindered amine

Sterically hindered amine is known as a modified primary or secondary amine, which has the ability to enhance absorption rates higher than primary or secondary amine. The formation of this amine is characterised by the amino group, whether attached to a tertiary carbon atom or a secondary tertiary carbon atom. It is classified as having intermediate to low stability, and the weak bond contributes to utilizing the high amine concentration in the solution. As a consequence, the energy penalty will be lower than primary and secondary amine by 20% and 15% for solvent consumption, respectively (Hüser et al.,2017).

### 2.4.3 Ionic Liquid

Ionic liquid is defined as the novel alternative to conventional amine-based solvents. It is classified as an organic salt because it has high boiling points and low vapour pressure, allowing it to selectively absorb CO<sub>2</sub> with a relatively low energy penalty. It is created by combining organic cations like phosphonium with either an inorganic anion like Cl<sup>-</sup> or an organic anion like RCO<sub>2</sub><sup>-</sup>. Anions play a vital role in increasing the performance of the absorption process in the absorber compared to cations, which have a lower impact on absorption. However, this solvent reacts with CO<sub>2</sub> as physical solvents, which enhancing the solubility of CO<sub>2</sub> by deploying Henry's law. It works on the same zwitterion mechanism as primary and secondary amines. Nonetheless, ionic liquids have drawbacks that make them unsuitable as a solvent. It has a higher viscosity during the absorption process than amine solvents, which limits mass transfer and causes operational issues.

Based on Luo and Wang (2017), it was reported that the reason for its high viscosity after CO<sub>2</sub> absorption is due to the generation of strong and dense hydrogen bonds between compounds. To overcome this limitation, some authors proposed that using non-amine functionalized ionic liquid is advantageous in terms of constraining the generation of hydrogen-bonded networks. Although it is noted that it is more expensive than amine solvents.

### 2.4.4 Solvents blend

A solvent blend may provide a significant improvement in energy consumption and solvent circulation rate by reducing the energy associated with amine regeneration. For example, adding primary or secondary amine to tertiary amine might enhance the absorption rate, increase the resistance to solvent degradation, and reduce energy consumption. For

these reasons, the researchers investigated several solvent blends to obtain the novel solvent for reducing the energy penalty. MDEA, as an example, which was the first amine, was added to faster-kinetic amine such as MEA and PZ, namely promoters. Table 2.5 presents the most relevant solvent blends from the previous studies.

**Table 2.5: Solvent blends of solvent-based PCC process**

Solvents blend	Abbreviation	Reference
Piperazine and potassium carbonate	PZ+K <sub>2</sub> CO <sub>3</sub>	Oexmann <i>et al.</i> ( 2008)
2-amino-2-methyl-1-propanol and Piperazine	AMP+PZ	Zhang <i>et al.</i> , 2017)
Methyl diethanolamine and piperazine	MDEA+PZ	Closmann <i>et al.</i> ( 2009)
Monoethanolamine and piperazine	MEA+PZ	Dugas and Rochelle (2011)

There are some advantages to using different solvent blends:

- There is an improvement in thermodynamic efficiency compared to single solvents.
- There is a reduction in solvent degradation and the operating costs.
- To achieve the highest efficiency, the composition range of solvents required for optimization can be chosen with flexibility.
- Solvent blends provides a higher absorption rate compared to single solvents.
- There is a reduction in the energy required for solvent regeneration.

#### 2.4.5 Water-free solvents

Utilizing water with the solvent has a profound role in reducing corrosion and viscosity. Nevertheless, it increases the parasitic energy required for solvent regeneration. As a result, some scientists have proposed various water-free solvents, such as amino-silicones and amines with superbase. A CO<sub>2</sub>-philic siloxane backbone and a CO<sub>2</sub>-reactive amino group distinguish amino-silicones. These solvents have a higher absorption efficiency compared to conventional amino groups due to the physisorption mechanism.



## 2.5 Steady-state simulation of solvent-based PCC

In recent decades, researchers have paid attention to first principles modelling because the experimental data has limitations in changing the operating conditions. It focuses on mass, heat transfer, and chemical reactions for solvent-based PCC. To improve the model, two columns should be deployed in this process. absorber column, which is operating at low temperature and atmospheric pressure, while the stripper is operating at elevated temperature and pressure, relying on the solvent characteristics.

This model's development requires two phenomena, including mass transfer and chemical reactions. These phenomena are classified as "model-level complexity." The level of complexity is classified based on two approaches: the equilibrium-based approach and the rate-based approach. The former expresses the consistent thermodynamic rule by calculating vapour pressure, heat capacities, and heat reactions. It considers that both phases, liquid and gas, are in equilibrium as theoretical stages. However, this approach is not able to provide the performance of the CO<sub>2</sub> capture process at a specific column size, so the latter is required. It will give accurate results as it consists of mass transfer and kinetic reactions. This approach is more reliable for analysing the performance of solvent-based PCC.

Figure 2.2 depicts the level of complexity for two approaches. Model (1) expresses both equilibrium in mass transfer and chemical reaction, while Model (2) has an equilibrium stage with reaction kinetics. Model (2) is still not reliable for model development because it cannot give accurate model predictions, such as CO<sub>2</sub> capture level and re-boiler duty related to chemical reactions and mass transfer as mentioned. Model (3) is different from models (1) and (2) because it expresses mass transfer but with an equilibrium reaction. It was used and provided satisfactory results in cases of fast reactions. Model (4) is similar to model (3) but with an improvement in the enhancement factor, which is defined as the ratio of the liquid mass transfer coefficient with or without reaction. Model 5, which considers reaction kinetics, reaction film, and electrolyte, is the most complex and accurate among the other models.

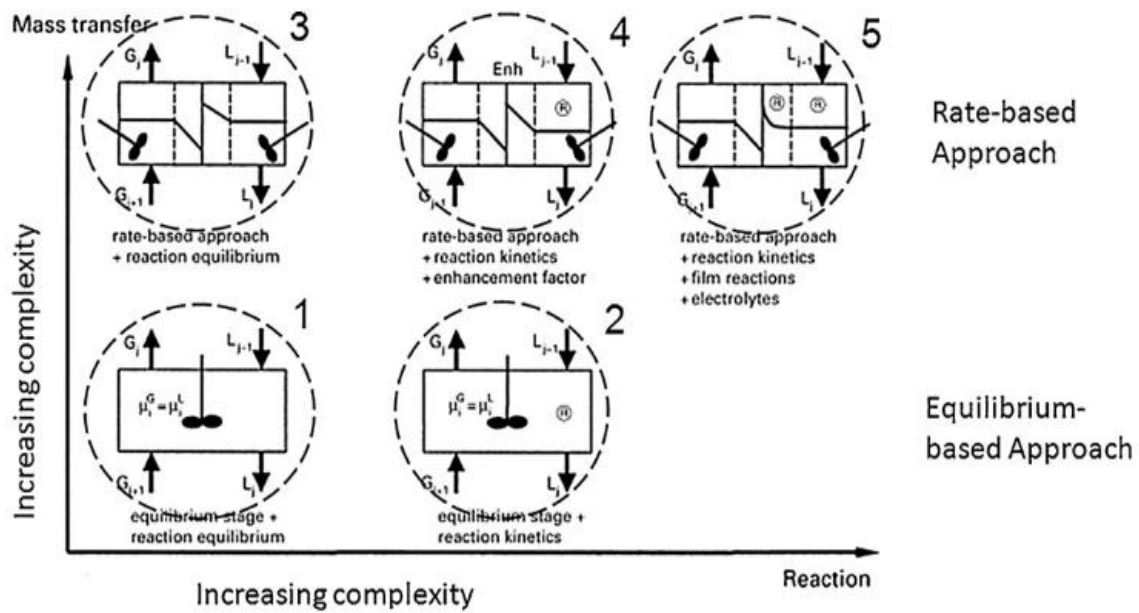


**Figure 2.2: A schematic of model level complexity for equilibrium -based model and rate-based model (Wang et al., 2011)**

There are several mass transfer theories for two phases, liquid and vapour, such as the two film theory and the penetration theory (Li et al., 2015). The two-film theory is more widely used due to its simplicity and ease of implementation. In both phases, there are two regions classified in this theory: bulk and film. The impact of mass transfer resistance is in the laminar film area. Penetration theory, on the other hand, operates on a different principle: the elements have the same exposure time on the surface of both phases, liquid and vapour, which has a strong influence on the mass transfer coefficient.

Pintola et al. (1993) developed a steady-state model for absorbers, conducting a rate-based model with an enhancement ratio to estimate the accurate absorption rate. Their finding of enhancement factors shows that there is a variation from the results by Tontiwachwuthikul *et al.*(1992). This discrepancy might have occurred because we used different correlations. It is emphasised that evaporation, condensation of water, and physical properties should be considered to provide accurate results against the pilot plant data. Moreover, the results confirmed that in the bottom of the absorber, the most  $\text{CO}_2$  removal occurred due to a high  $\text{CO}_2$  concentration. For the  $\text{CO}_2$  capture process, it is not sufficient to develop a standalone column so that there is a further steady-state model expressing the absorber and stripper by Alatiqi et al. (1994) in which rate-based calculation was conducted with different enhancement ratio correlations.

Abu-Zahra et al. (2007) performed a steady-state model for both columns using RadFrac using Aspen Plus®. A technical parametric analysis was conducted to improve the absorption rate and reduce the energy penalty. The experiment was carried out with a 30% MEA concentration, a CO<sub>2</sub> lean loading (mol CO<sub>2</sub>/mol MEA), CO<sub>2</sub> capture rate (%), lean solvent temperature (°C), and stripper pressure (kPa). It was noted that CO<sub>2</sub> lean loading has a profound effect on the performance of the entire process. Furthermore, energy savings occurred when MEA concentration and stripper pressure were increased. The economic study was performed by Abu-Zahra et al. (2007)

As shown in the Figure 2.2, there are two approaches to expressing the CO<sub>2</sub> medium with the target solvents. An equilibrium-based approach follows the principle of thermodynamic relations. Heat capacity, gas solubility, vapour pressure, heat of reaction, and molecular interaction are estimated using a set of parameters describing the chemical properties (Papadopoulos, 2017). Helmholtz formulation is used to obtain the chemical properties.

## **2.6 Control design of solvent-based PCC plant using packed bed with solvents**

Process control strategy is considered a necessity because it has a profound role in achieving safety and profitability for every process. It includes three entities consisting of the type of controller, control structure, and control design and tuning. Further detail will be discussed for previous studies on the process control of solvent-based PCC.

Most chemical processes are considered as an integrated process, which requires an appropriate controller based on control structure and design. The essential key is to select the manipulated and controlled variables properly, which are characterised by single input-single output (SISO) or multiple inputs-multiple outputs (MIMO).

Lawal et al. (2010) utilised a control scheme. The control structure is to control the temperature of the stripper by using a PI controller and manipulating the condenser and re-boiler heat for the bottom and top of the stripper. Because the temperature of the stripper has a vital impact on solvent absorption capacity and CO<sub>2</sub> loading from the bottom, Another controller was deployed, which is the P controller for keeping the re-boiler level by manipulating the re-boiler bottom flow rate. In addition, water balance was under control by manipulating the water makeup mass flowrate and water mass fraction in the lean solvent, which includes 30.48 wt.% MEA, 6.18 wt.% CO<sub>2</sub>, and 63.34 wt.% H<sub>2</sub>O.

Furthermore, the main goal is to control the CO<sub>2</sub> capture level by adjusting the lean solvent flow rate. The dynamic performance of solvent-based PCC was evaluated in this study using various disturbances such as increasing flue gas flow rate and CO<sub>2</sub> concentration in flue gas. The evaluation results show that the liquid to gas ratio (L/G) has a significant impact on the absorber, whereas the stripper is sensitive to the re-boiler heat duty. Similarly, Lin *et al.* (2011) performed the same procedure in the control structure. However, the manipulated variable for liquid level in the re-boiler was the water makeup flowrate; hence, it affected the water balance in the entire process. Despite the presence of disturbances such as flue gas flowrate, CO<sub>2</sub> content in the flue gas, and H<sub>2</sub>O concentration, the results of the dynamic analysis revealed that the process is operating well under the specified CO<sub>2</sub> capture level and CO<sub>2</sub> lean loading.

Mechleri *et al.* (2017) used two control structure strategies. Strategy one was to control CO<sub>2</sub> capture and re-boiler temperature by maintaining the lean solvent flowrate and steam flowrate, respectively. Whereas strategy 2 was to keep controlling CO<sub>2</sub> capture with a lean solvent flowrate by regulating the re-boiler temperature and lean solvent flowrate. The performance of the control structure was evaluated based on disturbance rejection, and the level of CO<sub>2</sub> capture was also controlled. The deviation from the set point was extremely low. The aforementioned step should be followed by controller selection, control design, and tuning. There are a variety of controllers that are essential in process control, such as decentralised or centralised loop control. An example of a decentralised control structure is the PID controller, whether it is feedback or feedforward. It can be utilised in such a way that each loop has a different structure. Several previous studies focused on the controllability of flexible operation for solvent-based PCC, Rodriguez *et al.* (2014). In this study, PI controllers were used in the process where CO<sub>2</sub> capture level was controlled by regulating the lean solvent flow rate. In addition, another PI controller was deployed to control the pressure in the condenser and re-boiler by manipulating the condenser vapour in the outlet stream and the re-boiler vapour outlet stream. The dynamic performance in the case of CO<sub>2</sub> capture level did not achieve the setpoint, which is 90%, because it rose to 93% and reduced to 87% in the presence of ramp disturbance. Furthermore, the P controller was utilised as well to control the condenser level.

Gaspar *et al.* (2015) implemented a decentralised control structure to control both CO<sub>2</sub> capture level and lean loading out of the re-boiler while the manipulated variables were

the lean solvent flowrate entering the absorber and the flowrate of steam entering the reboiler using a two-control structure with two P controllers.

## 2.7 Dynamic simulation and validation of solvent-based PCC using packed bed with solvents

Due to the inaccuracy of model development for the whole process at steady-state, the performance dynamic analysis is required to obtain the deep understanding of the process at transient condition. Hence, it will provide the knowledge for flexible operations (i.e., start-up and shutdown). The researcher investigated the dynamic performance by standalone packed columns. For example, a few researchers studied the dynamic performance of absorber column using the MEA benchmark (Kvamsdal *et al.*, 2009;2011; Lawal *et al.*, 2009; 2009a; Mac Dowell *et al.*, 2013; Posch and Haider, 2013). On the other hand, stripper was investigated by (Lawal *et al.*, 2009; Ziaii *et al.*, 2009; Greer *et al.*, 2010).

Kvamsdal *et al.* (2009) investigated the dynamic performance of a standalone absorber by changing the lean solvent flow rate and the thermodynamic state. In addition, the H<sub>2</sub>O content of the flue gas stream was increased. It was observed that this variable has a profound impact on the mass transfer zone position, which raises the condensability of the flue gas stream. On the other hand, Ziaii *et al.* (2009) analysed the dynamic performance for standalone stripper for two dynamic strategies (i.e., peak load and price). A negative step change in the steam flow rate was deployed with and without modifying the rich solvent flow rate. The results showed that in cases of steam flowrate reduction without adjusting rich solvent flowrate, the lean loading increased by 3%. However, the standalone packed column cannot provide accurate dynamic performance because of the coupling resistance between both packed columns. Hence, some research studies studied the performance of two integrated packed columns (Lawal *et al.*, 2010; Gáspár and Cormoş, 2011; Harun *et al.*, 2012; Biliyok *et al.*, 2012; Dietl *et al.*, 2012; Flø *et al.*, 2015)

Lawal *et al.* (2009) investigated the dynamic performance of the entire process using two integrated-packed columns. The results confirmed that the L/G ratio has a greater direct impact on absorber performance than the solvent flowrate or flue gas flowrate. (Walters *et al.*(2016) developed a rate-based model through an intercooling absorber using piperazine (PZ) in gPROMS. The regressed electrolyte non-random two liquid (eNRTL) property method was used, and the mass transfer liquid film was determined

experimentally using various CO<sub>2</sub> lean loadings. The model predictions (i.e., CO<sub>2</sub> capture level and temperature profile) illustrated that there is a high degree of agreement with the steady-state model developed in Aspen Plus<sup>®</sup>. Using the same software, Biliyok *et al.* (2012) implemented the dynamic model through the same configuration, which is an intercooled absorber. However, this model was modified from Lawal *et al.* (2009) using a rate-based model by two-layer film theory. For the need of simplicity, chemical reactions were assumed to be in equilibrium. In this study, three empirical cases from the SRP pilot plant at the University of Texas at Austin were deployed for dynamic validation. The first case was used for conventional configuration, while the other two were used for intercooling absorber configuration. The data were obtained with different input variables such as solvent flowrate, solvent temperature, CO<sub>2</sub> content in flue gas, flue gas flowrate, and flue gas temperature. The findings noted that the results predicted well the behaviour of the pilot plant in the case of dynamic change. After that, a another analysis was conducted to study the impact of increasing the moisture content and decreasing the intercooled solvent temperature. The simulated results showed that moisture content plays a critical role in the absorber temperature profile but has a marginal effect on capture level. Furthermore, using an intercooling absorber improved absorption efficiency, improving the absorber's performance, especially when the temperature bulge which is defined as the maximum increase in the temperature in the column. The temperature bulge is the result of chemical reactions between CO<sub>2</sub> in flue gas and the solvent in liquid phase.

Dynamic modelling and simulation through software should be validated in order to provide reliable knowledge for dynamic performance analysis. Kvamsdal *et al.*, (2011) developed a rate-based model using Matlab<sup>®</sup> software. The model was validated against two empirical datasets from the Validation of Carbon Capture (VOCC) rig in Norway. Two experimental data were tested in this validation: change in gas and liquid flowrate and change in CO<sub>2</sub> content in flue gas. The model predictions, including CO<sub>2</sub> capture level and CO<sub>2</sub> rich loading, were validated against the experimental data, and the results reflected the dynamic absorber performance well within an acceptable deviation. Furthermore, different reaction coefficients were evaluated, and the findings confirmed that the model fitted to a specific pilot plant may not be valid for other pilot plant data.

Åkesson *et al.* (2012) used Modalica® for dynamic rate-based model to be used for the entire process. The model was evaluated against experimental data from the Esbjerg Pilot Plant in Denmark, where it was performed in an open loop. A 30% step change was used to change the flue gas flow rate. The dynamic response of the CO<sub>2</sub> capture level increased rapidly in response to a reduction in flue gas flowrate, whereas flue gas flowrate has only a minor effect on re-boiler temperature. On the other hand, closed loop performance was deployed by Posch and Haider (2013) to obtain deep insight about the absorber temperature profile. A dynamic rate-based model was carried out in a closed loop in which two input variables were adjusted, including flue gas and lean solvent temperature, from 30 to 50 °C. The validation was performed using the experimental data from the CO<sub>2</sub> SEPPL test rig at the Durnrohr power station in Austria. The results indicated that the dynamic response of temperature change at different absorber heights was in agreement with the experimental data.

Enaasen *et al.*, (2014) developed a dynamic model that was validated against the Brindisi Pilot Plant in Italy. The key parameters studied in this model were steam flowrate, re-boiler duty, flue gas, and lean solvent flowrate. Reduction in steam flowrate for re-boiler duty had a minor impact on CO<sub>2</sub> rich loading but had a high probability of increasing CO<sub>2</sub> lean loading slowly. By the end, there is a reduction in CO<sub>2</sub> capture level and CO<sub>2</sub> flow rate generated from the top of the stripper. In lean solvent flowrate reduction, the CO<sub>2</sub> capture level decreased quickly, while the flue gas flowrate had a negligible impact on CO<sub>2</sub> rich and lean loading but had a major effect on the CO<sub>2</sub> capture level. After that, the transiently validated model was used in the K-Spice general simulation tool and evaluated against pilot data, where the prediction was in agreement with dynamic performance.

Gaspar *et al.* (2016) performed a comparison of dynamic performance between the DCAPCO<sub>2</sub> in-house model and experimental data from a 1 t/h CO<sub>2</sub> pilot plant, utilising 30 wt.% MEA. The comparison was based on flue gas flowrate change, while the responses of key parameters were: CO<sub>2</sub> concentration in treated gas, flowrate of CO<sub>2</sub> generated from the top of the stripper, and the temperature profile for the liquid phase in different columns' heights. The results showed that the model was reliable against experimental data with a small deviation. On the other hand, a steady-state deviation in the CO<sub>2</sub> concentration of treated gas occurred when it was below 0.5 mol% due to the inaccuracy of physical and thermodynamic measurements. The sump was not performed in this procedure; hence, the fluctuation was easily obtained compared to the pilot plant. Another investigation was

to scale-up the validated model to 200 t/h CO<sub>2</sub> capacity by applying two solvents, MEA, and PZ, at different concentrations (30 and 40 wt.%) followed by dynamic performance. The transient results showed that a reduction in the flue gas flow rate has a major effect on CO<sub>2</sub> capture levels. Another observation is that the time for MEA to reach steady-state was faster than for PZ for the specified concentration in case of a flue gas flowrate increase. The reason is that the flue gas flow rate has a greater impact on the temperature of PZ in comparison to MEA. Another investigation was to carry out the load following the use of solvent-based PCC at a different circulation rate. In the case of a solvent limit, it was essential to adjust the solvent flow rate to provide the target CO<sub>2</sub> capture level while reducing the fluctuation in re-boiler duty.

Haar *et al.*, (2017) developed a rate-based model, which is different from that of the researcher. The equilibrium-based model was implemented in Thermal Separation Modalica<sup>®</sup>. The parameters regulated were mass, heat transfer, and chemical reaction coefficients using steady-state experimental data in order to provide a reliable model at specific nominal operating conditions. In the case of a step change in flue gas flowrate, the model predictions, including CO<sub>2</sub> capture level and CO<sub>2</sub> rich loading, had good agreement with the experimental data, while the temperature profile had a large steady-state deviation, particularly in absorber columns, which was similar to the findings in Peng *et al.* (2003). Furthermore, a switch from steam to a re-boiler was proposed to improve the power plant's load-following performance. Also, transient analysis was conducted in the case of the steam to re-boiler step change. Table 2.6 provides a summary about dynamic and validation of solvent-based PCC.



Table 2.6: Summary of some project conducted dynamic modelling of solvent-based PCC using different solvents

Institute	Year	Solvent/software	Cases investigated	Validation data	Reference
Norwegian research program Climate, Norway	2011	MEA/ model (4) Matlab	CO <sub>2</sub> content in flue gas, liquid, and gas flowrate	Validation of Carbon Capture (VOCC) rig in Norway	Kvamsdal <i>et al.</i> (2011)
Telemark University College, Norway	2013	MEA/ model (4) Matlab	Up stream of power plant (load scenario Downstream of stripper	Separation Research Program at the university of Texas at Austin	Jayarathna <i>et al.</i> (2013)
European FP7 OCTAVIUS project	2014	MEA/K-Spice general dynamic simulation tool	Change in steam flowrate to re-boiler , Change in solvent flowrate , Change in flue gas flowrate	Brindisi pilot plant	Enaasen <i>et al.</i> (2014)
Bolyai University, Faculty of Chemistry and Chemical Engineering, Romania	2015	AMP	Flue gas flowrate (step change), liquid flowrate step change stripper liquid input stream	Experimental data from university of Denmark	Gabrielsen (2005)

Department of Chemical Engineering, at the university of Texas at Austin	2016	PZ/ model 5	Step change of pressure in stripper	Dynamic data from SRP at the university of Texas at Austin	Gaspar <i>et al.</i> (2016)
Propulsion & Power, Delft University of Technology (The Netherlands), Institute of Thermo-Fluid Dynamics, Hamburg University of Technology (Germany) and TNO (The Netherlands Organisation)	2017	MEA/Model 1 Modalica	Step change flowrate, CO <sub>2</sub> concentration	Experimental Pilot plant from the Maasvlakte power station power station in the Netherlands	(Van De Haar <i>et al.</i> , 2017)

## 2.8 Solvent-based PCC using Rotating packed bed for Process Intensification

Rotating packed bed (RPB) is classified as a device for process intensification where a high centrifugal field is produced by a torus-shaped rotor spinning. This method was deployed originally by Colin Ramshaw (Luo et al., 2012). The main fundamental of this approach is that the liquids flow as jets, which come from the liquid distributor and get into the inner periphery of the rotor. The liquid flows through the rotor's packing. In cases of high gravity, micro- or nano-droplets are produced by liquid distribution. The gas flows to the liquid in the rotor in three ways: counter-current, co-current, and crossflow. This approach has advantages over the conventional packed bed in terms of mass transfer rate between liquid and gas, which is 1-3 orders of magnitude faster than the conventional packed bed. A rotating packed bed's central component is the rotor. The previous studies focused on different aspects, such as pressure drop and mass transfer performance

Zheng *et al.* (2000) investigated pressure drop in a rotating packed bed in a counter-current flow. It was confirmed that using wet-packed beds has a significantly lower pressure drop compared to dry-packed beds within specific operating conditions. For the experimental status of a rotating packed bed at Newcastle University, the main parameters investigated were lean amine temperature and rotor speed, using different MEA concentrations of 30, 55, 75, and 100 wt.%. The packing type was expamet, with a surface area of 2132 m<sup>2</sup>/m<sup>3</sup> and a void fraction of 0.76. On the other hand, another operating condition was used where water was used as a solvent for hydrodynamic study in the rotating packed bed. The findings indicated that using a rotating packed bed enhanced the mass transfer, which is gas phase controlled. Therefore, it is suitable for gas sweetening applications (Jassim et al., 2007).

At Taiwan University, Chang Gung University, and Chung Yuan University, three solvents were used to assess the RPB column. It was found that using DETA is more efficient than MEA in terms of  $K_{Ga}$  and HTU because DETA has a higher absorption capacity compared to MEA. DETA also has a high boiling point but a low vapour pressure (Yu et al., 2012). A blend of solvents PZ and DETA had a higher CO<sub>2</sub> absorption capacity than a single DETA. On the other hand, at Iran intensification research, the packing was different from the aforementioned studies of the specific surface area and void fraction; the operating conditions included inlet flue gas with 5000 ppm CO<sub>2</sub> and flue gas and liquid flow rates of

10–40 L/min and 0.2–0.8 L/min, respectively. The rotor speed ranged from 400 to 1600 rpm. The finding confirmed that the height of the transfer unit of CO<sub>2</sub> carbon capture absorption ranged from 2.4–4 cm and depended on the rotor speed, solution concentration, and gas and liquid flow rates (Rahimi and Mosleh, 2015)

## 2.9 Summary

The previous literature on steady-state and dynamic modelling of solvent-based PCC processes through control structure and design has shown these highlights:

- A few previous studies were developed using software at pilot scale for solvent-based PCC processes using the benchmark solvent MEA. But it has two problems: it costs a lot to run and buy, and it uses a lot of energy because of the way it works and how the solvent is recycled.
- Limited previous studies on a commercial scale were implemented to meet the exact flue gas flowrate from the CCGT power plants. The scale-up method is reliable if the solvent-based PCC modelling is validated against experimental data. Furthermore, the scale-up procedure has no effect on the process's performance, whether it affects the physical or chemical properties.
- Limited dynamic modelling of solvent-based PCC at pilot and commercial scales using different solvents such as PZ, AMP, or mixed solvents is necessary because the majority of previous studies were evaluated using only the benchmark solvent MEA.
- Based on different solvents such as PZ and mixed solvents (e.g., PZ with AMP), they have superiority in reducing energy consumption because they have better properties of absorption ability and solvent degradation. The previous studies focused on standalone absorbers and strippers. Hence, limited model development for the entire process was investigated. The economic and technical analyses were not evaluated to figure out their efficiency in comparison to the benchmark solvent, MEA.

## Chapter 3: Process Simulation PCC using MEA

### 3.1 Overview

In this chapter, the process simulation of the PCC process will be discussed in detail. A Chemical absorption approach is utilised using the benchmark solvent (MEA). This solvent is the most commonly used in amine scrubbing applications. Sections 3.2 and 3.3 focused on the steady-state model development and validation of the solvent-based PCC process at pilot scale using MEA in Aspen Plus® v.11. Section 3.4 presents the scale-up of the validated PCC model to commercial scale. The Technical evaluation of a commercial-scale solvent-based PCC model is presented in Section 3.5. In Section 3.6, Economic evaluation, using Aspen Process Economic Analyser® is presented.

Steady-state the PCC model has limitations in providing a deep understanding of the transient behaviour of the entire process. Dynamic modelling of the commercial scale PCC model is presented in Section 3.7.

### 3.2 Steady-state model development of PCC using MEA at pilot scale

Solvent-based PCC involves an absorption process using an absorber column and solvent regeneration using a stripper column. The RadFrac model block is used to represent the respective columns in the solvent-based PCC process. RadFrac is a rigorous model block, available in Aspen Plus®, for simulating all kinds of multi-stage fractionation operations such as absorption, stripping, extractive distillation, and azeotropic distillation. The RadFrac model enables the implementation of the rate-based modelling approach to the absorber and stripper columns, which is more reliable for the performance evaluation of the solvent-based PCC process (Al-malah, 2017).

In this process, two phases are included: the gas phase, involving nitrogen, water, carbon dioxide, and argon. On the other hand, the liquid phase includes the MEA, CO<sub>2</sub>, and H<sub>2</sub>O.

Table 3.1 lists the components of CO<sub>2</sub>-MEA-H<sub>2</sub>O, along with their ions and flue gas compositions.

**Table 3.1: Components and ions in gas and liquid phase**

Gas phase	Liquid phase	
CO <sub>2</sub>	H <sub>2</sub> O	MEAH <sup>+</sup>
H <sub>2</sub> O	H <sub>3</sub> O <sup>+</sup>	MEACOO <sup>-</sup>
Argon	CO <sub>2</sub>	HCO <sub>3</sub> <sup>-</sup>
N <sub>2</sub>	CO <sub>3</sub> <sup>-2</sup>	MEA

There were specific assumptions used in this model development:

- Flow regime for plugs
- Linearity in pressure drop across the column
- The accumulation is zero in the liquid and vapour bulks as well as the vapour phase.
- Negligible oxygen in flue gas
- The reactions occur in the liquid phase.
- There is no heat loss to the surrounding
- MEA is defined as non-volatile, so solvent degradation is negligible.
- There is phase equilibrium occurring at the interface.

The type of model that provides an accurate evaluation of thermodynamic properties should be selected. Because of the presence of ions, this model must be chosen with the strong non-ideality of the liquid phase in. A variety of previous studies suggested that using Electrolyte Non-Random Two Liquid (ENRTL) is the most appropriate method for expressing the electrolyte interactions between CO<sub>2</sub>, H<sub>2</sub>O, and MEA.

The solvent-based PCC process is modelled in the simulation as two packed columns, such as absorber and stripper, heater, condenser, pumps, and cooler. The modelling is deployed as RadFrac using a rate-based model because it is more reliable than equilibrium. Table 3.2 details the absorber and stripper packed section specifications obtained from the pilot plant located at Separation Research Program (SRP), which includes packed section diameter and height, packing type, packing factor, and surface area. These specifications are relevant to carry out validation of the model developed at pilot scale.)(Canepa *et al.*, 2013).

**Table 3.2: Absorber and stripper packing material characteristics (Canepa et al., 2013)**

Specifications	Absorber	Stripper
Packing section diameter (m)	0.427	0.427

Packing section height (m)	6.100	6.100
Type of Packing	IMTP#40	FLEXIPAK 1Y
Packing factor (1/m)	78.700	168.200
Packing surface area (m <sup>2</sup> /m <sup>3</sup> )	145.000	420.000

Because the CO<sub>2</sub> heat of absorption in MEA is greater than the water heat of vaporization, the pressure in the stripper is always greater than the atmospheric pressure in the absorber.(Freguia et al., 2003). Moreover, based on the Clausius-Clapeyron equation, CO<sub>2</sub> vapour pressure is increasing rapidly compared to H<sub>2</sub>O vapour pressure. However, there is a limit for stripper pressure increases due to the limitation of MEA degradations. It has been noted that solvent degradation is negligible when keeping the re-boiler temperature below 110 °C (Davis et al., 2009). The specifications for the absorber and stripper are presented in Table 3.3, where pressure profile and re-boiler duty were taken from the experimental data provided by Canepa *et al.*(2013). On the other hand, the number of stages was specified based on the CO<sub>2</sub> composition profile in the liquid phase in both packed columns. Also, the amount of liquid held between packing materials, called "liquid hold-up," is chosen to match the pressure drop in the columns.

**Table 3.3: Absorber and stripper specification at pilot scale**

Input	Absorber	Stripper
Pressure profile (N/m <sup>2</sup> )	Top Stage: 97000 Bottom Stage: 106190	Top stage: 161702 Bottom stage: 162090
Liquid holdup (L)	0.09	0.1
Number of stages	10	20
Re-boiler duty (MW)	-	0.6

### 3.2.1 Correlations and reactions used

The correlations selected in this model were the mass transfer coefficient and the interfacial area estimated by selecting the Onda correlation(Onda et al., 1968). In the case of liquid holdup, the Stichlmair correlation was selected for the calculation in the absorber column. On the other hand, Bravo correlations were utilised in the stripper for mass transfer coefficient, interfacial area, and liquid holdup estimation(Bravo, 1985)

### 3.2.1.1 Mass transfer

While mass transfer resistance occurs in the liquid and vapour phases, the diffusivity of CO<sub>2</sub> in the liquid phase was estimated by the expression provided by Mahajani, (2005), and the diffusivity of CO<sub>2</sub> in the vapour phase was estimated using Fuller's equation. The mass transfer estimations for the liquid and vapour phases in the film were calculated using the correlation provided by Onda et al.,(1968), the correlation parameters, such as mass transfer coefficients  $k_G$  and  $k_L$ , and the effective area of packing  $a_w$  were used to obtain  $H_G$  and  $H_L$ .(Onda et al., 1968).

Equation 3.1 for effective area is shown as follow:

$$\frac{\alpha_w}{a} = 1 - \exp \left[ -1.45 \left( \frac{\sigma_C}{\sigma_L} \right)^{0.75} \left( \frac{L}{a\mu_L} \right)^{0.1} \left( \frac{L_w^{*2} a}{\rho_L^2} \right)^{-0.05} \left( \frac{L_w^{*2}}{\rho_L \sigma_L \alpha} \right)^{0.2} \right] \quad 3.1$$

Equations 3.2 and 3.3 for mass coefficients:

$$k_L \left( \frac{\rho_L}{\mu_L g} \right)^{1/3} = 0.0051 \left( \frac{L_w^*}{a_w \mu_L} \right)^{2/3} \left( \frac{\mu_L}{\rho_L D_L} \right)^{-1/2} (ad_p)^{0.4} \quad 3.2$$

$$\frac{k_G RT}{a D_v} = K_5 \left( \frac{V_w^*}{a \mu_v} \right)^{0.7} \left( \frac{\mu_v}{\rho_v D_v} \right)^{1/3} (ad_p)^{-2} \quad 3.3$$

Equations 3.4 and 3.5 for film transfer unit heights are provided as follow:

$$H_G = \frac{G_m}{k_G a_w P} \quad 3.4$$

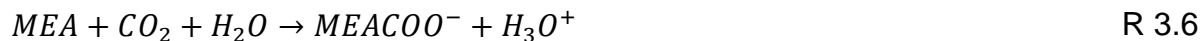
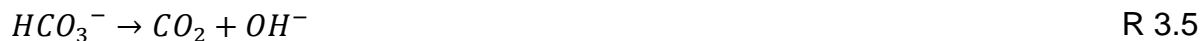
$$H_L = \frac{L_m}{k_L a_w C_t} \quad 3.5$$

### 3.2.1.2 Chemical reactions used in the model

The reactions added to this model include two reaction type: equilibrium and kinetic. Three ionic equilibrium reactions (R 3.1-R 3.3) and four kinetic reactions (R 3.4-R 3.7) in particular:







Based on the equilibrium reactions, equilibrium constants are defined as functions of temperature. There are two methods for determining it that Aspen Plus<sup>®</sup> offers: The first method is defined as standard Gibbs free energy change, using rigorous equation 3.6:

$$K_{eq} = \exp\left(\frac{\Delta G^\circ}{RT^L}\right) \quad 3.6$$

Where G is calculated using Aspen properties<sup>®</sup>. The second approach is parameter-based correlation, in which equation 3.7 used is as follow: equation 3.8 represents the kinetics reactions.

$$\ln(K_{eq}) = A + \frac{B}{T^L} + C \ln(T^L) + DT^L \quad 3.7$$

$$r = kT \exp\left(\frac{E}{RT}\right) \prod_{i=1}^N C_i^{\alpha_{ij}} \quad 3.8$$

Where the coefficients A, B, and C were added using literature (Canepa et al., 2013). In this model, parameter-based model is chosen because it is fully available in the previous study. Table 3.4 shows all the parameters required for both equilibrium constants and Kinetic expressions.

**Table 3.4: Coefficients for equilibrium constant and kinetic reactions(Canepa et al., 2013)**

Reaction no.	A	B	C	D
R 3.1	132.88	-13455.9	-22.47	0.0
R 3.2	-3.03	-7008.35	0.0	-0.003
R 3.3	216.04	-12431.7	-35.48	0.0
	k		E (cal/mol)	
R 3.4	4.32+13		13249.0	

R 3.5	2.38e+17	29451.0
R 3.6	9.77e+10	9855.8
R 3.7	2.18e+18	14138.4

### 3.2.2 Transport phenomena properties

The transport properties in this model include the liquid molar volume model, liquid viscosity, liquid surface tension, thermal conductivity, and binary diffusivity. All the transport properties are essential for mass transfer, heat transfer calculations using the NRTL property model. A Summary of these properties is given in Table 3.5:

**Table 3.5: Correlation models used for transport phenomena properties(AspenTech, 2010)**

Transport property	Liquid phase	Gas Phase
Viscosity	Jones-Dole electrolyte model	Chapman-Enskog-Brokaw model
Density	Clarke model	COSTALD model
Thermal conductivity	Riedel electrolyte correction model	Wassiljewa-Mason-Sexena model
Surface tension	Onsager-Samaras model	-
Binary Diffusivity	Nernst-Hartely model	Chapman-Enskog-Wilke-Lee model

Heat exchangers were connected as heaters and coolers between the absorber and stripper column, including one hot stream that is solvent leanout coming from the stripper. The second cold stream is a rich solvent leaving the absorber column. Moreover, the loop must be closed. Hence, it is obvious that mass and energy balance are achieved by adding MEA and water makeup to compensate for any losses in the entire process. Table 3.6 gives details of conditions (temperature and pressure) of the make-up MEA and water and the calculated flowrate of each make-up stream. The make-up stream accounts for the solvent loss and tops up the regenerated lean solvent flowrate. The make-up stream flowrate for MEA and water was calculated by carrying out a component mass balance in Aspen Plus. To assure convergence, the pressure and temperature of each make-up streams were selected as the regenerated lean solvent temperature and pressure after it has been cooled to 313.15 by a cooler (see Figure 3.1). to close the loop.

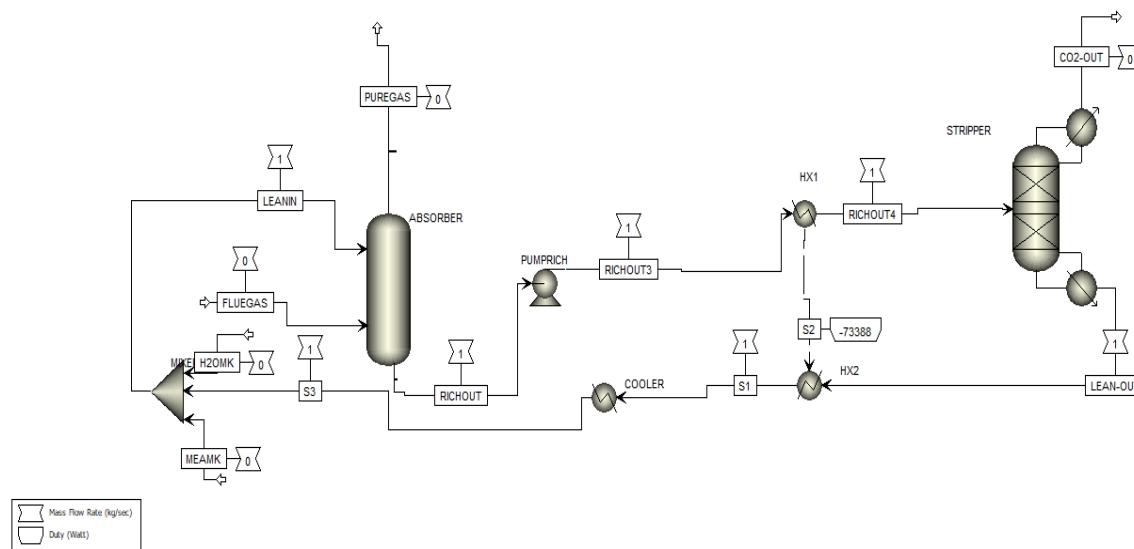


**Figure 3.1: A schematic of flowsheet of solvent-based PCC, showing closed loop**

Also, flowrate was calculated to have mass balance in the entire process for MEA and water.

**Table 3.6: Water and MEA make-up input and output specifications**

Specifications	MEA make-up	Water Make-up
Pressure (N/m <sup>2</sup> )	162090	162090
Temperature (K)	313.15	313.15
Output		
Flowrate (kg/h)	15.60	0.062

### 3.3 Steady-state model validation of PCC using MEA at pilot scale

#### 3.3.1 Pilot plant data

The model validation of a solvent-based PCC process was performed against the Separations Research Program (SRP) at the University of Texas at Austin. This research group was organised by Prof. Gary Rochelle. In both packed bed columns: (absorber, stripper), the diameter was 0.421 and a height of 6.1 m where each packed bed column was divided into two sections of 3.05 m. In the pilot plant data, there are 48 experimental cases conducted in this SRP. A solvent-based PCC was developed and validated using experimental data from case 28 as shown in Table 3.7.

**Table 3.7: Pilot plant data specifications for case 28 from SRP(Canepa et al., 2013)**

Specification	Case-28 Pilot plant data
Lean solvent volumetric flowrate (m <sup>3</sup> /min)	0.082
Lean solvent temperature (°C)	40.140
Flue gas volumetric flowrate (m <sup>3</sup> /min)	11.000
Flue gas temperature (°C)	48.080
Flue gas pressure (bar)	1.052
Condenser temperature (°C)	14.790
Re-boiler temperature (°C)	115.050
CO <sub>2</sub> content in flue gas (mol%)	16.540
Stripper pressure (bar)	1.621

### 3.3.2 Steady-state model validation of PCC using MEA at pilot scale

The PCC model validation includes the model predictions, including CO<sub>2</sub> capture level %, CO<sub>2</sub> rich loading mol<sub>CO2</sub>/mol<sub>MEA</sub>, CO<sub>2</sub> Lean Loading mol<sub>CO2</sub>/mol<sub>MEA</sub>, and Temperature Profile. Table 3.8 presents the model predictions, such as CO<sub>2</sub> capture level %, CO<sub>2</sub> rich loading mol<sub>CO2</sub>/mol<sub>MEA</sub>, CO<sub>2</sub> Lean Loading mol<sub>CO2</sub>/mol<sub>MEA</sub>, and re-boiler temperature against the SRP pilot plant data.

**Table 3.8: Model predictions validation against SRP pilot plant data**

Input	Rate-based model-	SRP experimental data	Relative percentage error (%)
CO <sub>2</sub> lean Loading (mol <sub>CO2</sub> /mol <sub>MEA</sub> )	0.287	0.286	0.348
Output			
CO <sub>2</sub> capture level (%)	86	80	6.9
CO <sub>2</sub> rich loading (mol <sub>CO2</sub> /mol <sub>MEA</sub> )	0.412	0.407	1.4
Re-boiler temperature (°C)	115.93	115.05	0.007

CO<sub>2</sub> capture level was calculated using the equation 3.9:

$$CO_2 \text{ capture level} = \frac{CO_2 \text{ in flue gas} - CO_2 \text{ out in treated gas}}{CO_2 \text{ in flue gas}} \% \quad 3.9$$

The relative percentage error was calculated by equation 3.10 for all model predictions to confirm that the model is reliable with high fidelity against the pilot plant data.

$$\text{Relative percentage error \%} = \frac{| \text{Measured (model)} - \text{real(pilot data)} |}{\text{real}} * 100\% \quad (3.10)$$

In the case of the temperature profile, the PCC rate-based model for both packed bed columns accurately predict the temperature profile from the experimental data, as shown in Figure 3.2. However, both columns have different temperature bulge locations. In the absorber, it was noted that its location was at the bottom of the packed column, where the L/G ratio was 5.95 (kg/kg). The temperature bulge does not have a profound impact on the absorber's performance.

CO<sub>2</sub> transfer is explained by two film theory, which it is a diffusion-based mechanism for characterizing gas mass transfer across a liquid phase. The assumptions are:

- 1- Laminar flow exists in gas and liquid film
- 2- The interface is in equilibrium and Henry's law is used with constant values of Henry's constant.
- 3- Chemical reactions and mass transfer occur in the films

The temperature profiles were extracted from Aspen Plus<sup>®</sup> for liquid phase, where chemical reactions occur between the CO<sub>2</sub> and the target solvent

Liquid bulk mass balance is shown by equation 3.11 and 3.12:

$$\frac{dM_i}{dt} = \frac{-1}{L \cdot A} \frac{\partial F_i^L}{\partial y} + N_i \cdot Sp \cdot MW_i \cdot \omega \quad (3.11)$$

$$\left. \frac{\partial F_i^L}{\partial y} \right| = 0 \quad (3.12)$$

where:

$$M_i = x_i \times M, \quad i = 1, \dots, n$$

$$\sum_{i=1}^n x_i = 1 \quad (3.13)$$

Regarding equation 3.11,  $y$  is defined as the axial location relative to the top of absorber packing, which means the top is counted zero to one or bottom of packing. The liquid energy balance is given by equations 3.14, 3.15, 3.16.

$$\frac{dU}{dt} = \frac{-1}{L.A} \frac{\partial F_H^L}{\partial y} + Sp \cdot \omega (H_{liquid}^{cond} + H_{liquid}^{conv} + H_{abs}) \quad (3.14)$$

$$\frac{\partial T|_{y=1}}{\partial y} = 0 \quad (3.15)$$

$$H_{abs} = N_{CO_2} \times h_{abs} \quad (3.16)$$

Where  $h_{abs}$  is defined as the specific heat of absorption where it is estimated as it is a function of temperature and  $CO_2$  loading from the literature (Oyenekan, 2007). In equation 3.14,  $F_H^L$  is the liquid enthalpy flow rate (J/s).

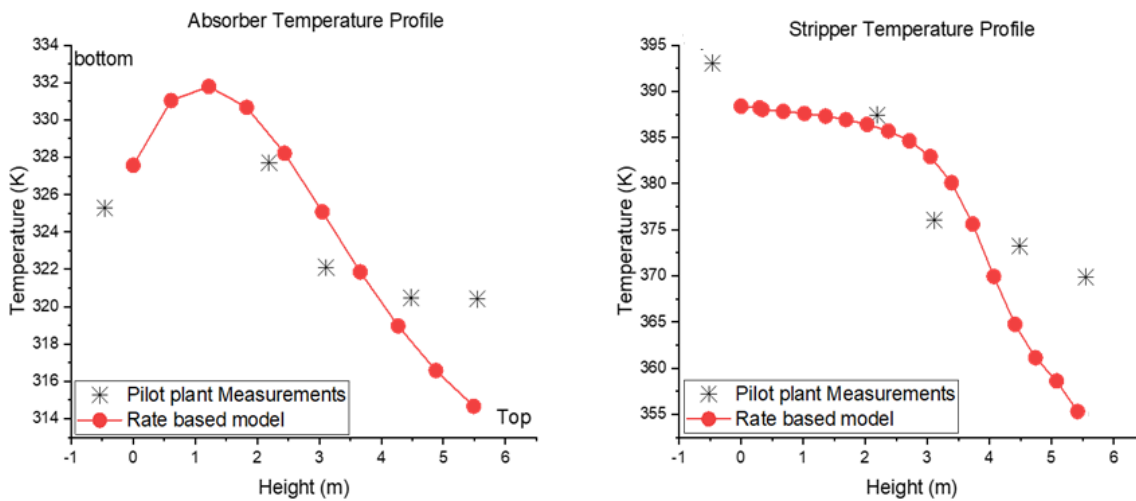


**Figure 3.2: Temperature profile for both packed columns: absorber and stripper**

In the stripper, it is clear that temperature bulge location is at the top of packed column. The L/G ratio affects the temperature bulge that happens when reactions happen in a packed column. L/G ratio for stripper was lower than absorber because the packing material, known Flexipac 1Y, used has higher surface area than IMTP no.40 in the absorber. At the packed column top in both plots, there is a difference between the experimental data and the rate-based model. In the case of the absorber, the feed's location difference for both streams (flue gas and lean solvent) to the absorber. In the case of the stripper, the feed operating conditions for the stripper were not provided in the experimental data, which might show this discrepancy.

### 3.4 Scale-up of solvent-based PCC using MEA to commercial scale

The solvent-based PCC model developed at pilot scale was scaled up to commercial scale to treat the flue gas flowrate from the commercial-scale power plant (250 MWe). This section highlights in detail the scale-up procedure's implementation. The CO<sub>2</sub> capture plant was designed to achieve a 90% CO<sub>2</sub> capture level using 30% wt. MEA solvent to treat a 356 kg/s flue gas flow rate.

- The CO<sub>2</sub> lean loading was 0.297 mol CO<sub>2</sub>/mol MEA, where was taken from the rate-based model at pilot scale as first guess to provide 90% CO<sub>2</sub> capture level at specific CO<sub>2</sub> lean loading.
- The CO<sub>2</sub> rich loading was 0.438 mol CO<sub>2</sub>/mol MEA, where was taken from the rate-based model at pilot scale as first guess to provide 90% CO<sub>2</sub> capture level at specific CO<sub>2</sub> lean loading.
- The CO<sub>2</sub> absorption capacity was assumed to be 0.18 mol CO<sub>2</sub>/mol MEA, which is defined as the difference between CO<sub>2</sub> Lean loading and CO<sub>2</sub> rich loading at 90% CO<sub>2</sub> capture which is different from the first value of CO<sub>2</sub> lean loadings taken from pilot plant (Canepa *et al.*, 2013).
- 

The scale-up calculations were focused on the solvent flow rate required and column diameter. The packed bed column height, on the other hand, was estimated using Aspen Plus®.

For scale-up calculations, there are a few things to keep in mind, which are explained below:

#### 3.4.1 Packing type

There are a variety of packing materials, but in this model, two packing materials were used. Random packing is defined as IMTP no. 40 for absorber columns. The packing material selection was implemented based on the nature of the fluid utilised and the operating temperature.

For the stripper, FlexiPac was selected because it has better mass transfer performance than random packing. This packing material is classified as a structure packing material

and is produced from a mesh or perforated metal sheet. It has a higher surface area, a high void fraction, and a high separation efficiency (Towler and Sinnott, 1969). FlexiPac is more efficient than random packing due to its low HETP and low pressure drop.

Structured packing material utilisation is used in systems with high separation difficulty, such as high vacuum distillation. However, it is very expensive compared to random packing material. Dugas (2006) investigated the performance of packing materials and concluded that structured packing materials are better than random packing materials by a factor of 1.5–2.

### 3.4.2 Packed column size

The absorber diameter was estimated based on the flue gas flow rate from the CCGT power plant, including specific operating conditions (e.g., temperature and pressure) and compositions. It was clear that the absorber had the largest size compared to the stripper. Generally, the flue gas flow rate at commercial scales is thousands of times that of a pilot plant. For instance, flue gas flow rates at commercial scale reported by Canepa *et al.*, (2013) and Lawal *et al.*, (2012) were higher by 5000 and 2200 times the flue gas flow rates from the pilot plant, respectively.

For packed column diameter estimation, solvent flow rate has to be calculated using the equation from the previous study (Agbonghae *et al.*, 2014). The flue gas flow rate was constant while the lean solvent flow rate varied to provide 90% CO<sub>2</sub> capture. Equation 3.17.

$$\text{Solvent lean flow rate} = \frac{\text{Gas flowrate} * X_{\text{CO}_2} * \varphi_{\text{CO}_2}}{100\zeta(\alpha_{\text{rich}} - \alpha_{\text{lean}})} \left[ \frac{M_{\text{MEA}}}{44.009} \left( 1 + \frac{1 - \omega_{\text{solvent}}}{\omega_{\text{solvent}}} \right) + \zeta\alpha_{\text{lean}} \right] \quad 3.17$$

$F_{\text{Lean}}$	Solvent mass flow rate (kg/s)
$F_{\text{FG}}$	Mass flow rate of flue gas (kg/s)
$X_{\text{CO}_2}$	Mass fraction of CO <sub>2</sub> in flue gas
$\Psi_{\text{CO}_2}$	Percentage of CO <sub>2</sub> captured in cleaned flue gas
$M$	Molar mass of lean amine solvent (PZ) (g/mol)
$\alpha_{\text{lean}}$	CO <sub>2</sub> lean loading solution
$\zeta$	Number of equivalents per mol of amine
$\alpha_{\text{Rich}}$	CO <sub>2</sub> rich loading solution
$\omega_{\text{amine}}$	Weight percentage of solvent



In the case of the stripper, the lean solvent flow rate is equal to the sum of the rich solvent flow rate and the reflux rate, while the gas flow rate to the stripper is equal to the boil-up rate that is needed to get the lean solvent flow rate.

The first step in scale-up calculation of column diameter is to calculate the flow parameter using some data from the pilot plant, such as density for both liquid and gas phases, kinematic viscosity for liquid, and a packing factor for the specified packing materials.

$F_{LV}$  is defined as defined as the liquid phase's kinetic energy multiplied by the gas phase's kinetic energy using equation 3.18

$$F_{LV} = \frac{L}{G} \sqrt{\frac{\rho_L}{\rho_G}} \quad 3.18$$

Where  $L$  is liquid mass flow rate (kg/s),  $G$  is gas mass flow rate (kg/s), while  $\rho_L$ ,  $\rho_G$  express the densities of both the liquid and gas phases. The flow parameter was used in the generalised pressure drop correlation (GPDC) chart to obtain  $K_4$ , which represents gas load as shown in Figure 3.3. The estimation was deployed based on the pressure drop assumption, where 42 mm of water/m of packed column was chosen, where it is defined as the default value for pressure drop per meter of packing height in packed columns (Sinnott, 2005).

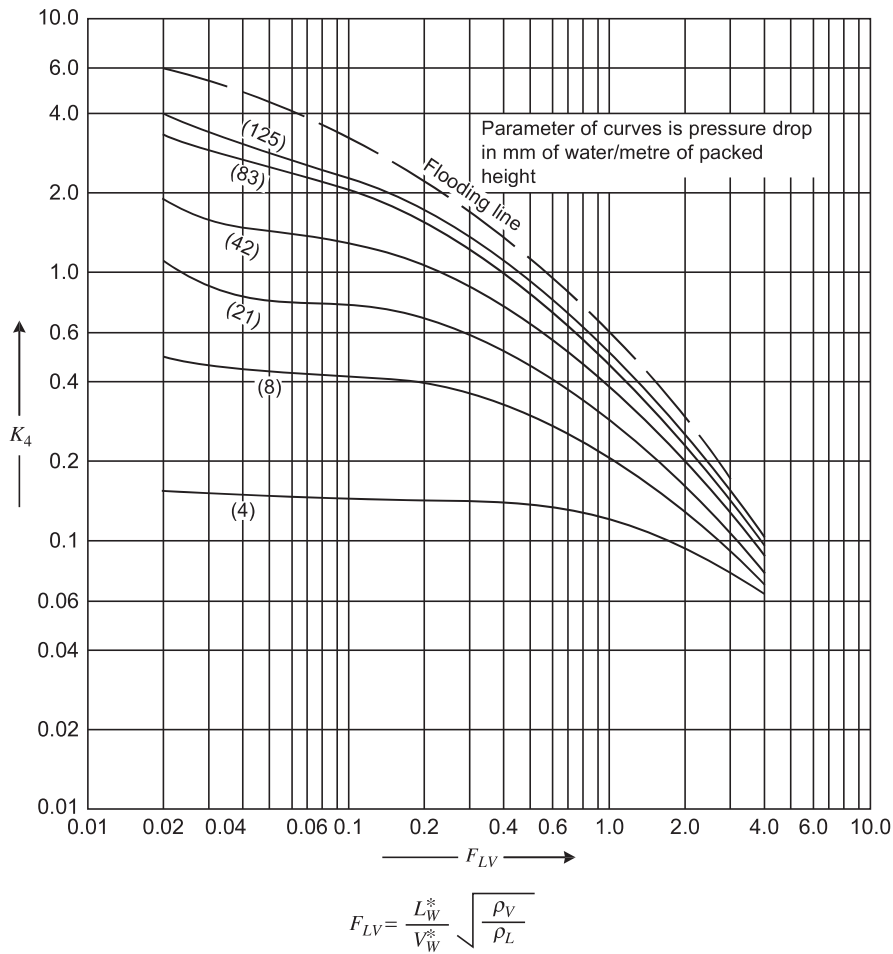


**Figure 3.3: Generalized pressure drop correlation (Towler and Sinnott, 1969)**

$K_4$  was used to calculate the gas mass flow rate per cross sectional area  $V_w$  in equation 3.19 (Sinnott, 2005).

$$K_4 = \frac{13.1 * V_w^2 * F_p * (\mu_L - \rho_L)^{0.1}}{\rho_V(\rho_L - \rho_V)} \quad 3.19$$

$F_p$	Packing factor ( $m^{-1}$ )
$V_w$	Gas mass flowrate per cross sectional area ( $kg/m^2 \cdot s$ )
$\mu_L$	Viscosity of liquid (Pa. s)
$K_4$	Gas load parameter

From the gas mass flowrate of gas phase per cross-sectional area  $V_w$ , cross-sectional area and absorber and stripper diameters were calculated

**Table 3.9: Input parameter and scale-up calculation results**

Inputs		
	Absorber	Stripper
$\rho_V$ (kg/m <sup>3</sup> )	1.0171	1.055
L /G	1.748	6.335
$\rho_L$ (kg/m <sup>3</sup> )	938.47	906.26
Pressure drop (mm H <sub>2</sub> O/ m Packing)	42	42
$\mu_L$ (Pa.s)	0.001268	0.000403
$F_p$ (m <sup>-1</sup> )	78.74	168.2
Results		
$F_{LV}$	0.0575	0.216
$K_4$	1.53	1.00
Cross-sectional area (m <sup>2</sup> )	152.77	50.10
Packed column diameter (m)	13.95	7.90

Table 3.9 details the input parameters for scale-up calculation and the scale-up calculation results. The liquid and gas densities ( $\rho_L$  and  $\rho_V$ ), as well as L/G ratio, are needed to determine the flow parameter ( $F_{LV}$ ) based on equation 3.18 (see Page 68). These input specifications ( $\rho_L$ ,  $\rho_V$ , and L/G ratio) were obtained from the rate-based pilot scale PCC model developed in Aspen Plus<sup>®</sup>. The determined ( $F_{LV}$ ) is then used to obtain the gas load parameter ( $K_4$ ) using the GPDC chart (see Figure 3.2). Using equation 3.19, the gas mass flowrate per cross-sectional area ( $V_w$ ) was determined. The packing factor ( $F_p$ ) and viscosity of liquid ( $\mu_L$ ) for both columns were obtained from Sinnott, 2005 and the rate-based pilot scale PCC model developed in Aspen Plus<sup>®</sup> respectively.

The cross-sectional area as well as the diameter of each column at large was determined as follows:(Sinnott, 2005)

Cross-sectional area of packed column = flue gas mass flow rate /  $V_w$

Area= (3.14/4)\* (diameter)<sup>2</sup>.

the absorber cross-sectional area is larger than that of the stripper. This is due to the absorber receiving a greater volume of flue gas than the stripper. Hence, the absorber diameter is larger than the stripper diameter.

### 3.5 Simulation of solvent-based PCC model at commercial scale and technical evaluation

#### 3.5.1 Commercial scale PCC simulation

Based on the pilot plant model, the PCC simulation was scaled up to 250 MWe of CCGT. The operating conditions for the commercial scale PCC were similar to those at the pilot scale. The simulation is deployed on Aspen Plus®. Table 3.10 shows the specifications for absorbers and strippers at commercial scale. While the flue gas flow rate and MEA solvent specifications, including mass flow rate, solvent weight, solvent molecular weight, and CO<sub>2</sub> capture level, are shown in Table 3.10.

**Table 3.10: Absorber and stripper input specification at commercial scale**

Specification	Absorber	Stripper
Number of Column	1	1
Packing material	IMTP #40	Flexipac 1Y
Pressure (kPa)	101	162
Diameter (m)	13.95	7.9
Packing height (m)	30	30

**Table 3.11: Flue gas and lean solvents specifications at commercial scale**

Conditions	Value
Mass flow rate of flue gas (kg/s)	356
Mass fraction of CO <sub>2</sub> in flue gas	0.076
CO <sub>2</sub> captured percentage (%)	90
Absorption capacity (mol CO <sub>2</sub> /mol MEA)	0.18
Molecular weight of MEA solvent (g/mol)	61.08
Mass fraction of MEA in solution	0.30
Calculated Solvent mass flow rate (kg/s)	622.43

#### 3.5.2 Technical evaluation

To determine the optimal value of the independent variable CO<sub>2</sub> lean loading on the dependent variables: L/G ratio and specific re-boiler duty, a technical evaluation is required. It was noted that the re-boiler duty required for solvent regeneration contributes to the energy penalty in the entire process. The technical evaluation was conducted by sensitivity analysis between the independent and dependent variables at a 90% capture level, as shown in Table 3.18. It was cleared from Figure 3.4 that there was an optimal

lean loading that has the lowest specific re-boiler duty. The trend was linear for the independent variable before the lowest re-boiler duty. After the optimal CO<sub>2</sub> lean loading, the trend becomes exponential. The L/G ratio, on the other hand, increases linearly until it reaches the lowest re-boiler duty.

The re-boiler duty decreases noticeably as CO<sub>2</sub> lean loading increases because it means less CO<sub>2</sub> is stripped, where it requires low steam for solvent regeneration. Hence, the specific re-boiler duty decreases as well. The CO<sub>2</sub> lean loading chosen is 0.19-0.33 mol CO<sub>2</sub>/mol MEA, where is the default CO<sub>2</sub> lean loading in literature, and the re-boiler duty range is 171.4-102.35 MW, which was obtained for this CO<sub>2</sub> lean loading range. This range decreases linearly until the optimal value of 0.29 mol CO<sub>2</sub>/mol MEA CO<sub>2</sub> lean loading while re-boiler duty is 4.137 GJ/tonne CO<sub>2</sub> is reached. Another issue observed is that with increasing CO<sub>2</sub> lean loading, the condenser temperature reduces, although the condenser duty is fixed until the optimal CO<sub>2</sub> lean loading. Because of the lower re-boiler duty and the lower reflux ratio, the condenser duty decreases to provide a converged stripper. The relationship between CO<sub>2</sub> lean loading and dependent variables (specific re-boiler duty and liquid-to-gas ratio (L/G) kg/kg) is shown in Table 3.12,

**Table 3.12: Technical evaluation results of commercial PCC model using MEA**

CO <sub>2</sub> lean loading (mol CO <sub>2</sub> /mol MEA)	Lean solvent Flowrate (kg/s)	L/G ratio (kg/kg)	Re-boiler duty (MW)	Specific re-boiler duty (GJ/tonne CO <sub>2</sub> )
0.19	378.47	1.06	171.42	7.033
0.20	391.53	1.10	157.05	6.493
0.21	405.52	1.14	144.61	5.951
0.22	420.53	1.18	133.83	5.541
0.23	436.67	1.23	124.51	5.117
0.24	454.08	1.28	116.50	4.836
0.25	472.93	1.33	109.76	4.505
0.26	493.40	1.39	104.36	4.350
0.27	515.75	1.45	102.67	4.213
0.28	540.29	1.52	100.87	4.140
0.29	567.49	1.59	100.79	4.137
0.30	597.80	1.68	100.97	4.144

0.31	632.13	1.78	101.22	4.155
0.32	671.72	1.89	101.62	4.172
0.33	719.09	2.02	102.35	4.201

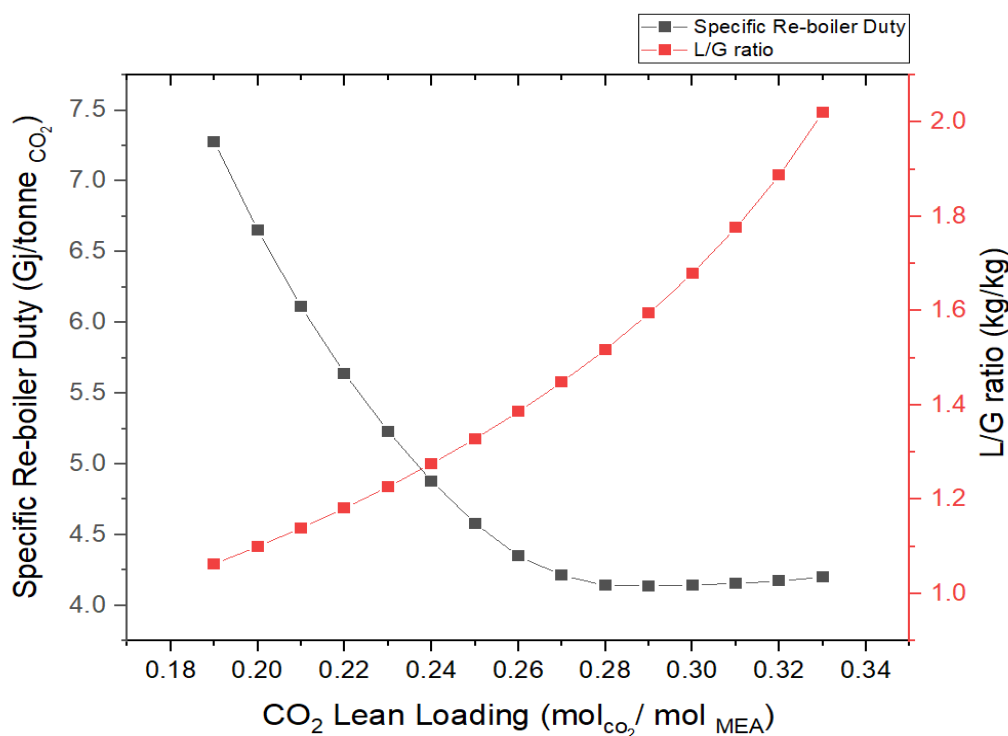


**Figure 3.4: Technical evaluation plot showing the correlation between L/G ratio with specific re-boiler duty and CO<sub>2</sub> lean loading**

In Figure 3.4 low CO<sub>2</sub> lean loading means low solvent flowrate require to provide 90% CO<sub>2</sub> capture level. However, high re-boiler duty is needed to strip the CO<sub>2</sub> rich solvent liquid to match the desired CO<sub>2</sub> lean loading. Furthermore, increased CO<sub>2</sub> lean loading expresses more CO<sub>2</sub> in rich solvent, resulting in lower re-boiler duty, lower absorption capacity, and an increase in the L/G ratio. Compared to previous study (Canepa et al., 2013). The optimal CO<sub>2</sub> lean Loading was 0.3 (mol CO<sub>2</sub>/ mol<sub>MEA</sub>), providing a specific re-boiler duty of 4.97 (GJ/tonne CO<sub>2</sub> and a 2.02 L/G ratio (kg/kg), which was the lowest value for energy consumption. Moreover, the re-boiler duty was 121 MW at the optimal CO<sub>2</sub> lean loading, while in this study the re-boiler duty is 100.8 MW, which is lower than Canepa *et al.*, (2013). Hence, lower energy consumption, which is strongly connected to the stripper, and lower capital and operating costs, which will be discussed in section 3.6.

### 3.6 Economic evaluation of commercial solvent-based PCC model using MEA

To select the proper case for dynamic analysis for the whole process, economic evaluation is required, which is conducted in the Aspen Plus economic analyser<sup>®</sup>.

An economic evaluation is performed to provide full detail about the entire PCC process, discussing the cost for each piece of equipment at different CO<sub>2</sub> lean loadings, in order to analyse the operating and capital cost per tonne CO<sub>2</sub>. The cost breakdown was taken from the previous study (Akinola *et al.*, 2019). The cost breakdown included in this procedure is shown in Table 3.13. The percentage of each cost is considered for annualised capital and operating costs. MEA cost and water, they are assumed to be 0.925 £/kg and 0.00037 £/kg, respectively (Karimi *et al.*, 2011). The cost breakdown involves the total capital cost (TCC) including direct cost, indirect cost, working capital cost, start-up cost, initial solvent cost which is illustrated in Table 3.13. Total operating cost (TOC) including variable and fixed operating cost breakdowns.

**Table 3.13: Total capital cost breakdown for economic evaluation of PCC model using MEA**

Total Capital Cost Breakdown	Percentage of cost
Direct Cost	
Installed Cost	10% of Equipment Cost
Instrumentation and Control	20% of Equipment Cost
Pipe	30% of Equipment Cost
Electrical cost	5% of Equipment Cost
Building and Building Service	10% of Equipment Cost
Yard Improve	10% of Equipment Cost
Land	5% of Equipment Cost
Miscellaneous	2% of Equipment Cost
Indirect Cost	
Engineering and Supervision	15% of Direct Cost
Contingency	11% of Direct Cost
Procurement cost	2% of Direct Cost
Total Capital cost	

Fixed Capital Cost	Direct and Indirect Cost
Start-up Cost	1% of Fixed Capital Cost
Working Capital Cost	15% of Fixed Capital Cost
Initial Solvent Cost	Solvent flowrate* Cost
Total Operating Cost Breakdown (VOC+FOC)	
Variable Operating Cost	
Cooling Water Utility (£/GJ)	0.157
Steam Utility Cost (£/GJ)	1.63
Electricity Utility Cost (£/kWhr)	0.057
Make-Up of MEA Cost (£/kg)	0.925
Make-Up of Water Cost (£/kg)	0.00037
Miscellaneous Operating Cost	2% of Variable Operating Cost
Fixed Operating Cost	
Admin Cost	15% of Operating Labour
Insurance Cost	1% of Fixed Capital Cost
Local Tax	1% of Fixed Capital Cost
Operating Labour	26.64£ per hr
Lab Cost	20% of Operating Labour
R and D Costs	5% of Operating Cost
Maintenance	3% of Fixed Capital Cost
Supervision	20% of Operating Labour
Distribution and Marketing	0.5% of Operating Cost
Operating supplies	15% of Maintenance
Plant Overheads	50% of Operating Labour

From capital cost and operating cost breakdowns, the annualised capital cost is calculated using equation 3.20,3.21:

$$ACC = \frac{TCC}{((1+r)^n - 1)/r(1+r)^n} \quad 3.20$$

$$ATC = OC + ACC \quad 3.21$$

Where:

ACC

Annualised Capital Cost



---

TCC	Total Capital Cost
ATC	Annualised total cost
OC	Operating cost
r	Project Lifetime
n	Project Interest

The project lifetime is assumed to be 20 years with an interest rate of 10%. The annualised capital cost is calculated at different CO<sub>2</sub> lean loadings ranged from 0.19-0.33 mol<sub>CO<sub>2</sub></sub>/mol<sub>MEA</sub>. It is noticed from the Figure 3.5 that the trend of the annualised Capital Cost with increasing CO<sub>2</sub> lean loading reduces from 3.1 (M£/Year) to reach the lowest cost of 1.36 (M£/ Year) at 0.28 CO<sub>2</sub> lean loading, then the Cost started to be increased because the change in re-boiler duty. The annualised operating cost, on the other hand, is between 19.5 million pounds per year at 0.19 CO<sub>2</sub> lean loading and 15.3 million pounds per year at the optimal CO<sub>2</sub> lean loading of 0.28 mol CO<sub>2</sub>/mol MEA. Moreover, in Figure 3.5, The fluctuation was caused by an increase in condenser duty at 0.25 CO<sub>2</sub> lean loading in the stripper, which raises the annualised total cost, which equals the sum of annualised operating and capital costs. After 0.28 CO<sub>2</sub> lean loading, which is the optimal value where it has the lowest annualised capital cost because it lowers the operating cost because of lower re-boiler duty , the total cost rises as the lean loading increases.

Annualised total cost = annualised operating cost + annualised capital cost.

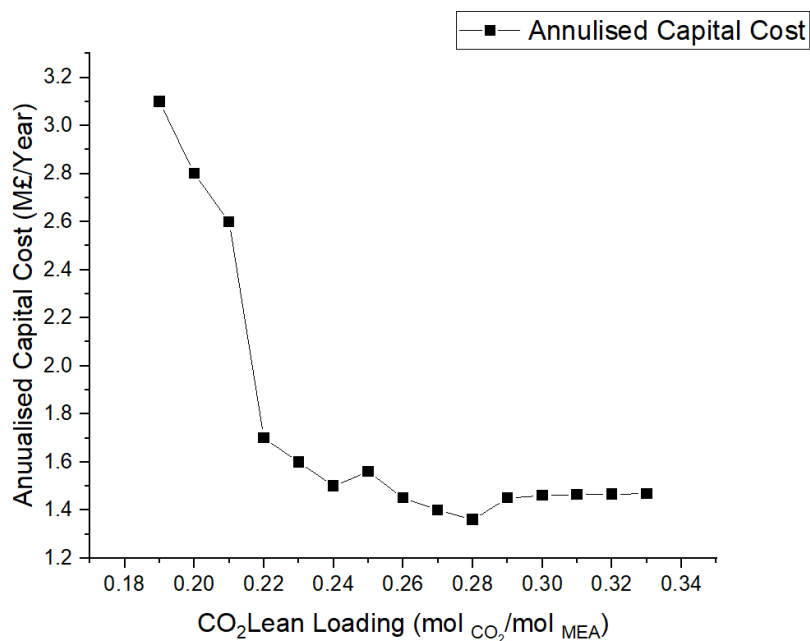


**Figure 3.5: Annualised capital cost correlation with changing CO<sub>2</sub> lean loading**

In terms of annualised total cost, the cost ranges from 22.6 (M£/Year) at 0.19 CO<sub>2</sub> lean loading to 16.53 (M£/Year) at 0.28 mol CO<sub>2</sub>/mol MEA. At 0.33 CO<sub>2</sub> lean loading, the cost increases to 18 M£/Year. In previous study (Otitoju *et al.*, 2021), the annualised total cost for 30 wt.% MEA at the optimal CO<sub>2</sub> lean loading was 58.5 M£/year which means a lower cost in the current study resulting in a lower energy penalty as shown in Figure 3.6

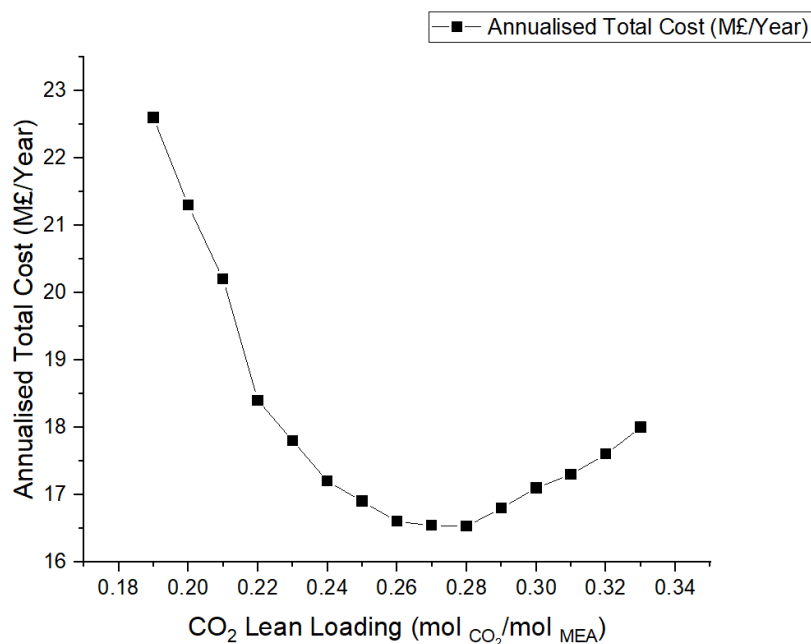


**Figure 3.6: Annualised total cost correlation with changing CO<sub>2</sub> lean loading**

The total cost per tonne CO<sub>2</sub> is considered to analyse cost regarding how much CO<sub>2</sub> captured from the top of stripper at different CO<sub>2</sub> lean loading ranged from 29.4 £/tonne CO<sub>2</sub> to 21.5 £/tonne CO<sub>2</sub> at the optimal CO<sub>2</sub> lean loading as shown in Figure 3.7. At 0.28 CO<sub>2</sub> lean loading, the total cost is 21 £/tonne CO<sub>2</sub> as illustrated in the Figure 3.7. on the other hand, Otitoju et al.,(2021) estimated the total cost of 30 wt.% MEA at around 80.9 M£/tonne CO<sub>2</sub>

It is indicated from the technical and economic evaluations that the optimal CO<sub>2</sub> lean loading 0.28 is the more effective CO<sub>2</sub> lean loading for 30 wt.% MEA regarding lowest energy consumption and total operating and capital cost per tonne CO<sub>2</sub>. Solvent-based PCC model at 0.29 CO<sub>2</sub> lean loading is selected for dynamic performance analysis because it has the lowest specific re-boiler duty, using Aspen Dynamics®.

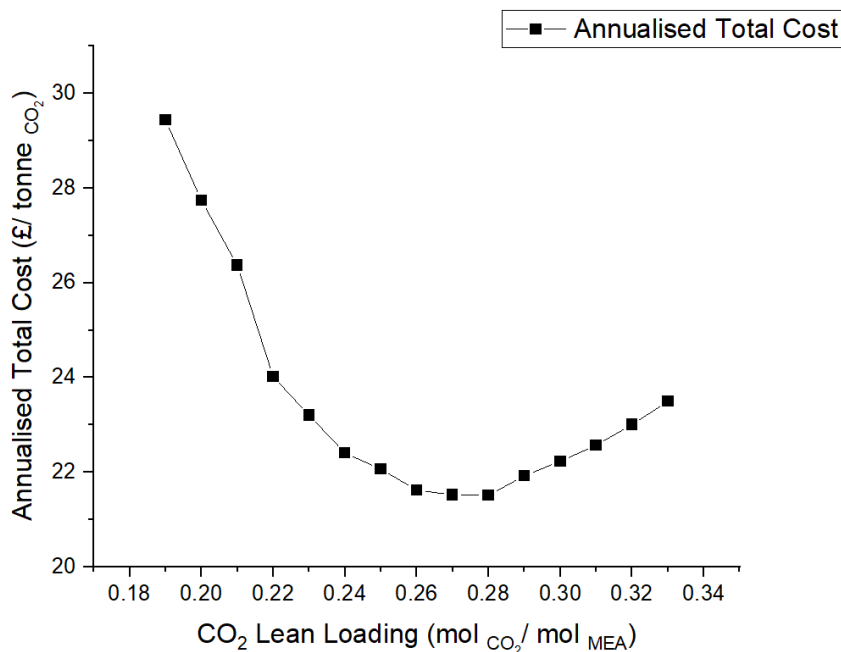
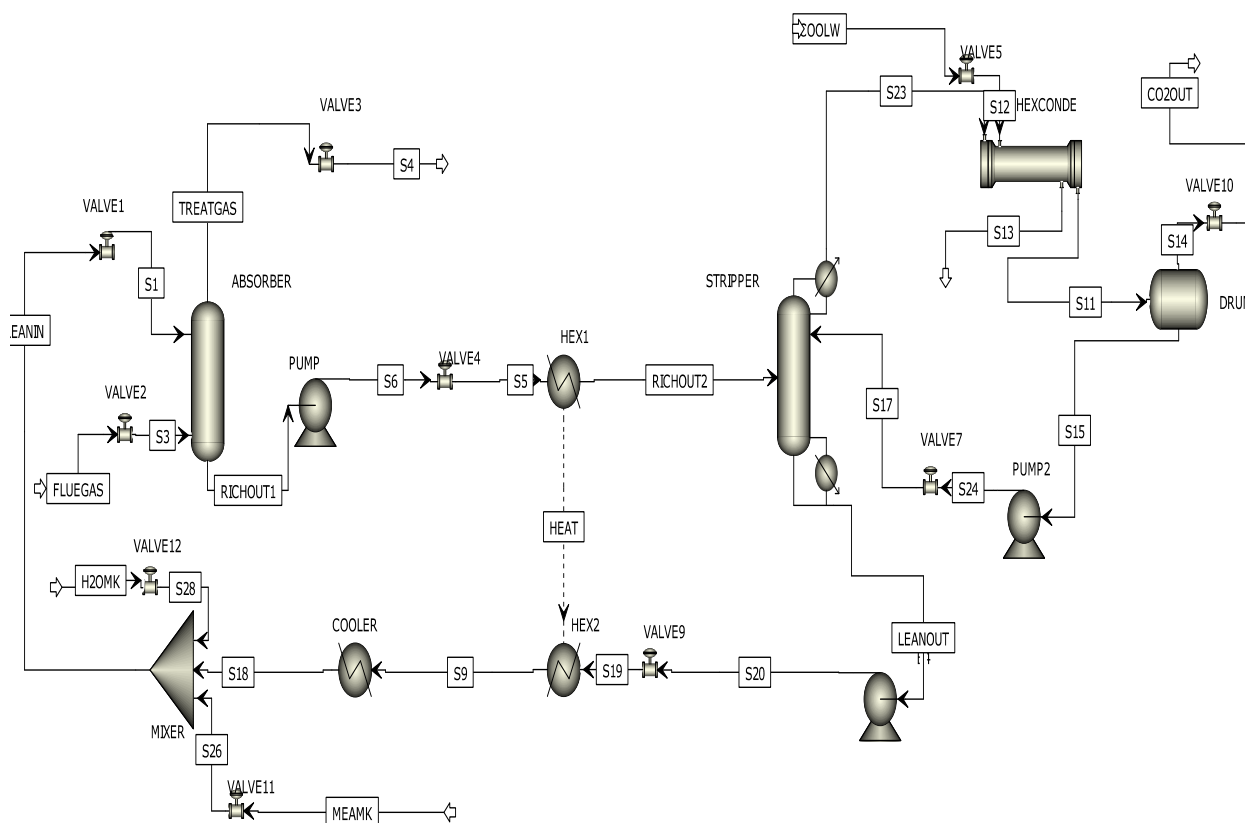


Figure 3.7: Annualised total cost per tonne CO<sub>2</sub> correlation with changing CO<sub>2</sub> lean loading

### 3.7 Dynamic modelling of commercial scale solvent-based PCC model using MEA

This section explains the dynamic simulation analysis using MEA as a solvent for commercial scale solvent-based PCC. Moreover, control structure and design, which are performed based on open loop analysis, The base case model is selected based on the economic evaluation in Section 3.6. This case study has the lowest annual total capital and operating costs. It is the commercial scale of the validated PCC model against SRP research pilot plant data. The flowsheet of the PCC model is shown in Figure 3.8.



**Figure 3.8: PCC commercial model flowsheet with valves and external condenser using MEA**

To conduct a dynamic model of commercial PCC, some equipment are added to stabilise the transient behaviour in Aspen Plus® and to monitor the water balance in the entire process, which might have a negative impact on packed bed flooding, including an absorber sump, stripper sump, an external condenser, including a heat exchanger and a reflux drum, and a buffer tank for water and solvent make-up to compensate for the loss in entire process.

For the sump, reflux drum, and buffer tank, the size should be estimated before exporting the steady-state model to Aspen Dynamics®. The calculations are conducted based on the flowrate at a steady-state. Table 3.14 shows the base operating conditions for the commercial PCC model, which are used as the setpoint for the transient behavior.

**Table 3.14: Base case operating conditions of absorber for commercial PCC model using MEA**

Parameter	Value
Absorber	
Flue gas flowrate (kg/s)	356

Lean solvent flowrate (kg/s)	540.292
Absorber diameter (m)	14
Packing height(m)	30
Operating pressure(N/m <sup>2</sup> )	97000
Absorber pressure drop(bar)	0.1
Packing material	IMTP#40
Number of stages	20
Sump level(m)	0.496
Sump diameter(m)	14
CO <sub>2</sub> capture level (%)	90
Model type	Equilibrium-based model

The stripper specification with external condenser including heat exchanger, reflux drum ,and buffer tank is given in Table 3.15:

- Operating pressure was taken from rate-based model, where absorber is operated at atmospheric pressure to reduce the solvent degradation.
- Number of stages: It is estimated based on the CO<sub>2</sub> composition profile in liquid phase. It is specified when there is equilibrium transfer in its composition.
- CO<sub>2</sub> capture level: it was specified to be 90 % to have tradeoff between profit and efficiency.
- Sump diameter: It was included in the packed column, where it assumed to be the same absorber diameter.
- Sump level: It was assumed by taken the flowrate of the packed column last stage and assume 10 min hold up time residence to fill the whole packed column.
- Model type: it is an equilibrium-based model to be prepared for Aspen Dynamics because this software does not support kinetic reactions.

**Table 3.15: Base case operating conditions of stripper for commercial PCC model using MEA**

Parameter	Value
Packing height(m)	30
Stripper diameter(m)	7.9
Operating pressure(N/m <sup>2</sup> )	162090
Stripper pressure drop	0.1
Number of stages	20

Model type	Equilibrium-based model
Packing material	FLEXIPAC 1Y
Re-boiler duty (MW)	100.87
Re-boiler temperature(K)	388.229
Condenser Temperature(K)	363.65
Reflux drum level(m)	0.9
Sump level(m)	0.447
Sump diameter(m)	8.2
Buffer tank level(m)	11.232
Buffer tank diameter(m)	5.76

### 3.7.1 Dynamic considerations

This consideration is essential before exporting the entire process from Aspen Plus® to Aspen Dynamics®. Some blocks, such as valves, a packed column sump, and an external condenser, are added to ensure that the process is fully pressure driven. Before dynamic analysis performance, several considerations were made, such as using an equilibrium-based model because Aspen Dynamics® does not support a rate-based model. Hence, stage efficiency is added to the equilibrium-based model to meet the target CO<sub>2</sub> capture level of approximately 90%. Additionally, valve addition in each stream is required in order to accurately configure the fully pressure-driven system without any fatal errors or warnings. The acceptable pressure drop range between upstream and downstream valves should be 2-4 atm (Luyben, 2016). Hence, the accurate pressure drop will enhance the level of controllability in the entire process. The valve design for liquid and gas phases has different procedures, which is discussed in the following paragraph. In the case of a liquid stream, valve design is used to specify the required pressure drop needed to avoid choking and cavitation.

Choking in the liquid phase, on the other hand, occurs for two reasons: the presence of vapour produced by cavitation or flashing increases. Hence, the specific volume rises while the pressure decreases until the sonic value is obtained. Cavitation is defined as the occurrence of vapour bubbles, which form when the pressure in the liquid decreases below the vapour pressure. As a result, noise, vibration, and erosion damage will occur. Flashing is defined as the presence of vapour bubbles generated at the vena cava that contract without collapsing when the outlet pressure is lower than the vapour pressure,

resulting in high extreme velocities and the possibility of erosion and pipe damage. Regarding the flow pattern, which is assumed to be turbulent flow, this expression is applied to calculate the CV regarding the flow rate in each stream using equation 3.22. In addition, the choking and cavitation are considered in this calculation (Baumann, 2009).

$$CV = flow \sqrt{\frac{SG}{\Delta p}} \quad 3.22$$

Where CV is flow capacity calculated based on the flowrate, SG is the specific gravity at flowing temperature,  $\Delta P$  is the pressure drop between valve streams (inlet and outlet). In Aspen Plus®, the valve specification is added after calculating the flow capacity CV, pressure drop ratio factor  $X_t$ , and pressure recovery factor  $F_L$ . Pressure drop ratio factor  $X_t$  is estimated using equation 3.23:

$$X_t = \frac{P1 - P2}{P1} \quad 3.23$$

Where P1 is the valve's inlet pressure and P2 is its outlet pressure. This factor predicts the choking point when more pressure drops. It is calculated by valve geometry in accordance with  $F_L$ , depending on valve type but in this study the valve design in Aspen Plus was based on  $C_v$  calculations. In the case of pressure recovery factor  $F_L$ , it forecasts how pressure will be retrieved between the pressure vena contracta and the pressure outlet.

The capacity calculation is affected by the internal geometry, depending on the valve type, such as butterfly and ball valves, which have high pressure recovery. On the other hand, they have low vena contracta pressure. The globe valve has a lower recovery pressure at the same pressure compared to the former valves. Consequently, the former valves have a higher likelihood of choking or cavitation at lower pressure than globe valves (Towler and Sinnott, 1969). The estimation is the square root of the pressure drop ratio factor considering the pressure at the vena contracta, where it is assumed to be 1/3 of the inlet pressure.

In case of gas stream, the following formula is used, which is equation 3.24 to calculate the  $C_v$  because the gas phase is compressible compared to non-compressible fluid (Liquid) which is affecting by temperature shown as follow (Engineering world, 2018):

$$CV = Q_G \frac{\sqrt{SG \cdot T}}{816 \cdot P1} \quad 3.24$$



here  $Q_G$  is the gas volumetric flow rate (ft<sup>3</sup>/hr),  $S_G$  is the specific gravity of medium air at 70°F and 14.7 psia = 1,  $T$  is the absolute temperature (°R), and  $P_1$  is the inlet pressure (psi). This formula is constrained by critical flow, where the upstream pressure is higher than the double of the downstream pressure.

In the packed columns (absorber and stripper), equilibrium reactions are considered in dynamic simulation because Aspen Dynamics® does not support kinetic reactions. The absorber column has the same function as the commercial scale, while the stripper is modelled with an external condenser and internal re-boiler. When pressure checker is used, converting the normal RadFrac with an internal condenser and stripper results in fatal errors. This issue is figured out using RadFrac with an external condenser and re-boiler. This method enhances stripper convergence. So, the stripper is modelled with two heat exchangers, duplicating the function of the condenser and re-boilers in the normal RadFrac. The external condenser is modelled as a heat exchanger between cold water at specific operating conditions required to provide 10 MW condenser duty, where it is taken from pilot plant data as provided in equation 3.25, while re-boiler duty is calculated using equation 3.26 (Harun et al., 2012)

$$\frac{dE_{Cond}}{dt} = F_{in}H_{in} - F_vH_v - F_LH_L - Q_{cond} \quad 3.25$$

$$\frac{dE_{reb}}{dt} = F_{in}H_{in} - F_vH_v - F_LH_L + Q_{reb} \quad 3.26$$

$E_{cond}$  and  $E_{reb}$  defined as the accumulated energy in both the condenser and the stripper. In the case of a condenser,  $F_{in}$  is the inlet flowrate, while  $F_v$  and  $F_L$  express the vapour and liquid flowrates, respectively.  $Q_{cond}$  stands for heat duty required in the condenser.  $H_{in}$  and  $H_v$ , on the other hand, represent the enthalpies of inlet and outlet vapour, respectively. In a re-boiler,  $F_{in}$  stands for the inlet stream flowrate for the liquid phase, while  $F_L$  presents the outlet stream, which is the solvent lean out flowrate. The enthalpies  $H_{in}$ ,  $H_v$ ,  $H_L$  represent the liquid stream inlet, outlet vapour, and outlet liquid, respectively.

The heat exchanger is modelled as a shell and tube, and its function is to transfer the heat required from a lean solvent flow rate to a rich solvent flow rate. Fluid temperature was used to determine fluid allocation, with lean solvent solution leaving the stripper having a higher temperature than rich solvent solution leaving the absorber. As a result, the rich solvent solution flows in the shell while the lean solvent flow rate is allocated in the tube.

This method enhances tube cleaning in cases of fouling and reduces corrosion. The energy balance for single tube and shell (Incropera et al., 1996) are shown in equation 3.27, 3.28, respectively.

$$\frac{\partial T_{tube}}{\partial t} = \frac{-u_{tube}}{L} \frac{\partial T_{tube}}{\partial Z} + UT_{LM} \frac{\Pi D_{tube}}{\rho_{tube} A_{tube} C_{p,tube}} \quad 3.27$$

$$\frac{\partial T_{shell}}{\partial t} = \frac{-u_{shell}}{L} \frac{\partial T_{shell}}{\partial Z} - UT_{LM} \frac{n_{tube}(\Pi D_{tube})}{\rho_{shell} A_{shell} C_{p,shell}} \quad 3.28$$

For the column sump diameter and height, the liquid volumetric flowrate was considered from the commercial scale case. The accurate information will provide reliable dynamic analysis for the entire process. Dynamic information should be filled in before exporting the process from steady-state to dynamics. The hold up residence time is assumed to be 10 minutes to calculate the volume of the column, where is the acceptable range is between 5-10 min (Towler and Ray Sinnott, 1969). The sump diameter is assumed to be equal to the column diameter for both columns because it included in the packed column while the sump height is estimated for both columns, by multiplying the volumetric flowrate with 10 min liquid hold up as shown in Table 3.16.

**Table 3.16: Sump input value for absorber and stripper**

Specification	Absorber	Stripper
Sump diameter (m)	13.95	7.90
Sump height (m)	4.00	6.30

With the specifications, the commercial-scale equilibrium PCC model is ready for Aspen Dynamics® to conduct the open loop analysis required before control structure development and controller design.

### 3.7.2 Open loop analysis

Open loop analysis is conducted to provide the relationship between the manipulated variables and the controlled variables because open loop analysis is selected to determine how the pair loop should be selected between variables in the control structure. The response of an open loop is aimed at offering knowledge of the non-linear behaviour of controlled variables during dynamic conditions such as CO<sub>2</sub> capture level, re-boiler temperature in case of disturbance rejection (flue gas flowrate) and manipulated variable step change (lean solvent flowrate and re-boiler duty). The findings of the open loop analysis response are discussed as follows:

### 3.7.2.1 Flue gas flowrate step change

The scenario represents the disturbance step change, which is defined as flue gas flowrate in the commercial PCC model, to analyse its effect on the controlled variables: CO<sub>2</sub> capture level and re-boiler temperature. The base operating condition is 356 kg/s of flue gas flowrate. Aspen Dynamics® was used to perform the flue gas flowrate step change (5% and 10%) analysis. Figure 3.9 and Figure 3.10 A and B, demonstrate the correlations between flue gas flowrate and controlled variables (CO<sub>2</sub> capture level and re-boiler temperature). The dynamic performance of this process includes the same flow and heat generated at steady-state but with variable accumulation, where there is change in the variable with time at transient behaviour.

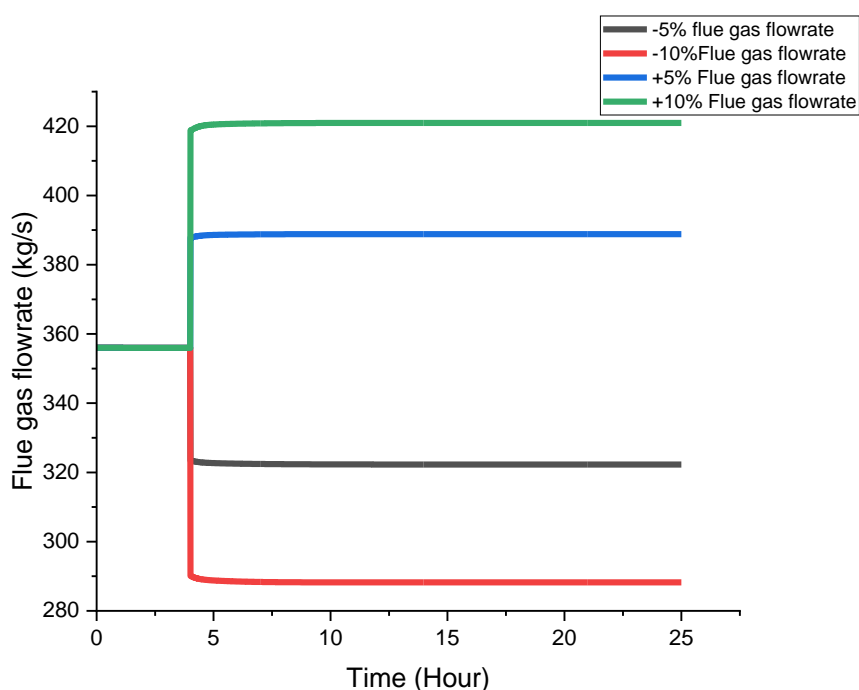
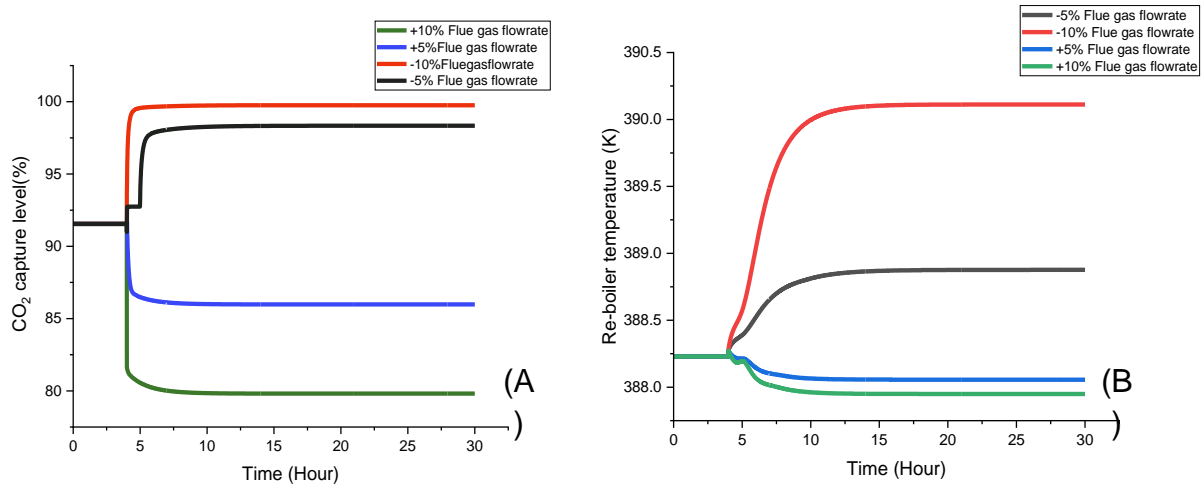


Figure 3.9: Flue gas flowrate step change



**Figure 3.10: (A) CO<sub>2</sub> capture level correlation on changing flue gas flowrate. (B) Re-boiler temperature correlation on changing flue gas flowrate**

It is noted from Figure 3.10 A and B that the controlled variables CO<sub>2</sub> capture level and reactor temperature have an inverse correlation with increasing (or decreasing) flue gas flowrate. The range of CO<sub>2</sub> capture levels is between 99.9 and 79% with a settling time of 5 hours, while the re-boiler temperature range is between 391.1 and 387.9K with a settling time of 11 hours. This step in Figure 3.10 (A), where is at -5% step change, might occur because the couple presence between flue gas flowrate and the amount of lean solvent in the case of flue gas step change due to the integration of this process, which need decoupling between the variables.

In addition, the effect of the flue gas step change is extremely strong on CO<sub>2</sub> capture level compared to the re-boiler temperature. The rich solvent temperature at the bottom of the absorber decreases as the flue gas flowrate increases (or decreases). This means that at a constant lean solvent flowrate and re-boiler duty, the reducing rich solvent temperature decreases (increases). Hence, an increase (or decrease) in the CO<sub>2</sub> lean loading occurs when the CO<sub>2</sub> content is increased (or decreased) in the lean solvent flow rate recycled to the absorber, resulting in a big difference between CO<sub>2</sub> rich loading and CO<sub>2</sub> lean loading at constant solvent circulation. This finding has a similar trend correlation as in Lawal et al.(2010). Also it is in agreement with Nittaya *et al.*(2014b).

The open loop gain, which is calculated by the ratio of change process variable to the change in manipulated variable and the time constant, which is calculated by specifying the time, where the process variables reach 63.2% of final value, are two characteristics

that must be calculated during the open loop process. For accuracy. Different step changes were conducted to obtain the average open loop and time constant. shows the estimated characteristics of CO<sub>2</sub> capture level and re-boiler temperature for the specific flue gas flow rate step change.

Table 3.17 shows the estimated characteristics of CO<sub>2</sub> capture level and re-boiler temperature for the specific flue gas flow rate step change.

**Table 3.17: Open loop characteristics for CO<sub>2</sub> capture level and re-boiler temperature**

CO <sub>2</sub> capture level		
Step change %	Open loop gain	Time constant (min)
5% flue gas flowrate	-0.172	12
-10% flue gas flowrate	-0.114	3.6
-5% flue gas flowrate	-0.198	66.6
+10% flue gas flowrate	-0.18	0.6
Average	-0.1666	20.7
Re-boiler temperature		
5% flue gas flowrate	-0.0052	150
-10% flue gas flowrate	-0.0265	166.2
-5% flue gas flowrate	-0.019	166.8
+10% flue gas flowrate	-0.0043	135
Average	-0.011	123.6

### 3.7.2.2 Lean solvent step change

This scenario depicts the effect of a step change in lean solvent flowrate on controlled variables in Figure 3.11. The controlled variables include CO<sub>2</sub> capture level and re-boiler temperature, as shown in Figures 3.12 A and B . The base operating condition is 540.292 kg/s, which results in a 91.547% CO<sub>2</sub> capture level. Moreover, the lean solvent step change has a similar percentage of flue gas step change (5% and 10%). Figures 3.12 A and B show the trend correlation of the controlled variables (CO<sub>2</sub> capture level and re-boiler temperature) in the case of a lean solvent step change. dynamically. It indicates that using a higher lean solvent flowrate results in a higher CO<sub>2</sub> capture level without a recycling loop, indicating a proportional correlation. Figure 3.12 A shows a small spike which might be because this integrated process, where decoupling is required to reduce

the effect of some parameters with each others. When the loop is recycled, the step change reduction in lean solvent increases CO<sub>2</sub> capture because the overall circulation rate of the solvent is decreased. Consequently, the driving force of solvent regeneration will be higher, which will reduce the re-boiler duty. The results were similar to the previous studies (Kvamsdal et al., 2009; Lawal et al., 2009; Nittaya et al., 2014a). Compared to the flue gas step change, the CO<sub>2</sub> capture level and re-boiler temperature settling time are, respectively, 8 and 7.5. The open loop gain and the time constant are two characteristics that must be calculated during the open loop process. Different step changes were conducted to obtain the average open loop and time constant. Table 3.18 shows the estimated open loop characteristics for the specific lean step change.

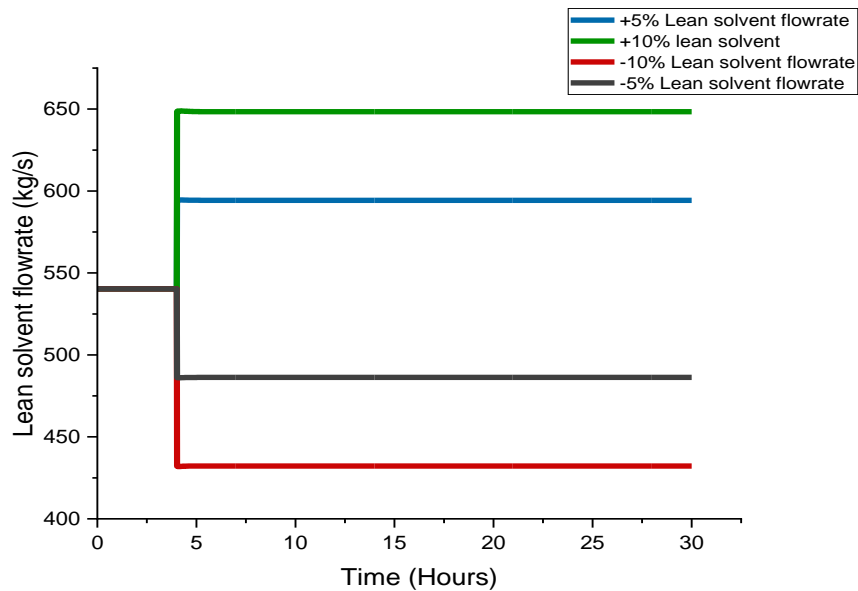
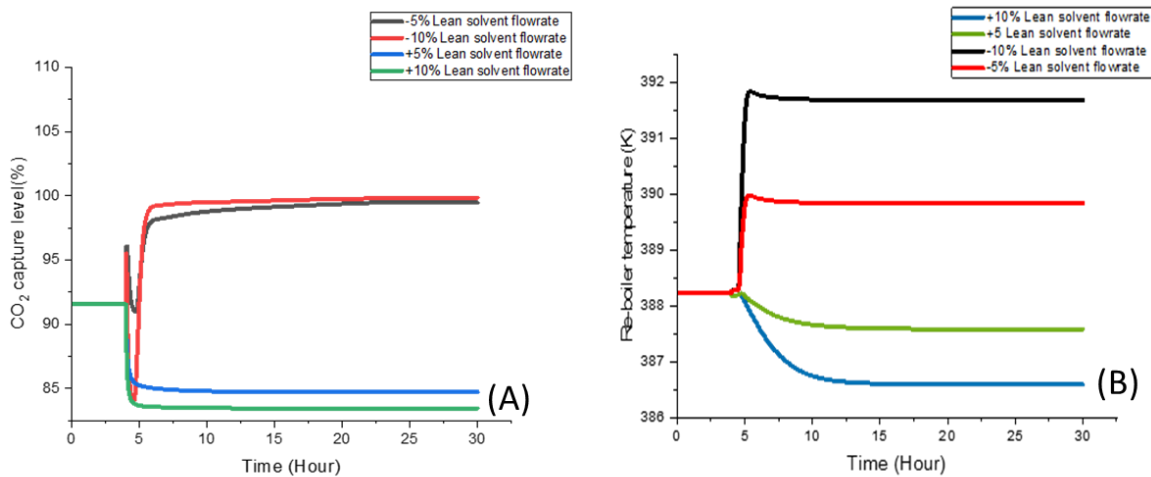


Figure 3.11: Lean solvent flowrate step change



**Figure 3.12: (A) CO<sub>2</sub> capture level correlation on changing lean solvent flowrate. (B) Re-boiler temperature correlation on changing lean solvent flowrate**

**Table 3.18: Open loop characteristics of CO<sub>2</sub> capture level and re-boiler temperature on changing lean solvent flowrate**

CO <sub>2</sub> capture level		
Step change %	Open loop gain	Time constant (min)
5% lean solvent flowrate	-0.126	3.6
-10% lean solvent flowrate	-0.0763	102
-5% lean solvent flowrate	-0.130	72.6
+10% lean solvent flowrate	-0.0748	5.4
Average	-0.102	45.9
Re-boiler temperature		
5% lean solvent flowrate	-0.012	162.6
-10% lean solvent flowrate	-0.0319	49.8
-5% lean solvent flowrate	-0.029	48
+10% lean solvent flowrate	-0.015	184.2
Average	-0.0176	88.92

### 3.7.2.3 Re-boiler duty step change

This scenario explores the significance of a re-boiler duty increase (decrease) step change, as shown in Figure 3.13. The controlled variables CO<sub>2</sub> capture level and re-boiler temperature are shown in Figures 3.14 and 3.15, respectively. It is clear from Figure 3.14 that increasing or decreasing re-boiler duty raises or reduces the CO<sub>2</sub> capture level because an increase in CO<sub>2</sub> lean loading from the stripper results in higher CO<sub>2</sub> lean loading, which means more CO<sub>2</sub> to be stripped in the stripper. Hence, more steam is required, resulting in an increase in the re-boiler. Hence, the absorption level is enhanced in the absorber. There is a small spike in CO<sub>2</sub> capture level due to controllability issue which might affect the transient performance of the entire process. The settling times of both controlled variables (CO<sub>2</sub> capture level and re-boiler temperature) were 11 and 12 hours, respectively. The open loop characteristics of a step change in re-boiler duty on CO<sub>2</sub> capture level and re-boiler temperature are shown in Table 3.19.

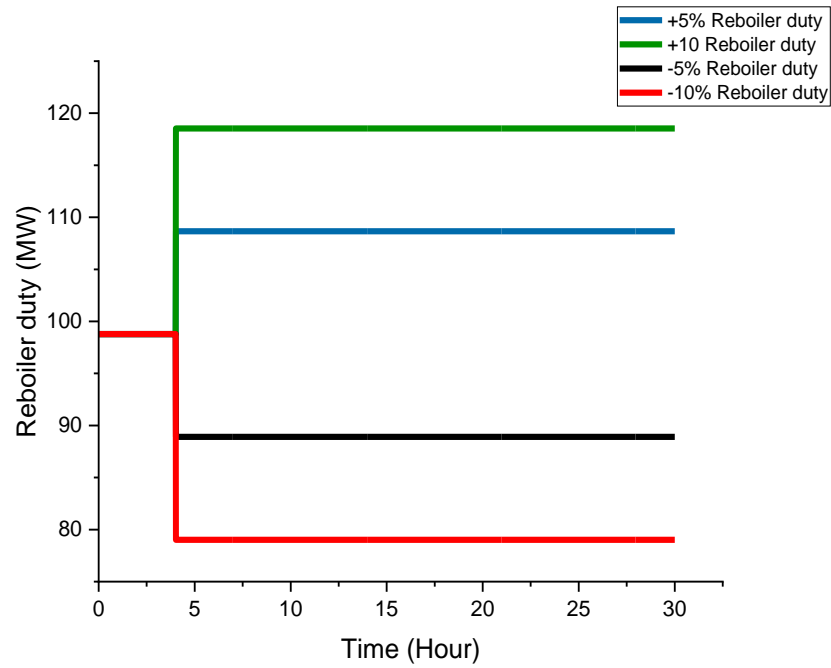


Figure 3.13: Re-boiler duty step change

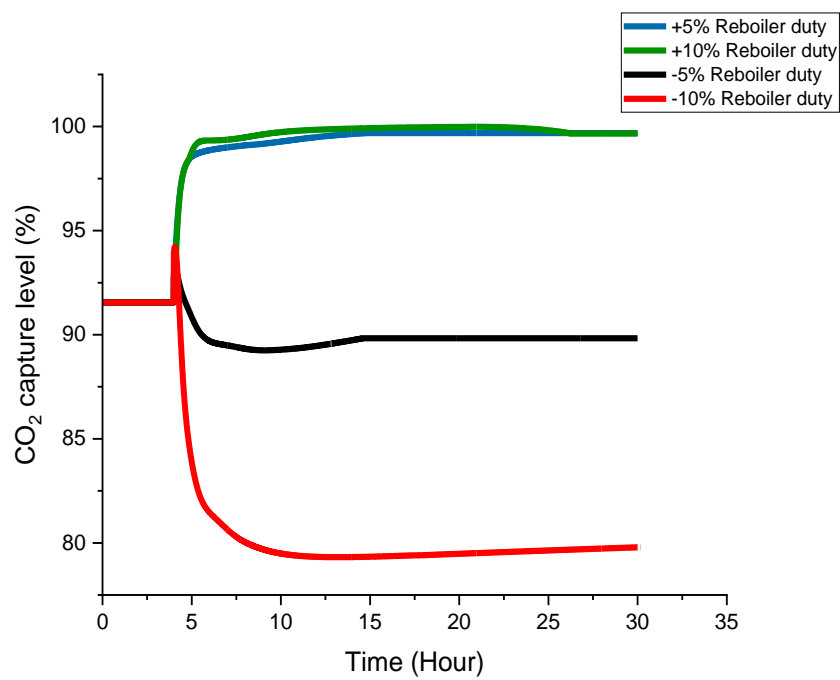


Figure 3.14: CO<sub>2</sub> capture level correlation on changing re-boiler duty



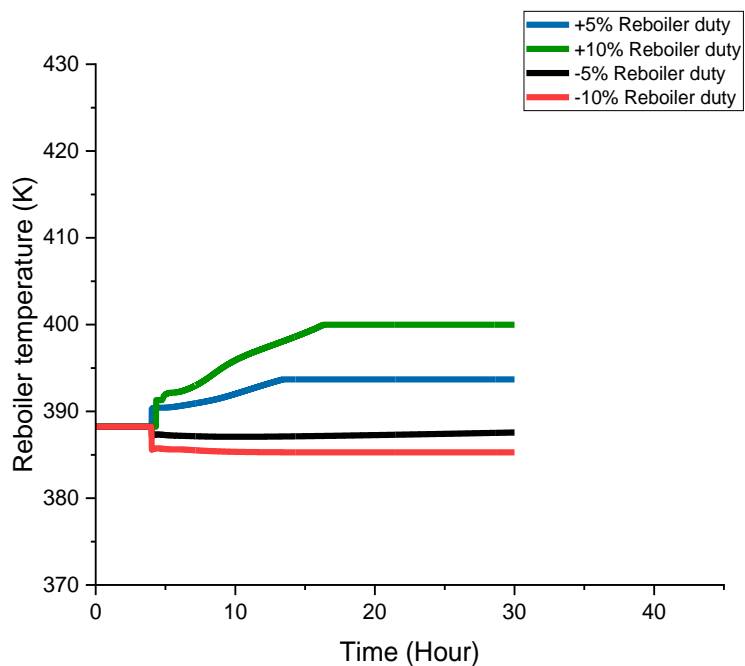


Figure 3.15: Re-boiler temperature correlation on changing re-boiler duty

Table 3.19: Open loop characteristic for CO<sub>2</sub> capture level and re-boiler temperature on changing re-boiler duty

CO <sub>2</sub> capture level		
Step change %	Open loop gain	Time constant(min)
5% Re-boiler duty	0.815	19.8
-10% Re-boiler duty	0.634	63.6
-5% Re-boiler duty	0.176	21.00
+10% Re-boiler duty	0.422	21.000
Average	0.512	25.080
Re-boiler temperature		
5% Re-boiler duty	0.555	309.000
-10% Re-boiler duty	0.149	0.600
-5% Re-boiler duty	0.094	22.800
+10% Re-boiler duty	0.590	343.200
Average	0.266	135.12

### 3.7.3 Control structure and design

Control structures are selected based on open loop analysis, where it is represented in Figure 3.16. For CO<sub>2</sub> capture, it was controlled by comparing the CO<sub>2</sub> mass flow in the flue gas stream entering the bottom of the absorber with the CO<sub>2</sub> mass flow in the vented gas stream leaving the top of the absorber and then adjusting the lean solvent flow rate. Condenser temperature was controlled by manipulating condenser heat duty. Also, the re-boiler temperature was controlled by adjusting the re-boiler heat duty in the stripper. Water makeup was paired with water mass fraction in lean solvent flowrate, which was treated as a variable to be manipulated.

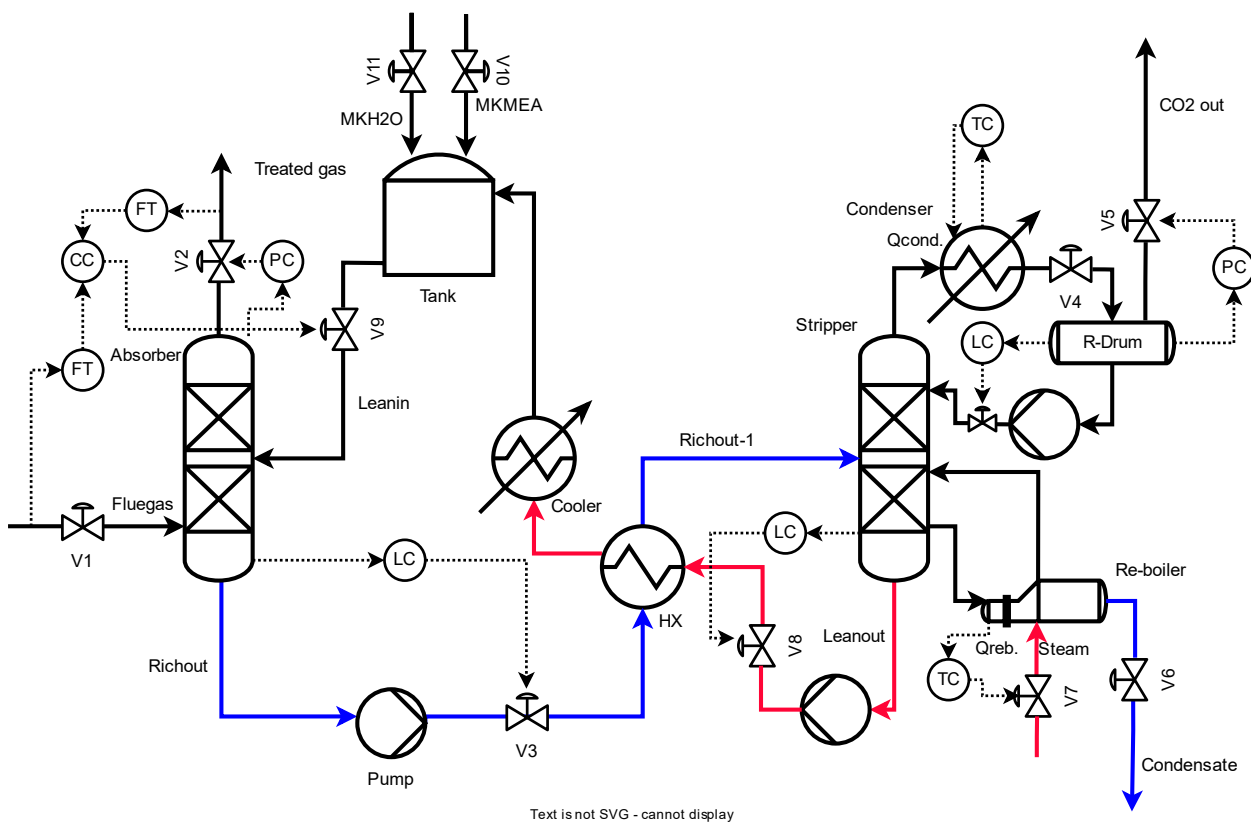


Figure 3.16: Flowsheet of PCC process with control structure

The absorber sump level was controlled by manipulating the valve (3) for packed column sump level. By adjusting the valve (8), the stripper sump level can be tightly controlled. The drum level is controlled by manipulating the valve located after the reflux drum. Liquid levels in the whole process should be tightly controlled to enhance the controllability of the CO<sub>2</sub> capture level and re-boiler temperature. The controller type used in this process is conventional control P/PI. P controller is proportional controller, where it is used to adjust the level because it is not important to have offset or not against the setpoint. On

the other hand, PI controller is defined as proportional integral, which is used to reduce the offset between process variable and the setpoint, such as re-boiler temperature and duty. On the other hand, CO<sub>2</sub> capture level, re-boiler temperature, and condenser temperature were controlled using a PI controller. The tuning parameters for the conventional controllers are given in Table 3.20. In this study, CO<sub>2</sub> capture level and re-boiler temperature were assessed dynamically against setpoint tracking and disturbance change, which are discussed in the next sections.

**Table 3.20: Tuning parameter for conventional controllers**

Manipulated variables	Controlled variables	Controller type	$\tau_i$ (min) time integral	K <sub>C</sub> gain	setpoint
Valve 3	Absorber sump Level (m)	Proportional	-	40	0.3
Valve 8	Stripper sump Level (m)	Proportional	-	80	0.2
Valve 12	Drum level (m)	Proportional	-	140	2
Lean solvent flowrate	CO <sub>2</sub> capture level (%)	Proportional/Integral	23	15	90
Re-boiler duty	Re-boiler temperature (K)	Proportional/Integral	55	10	389.229
Condenser duty	Condenser temperature(K)	Proportional/Integral	10	5	364.65

### 3.7.4 Process control evaluation

PCC process control evaluation was assessed using two criteria: disturbance rejection, which is expressed by flue gas flowrate change, which illustrates the fluctuation in the operation of power demand, and its response to reject the effect of flue gas flowrate fluctuation. The second evaluation is the CO<sub>2</sub> capture level setpoint step change.

#### 3.7.4.1 Flue gas step change

This scenario is expressed by a 10% step-change increase in flue gas flowrate where the setpoint is 356 kg/s to analyse its effect on CO<sub>2</sub> capture level and re-boiler temperature. Figures 3.18 and 3.19 show that a +10 flue gas step change reduces CO<sub>2</sub>

capture level and re-boiler temperature. It is difficult to monitor what is happening when there are setpoint tracking and disturbance rejection. This issue is part of the result limitation. Moreover, this process is integrated which means decoupling should be performed to enhance its controllability. However, re-boiler temperature had a spike due to valve opening for lean solvent flowrate to compensate the reduction in the CO<sub>2</sub> capture level. The reduction in re-boiler temperature was achieved by increasing the re-boiler duty required in the re-boiler. This dynamic performance has a similar trend as previous studies (Lawal, 2011; Nittaya, 2014). Additionally, it is observed that the dynamic performance on the commercial scale has similar behaviour to that on the pilot scale. Both variables have settling times of 8, 9, and 2 hours for CO<sub>2</sub> capture level and re-boiler temperature,

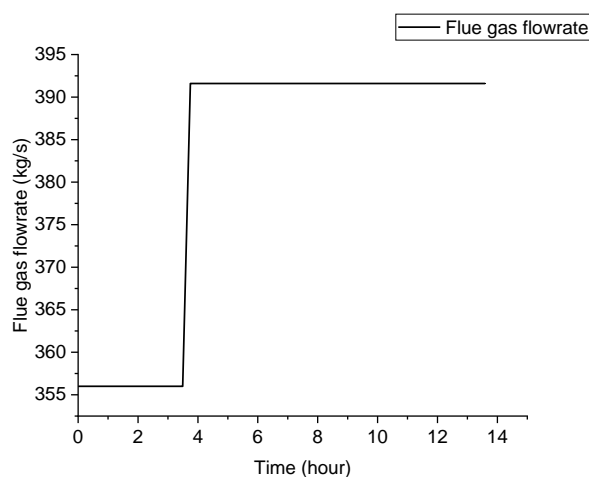


**Figure 3.17: Flue gas step change for PCC process using 30wt.% MEA**

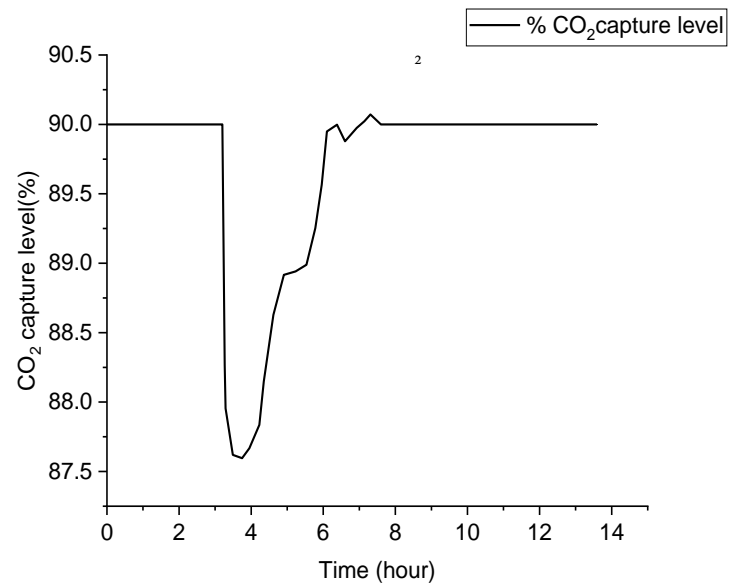


Figure 3.18: CO<sub>2</sub> capture level performance with 10% flue gas step change

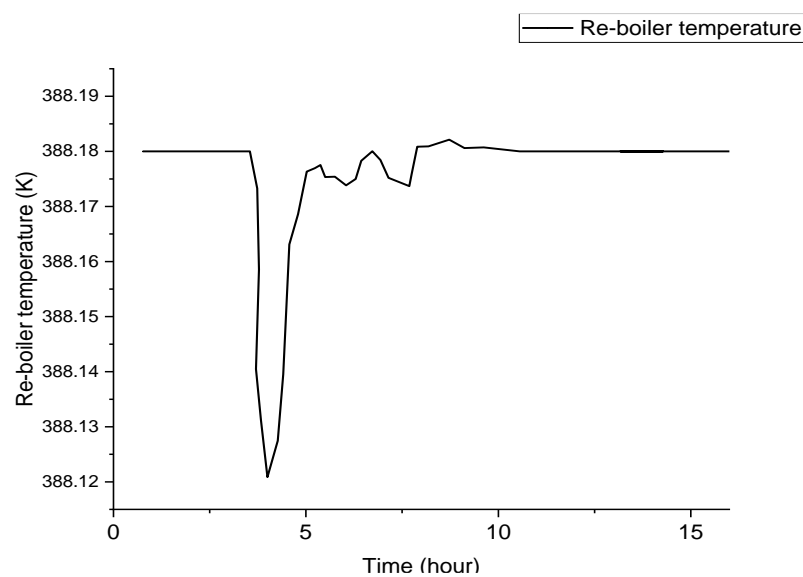


Figure 3.19: Re-boiler temperature performance with 10% flue gas step change

#### 3.7.4.2 CO<sub>2</sub> capture level step change

This scenario was evaluated by increasing the setpoint CO<sub>2</sub> capture level from 90 to 85% to investigate its impact on re-boiler duty in the stripper. Figure 3.21 depicts the trend of re-boiler duty with decreasing CO<sub>2</sub> capture level, where it decreases as the lean

solvent flow rate decreases. Consequently, a low vapour flow rate is provided in the stripper. Moreover, the settling time is long, at 10 hours to reach the first steady-state. It is clear from the Figure that there is fluctuation because it is difficult to monitor what is happening when there are setpoint tracking and disturbance rejection. This issue is part of the result limitation. Moreover, this process is integrated which means decoupling should be performed to enhance its controllability.

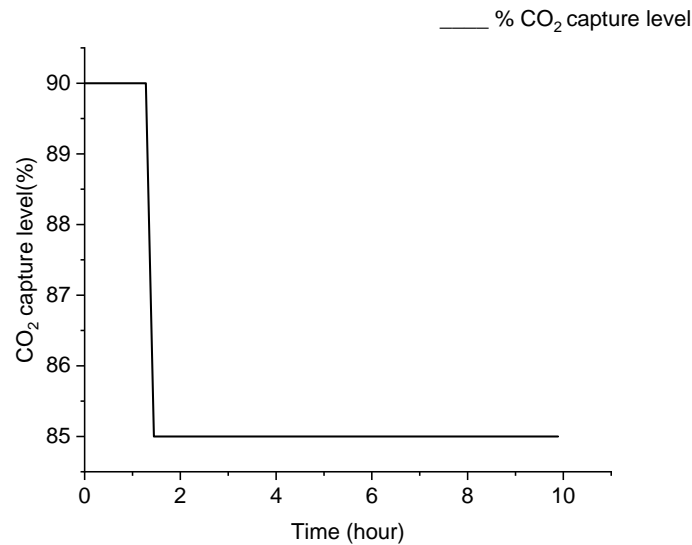


Figure 3.20: CO<sub>2</sub> capture level step change of -5.5%

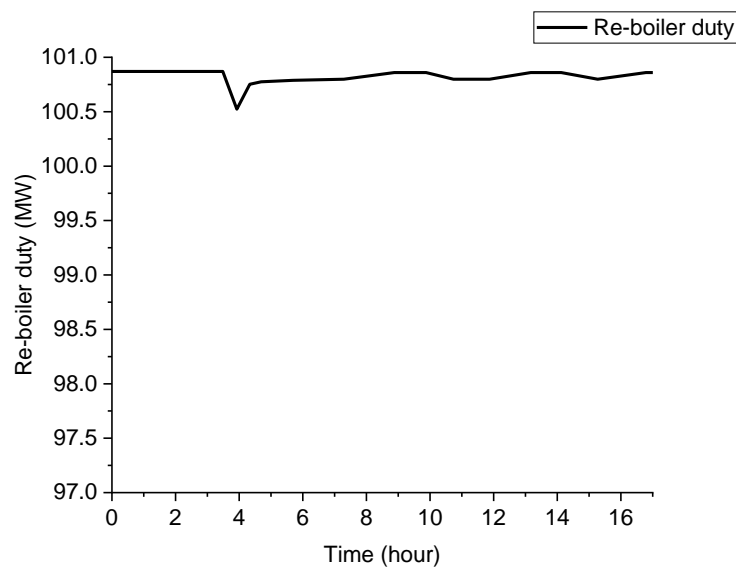


Figure 3.21: Re-boiler duty performance with step point reduction in CO<sub>2</sub> capture level -5.5%

### 3.8 Conclusion

In this chapter, Aspen Plus® was used to develop steady-state modelling of solvent-based PCC processes using 30% wt. MEA. Model validation was performed at a pilot scale against the experimental data from the separation research programme (SRP). The model validation findings confirmed that the rate-based model is in agreement with the experimental data. To meet the needs of a 250 MWe CCGT power plant, a scale-up procedure was carried out using the same method as in the previous study (Canepa et al., 2013) to meet 250 MWe CCGT power plant. A technical evaluation was implemented to obtain the optimal value of CO<sub>2</sub> lean loading that minimises energy consumption and operating and capital costs for the operating conditions. Additionally, economic evaluation was investigated. Finally, control structure and design were analysed in Aspen Dynamics®. The following key findings are presented in this chapter:

- The rate-based model was validated against the experimental data with a lower than 7% deviation. Furthermore, the temperature profile for both packed columns accurately predict the temperature profile in the experimental data, demonstrating that the temperature bulge is located at the bottom or top of the packed columns.
- The scale-up procedure was performed from the pilot scale to the 250 MWe CCGT power plant to obtain the packed column sizes. The absorber diameter was 13.95 m, while the stripper diameter was 7.9 m. The packed columns' height was assumed to be 30 m. The scale-up method predicts similar behaviour in the performance of absorber and stripper at pilot scale.
- Technical evaluation showed that L/G ratio and specific re-boiler duty are affected by CO<sub>2</sub> lean loading, where the optimal CO<sub>2</sub> lean loading was 0.28 mol CO<sub>2</sub>/mol MEA, the specific re-boiler duty was 4.14 GJ/tonne CO<sub>2</sub> and the L/G ratio was 1.49 kg/kg. To conclude, the correlation between specific re-boiler duty and CO<sub>2</sub> lean loading exhibits decreasing trend, which mean at higher CO<sub>2</sub> lean loading, lower specific re-boiler duty will be obtained. In terms of L/G ratio, it was increasing with increasing CO<sub>2</sub> lean loading. Hence, it will be beneficial to apply tradeoff between L/G ratio and energy consumption.
- Economical evaluation showed that the annualised total cost of the solvent-based PCC using MEA is 22.6 M£/year at 0.19 CO<sub>2</sub> lean loading. It was 15.53 M£/year at

the optimal CO<sub>2</sub> lean loading 0.28 mol CO<sub>2</sub>/mol MEA. It was increased to 18 M£/year at 0.33 CO<sub>2</sub> lean loading.

- Dynamic analysis of solvent-based PCC shows that the settling times for CO<sub>2</sub> capture level and re-boiler temperature in the case of a 10% flue gas step change were 8.2 and 9.2 hours, respectively. On the other hand, the re-boiler duty settlement time was 10 hours. The specified control structure effectively monitors the process's performance under disturbance rejection and setpoint tracking based on the settling time to reach the steady-state.

-



# Chapter 4: Process Simulation of PCC using PZ

## 4.1 Overview

This chapter represents the process simulation of PCC using PZ solvent to reduce the energy penalty that is connected to the benchmark MEA solvent. PZ solvent is known as a promotor, it has 10 time faster rate of reaction than MEA (Bishnoi et al., 2000). Hence, it can reduce the energy consumption of PCC. Section 4.3 presents the steady-state model development and validation of solvent-based PCC at pilot scale using PZ in Aspen Plus® v.11. In Section 4.4, the validated PCC model was scaled-up to commercial scale. In Section 4.5, technical evaluation for the scaled-up PCC model was presented. Economic evaluation is illustrated in detail in Section 4.5 in Aspen Process Economic Analyser®.

As steady-state model of PCC has limitation in providing the deep understanding of transient behaviour of the entire process, dynamic modelling of scaled model is presented in Section 4.7

## 4.2 Steady-state model development of PCC using PZ at pilot scale

This section provides the details of the steady-state model development of PCC using PZ. This development was carried out in Aspen Plus® v.11. A rate-based model was implemented to account for mass transfer and reaction kinetics. Model development involves thermodynamic properties, kinetics, and equilibrium reactions. The liquid and vapour phases have an interface as shown in Figure 4.1. Chemistry uses equilibrium reactions to calculate mass and heat transfer. Moreover, the correlations for heat transfer, mass transfer, and interfacial area were used.

Some assumptions were used to develop this model:

- All the reactions and mass transfer occur in liquid phase.
- The flow of liquid and vapour phase is counter-current
- No reactions exist in liquid and gas film.

- The vapour film is considered.
- Liquid phase contains these ions:  $H_3O^+$ ,  $OH^-$ ,  $HCO_3^-$ ,  $CO_3^{2-}$ ,  $PZH^+$ ,  $PZCOO^-$ ,  $HPZCOO$ ,  $PZ(COO^-)_2$ , Also the molecule of  $CO_2$ ,  $N_2$ ,  $H_2O$ , and  $PZ$ .
- No heat losses to the environments
- No oxygen content in flue gas stream

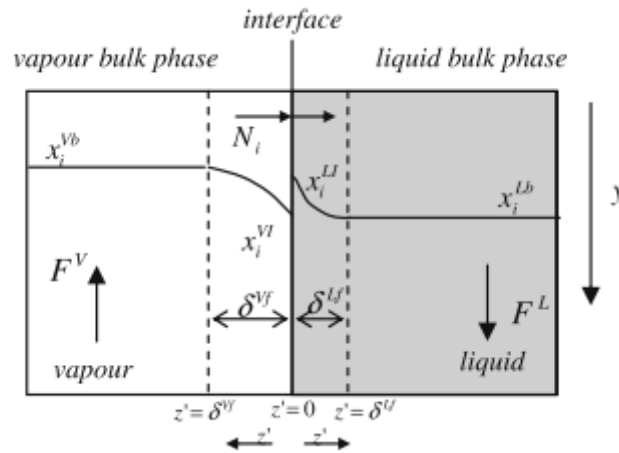


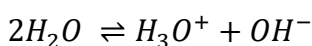
Figure 4.1: Vapour and liquid phase with interface accounted in model development (A. Lawal et al., 2009)

#### 4.2.1 Thermodynamic properties

The electrolyte solution of PZ- $CO_2$ - $H_2O$  in the liquid phase requires an accurate base method that accounts for the actual electrolyte solution's characteristics. To account for this electrolyte's liquid phase, the Electrolyte Non-Random Two-Liquid (ELENRTL) (Chen et al., 1986) base method was chosen, while the Redlich-Kwong (RK) base method was chosen for the vapour phase. Aspen properties and VLE data regression predicted a variety of properties, including Henry's constant, vapour pressure, and specific heat capacity, where predicted by Aspen properties and VLE data regression.

#### 4.2.2 Chemical reactions used in this model

The chemistry for this model was indicated by set of equilibrium reactions (R 4.1-R 4.7). They express the forward and backward reactions in the entire process. (Ermatchkov et al., 2006; Otitoju et al., 2021).



R 4.1

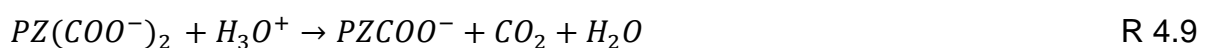


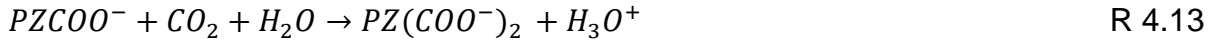
Regarding the temperature-dependant equilibrium constants, the above reactions are expressed as molar concentration scale using equation 4.1:

$$K_j = \exp\left(-\frac{\Delta G_j^0}{RT}\right) \quad (4.1)$$

The reactions R 4.1, R 4.5, and R 4.6 represent the water dissociation, the carbonate formation and bicarbonate. The coefficients in the equation 4.1. were considered from (Posey and Rochelle 1997). The reaction R 4.2 expresses the PZ Protonation, in which the coefficients of this reaction were taken from Hetzer *et al.*, (1968). The reactions R 4.3, R 4.4, and R 4.7 consists the carbamate PZ species, including piperazine mono-carbamate, dissociation of protonated carbamate zwitterion, and the piperazine di-carbamate, respectively. Their reaction coefficients were considered from the previous study (Ermatchkov *et al.*, 2006). On the other hand, kinetic reactions were provided to account the mass transfer in the liquid phase.

The kinetics-controlled reaction involves set of reactions where they were provided in both columns (absorber, stripper). These reactions express the rate-controlled for absorption rate which increases mass transfer efficiency from vapour to liquid phase.





These kinetic reactions have the reactions rate( $k_j$ ) that is calculated using power-law expression by equation 4.2:

$$k_j = k_j^\circ \exp\left(\frac{-E_j}{RT}\right) \prod_{i=1}^N C_i^{a_{ij}} \quad (4.2)$$

where the parameters in this equation are expressed as follows:  $k_j^\circ$  represents the pre-exponential factor,  $E_j$  expresses the activation energy,  $T$  is the environmental temperature,  $R$  is the universal gas constant,  $C_i$  depicts the concentration of species  $i$ ,  $a_{ij}$  is the reaction order for species  $i$  in the reaction  $j$ . Table 4.1 illustrates the kinetic reactions and activation energy used to calculate the reactions rate R 4.8-R 4.13.

**Table 4.1: Pre-exponential factor and activation energy parameters used in the kinetic reactions**

Reaction number	$k_j^\circ$ (m <sup>3</sup> /kmol. s)	$E_j$ (kJ/kmol)	Reference
R 4.8	4.23e+13	5.55e+4	(Pinsent et al., 1956)
R 4.9	2.38e+17	1.23e+5	(Pinsent et al., 1956)
R 4.10	4.14e+10	3.36e+4	(Bishnoi et al., 2000)
R 4.11	7.94e+21	6.59e+4	(Otitoju et al., 2021)
R 4.12	3.62e+10	3.36e+4	(Bishnoi et al., 2000)
R 4.13	5.56e+25	7.69e+4	(Otitoju et al., 2021)

#### 4.2.3 Model development of PCC using PZ at pilot scale

The modelling of PCC using PZ solvent has similar configuration to MEA solvent, where it has similar equipment. The modelling was implemented in Aspen Plus® v.8, v.11 using two main columns (absorber, stripper) where RadFrac block was selected to account the packed columns. The model type was rate-based model which considers the Column

hydraulics. This model has better performance than equilibrium-based model. The packing materials that were used are MELLAPAK 2X for absorber and stripper as provided in experimental data. The packing surface area was  $205 \text{ m}^2/\text{m}^3$  for absorber whereas the packing surface area for stripper was  $250 \text{ m}^2/\text{m}^3$  (Plaza and Rochelle, 2011; Van Wagener, 2011).

The absorber specifications considered to implement this model are shown in Table 4.2 (Plaza and Rochelle, 2011; Van Wagener, 2011).

**Table 4.2: Absorber specifications for model development of PCC at pilot scale(Plaza and Rochelle, 2011; Van Wagener, 2011)**

Absorber Specifications	
Number of stages	25
Leanin volumetric flow rate (gpm)	15.1
L/G ratio (kg/kg)	5.19
Diameter and packing type (m)	0.427, MELLAPAK 2X
Gas volumetric flow rate ( $\text{m}^3/\text{s}$ )	0.165
Column pressure (atm)	1
Gas temperature ( $^{\circ}\text{C}$ )	30
Leanin temperature ( $^{\circ}\text{C}$ )	40
Column height (m)	6.1

In case of stripper, the specifications required are given in Table 4.3 (Plaza and Rochelle, 2011; Van Wagener, 2011). Number of stages were specified by  $\text{CO}_2$  composition profile in liquid phase.

**Table 4.3: Stripper specifications for model development of PCC at pilot scale( Plaza and Rochelle, 2011; Van Wagener, 2011)**

Stripper Specifications	
Stripper Pressure (kPa)	136
Number of Stage	25
Stripper Temperature ( $^{\circ}\text{C}$ )	115
Re-boiler Duty (kW)	110

Reflux Ratio	0.8
--------------	-----

The PZ model was developed with 25 stages for the absorber and stripper of the column, with bulk properties playing the most significant role in calculating reaction rates. In both columns, mass transfer and energy flux were expressed using the counter-current flow model. The counter-current flow model is considered an accurate model for explaining the flow in a packed column when the bulk properties for gas and liquid phases are derived from the average of the inlet and outlet properties (Razi *et al.*, 2013). Nevertheless, the use of a counter-current flow model can result in an unstable solution and temperature profile oscillations. In the liquid phase, reactions occur, which are considered to be rapid reactions. The *discrxn* option was chosen to express diffusion resistance with liquid film reactions. Consider that in the gas phase, film is selected under the assumption that there are no chemical reactions.

#### 4.2.4 Mass transfer heat transfer correlations

In the model, liquid and vapour films demonstrate mass transfer resistance, and CO<sub>2</sub> diffusivity in the liquid phase is estimated using the Mahajani (2005) expression. The vapour phase CO<sub>2</sub> diffusivity was estimated using Fuller's equation. Similar to equations 3.1-3.6, the mass transfer coefficients  $k_G$  and  $k_L$ , as well as the effective area of packing  $a_w$ , are used to calculate  $H_G$  and  $H_L$  in the film Onda *et al.*, (1968). As shown in Table 4.4, correlations between mass transfer, heat transfer, and interfacial area were used to account for mass and heat transfer.

**Table 4.4: Correlations used in model development of PCC process**

Specification	Absorber	Stripper
Mass transfer	(Bravo, 1985)	(Bravo <i>et al.</i> , 1992)
Heat transfer	(Chilton <i>et al.</i> , 1934)	(Chilton <i>et al.</i> , 1934)
Hold-up liquid	(Stichlmair <i>et al.</i> , 1989)	(Stichlmair <i>et al.</i> , 1989)
Interfacial area	(Bravo, 1985)	(Bravo <i>et al.</i> , 1992)

#### 4.2.5 Transport properties

This model's transport properties include the major transport properties required for heat and mass calculations. For instance, the Rackett model was applied to define density in the liquid phase, whereas the Redlich-Kwong EOS model was implemented to define density in the gas phase. In the liquid phase, the Jones-Dole model was used to express viscosity, while the Chapman-Enskog model was performed in the gas phase. In the liquid phase, thermal conductivity was expressed using the Riedel model, while in the gas

phase, the Wassilijewa-Mason-Saxena model was used. The Wilki-Chang model was used to express the liquid phase diffusivity, while the Chpman-Enskog-Wilke-Lee model was applied to the gas phase. In the case of surface tension, Hakim-Steinberg-model Stiel's with Onsager-model Samaras's in the liquid phase are considered. Table 4.5 provides a summary of these properties (AspenTech, 2010):

**Table 4.5: The models used for transport properties for PCC process (AspenTech, 2010)**

Transport property	Gas Phase	Liquid phase
density	Redlich-Kwong EOS model	Rackett model
Surface tension	-	Hakim-Steinberg-Stiel with Onsager-Samaras model
Binary diffusivity	Chapman-Enskog-Wilke- Lee model	Wilki-Chang model
Thermal conductivity	Wassilijewa-Mason - Saxena model	Riedel model
Viscosity	Chapman-Enskog model	Jones-Dole model

### 4.3 Steady-state model validation of PCC using PZ at pilot scale

#### 4.3.1 Pilot plant data

To validate the rate-based model based on model predictions, such as CO<sub>2</sub> capture level, CO<sub>2</sub> rich loading, re-boiler duty, and specific re-boiler duty at the pilot plant, experimental pilot plant data was used. The CO<sub>2</sub> capture facility at the J.J. Pickle Research Center provided SRP at the University of Texas at Austin with 14 experimental runs. At the pilot plant, both the absorber and stripper have the same diameter of 0.427 metres and are divided into two sections of 3.05 metres. The fourteen experimental pilot plants had a constant volumetric flue gas flow rate (0.165 m<sup>3</sup>/s). As shown in Table 4.6, the CO<sub>2</sub> concentration in flue gas was 12 mol%, while the PZ concentration was in a different range. As shown in Table 4.6, while further details about this pilot plant data can be found in previous studies ( Plaza and Rochelle, 2011; Van Wagener, 2011)

Table 4.6: pilot plant data for 14 runs of model validation (Van Wagener, 2011)

Specificatio n	Runs													
	1	2	3	4	5	6	7	8	9	10	11	12	13	14
Leann flowrate (kg/s)	1.04	1.07	1.05	1.09	0.84	1.28	1.07	0.85	1.26	1.08	1.24	1.22	1.01	0.81
Lean Temperatur e (K)	323.0 5	319.6 5	322.6 5	312.8 5	317.2 5	318.5 5	321.3 5	318.0 5	324.8 5	318.4 5	317.9 5	321.7 5	319.6 5	315.7 5
CO <sub>2</sub> lean loading (mol/mol)	0.3	0.31	0.25	0.39	0.28	0.303	0.305	0.298	0.27	0.331	0.316	0.274	0.257	0.262
Re-boiler temperature (K)	380.3 5	376.1 5	382.0 5	360.6 5	378.8 5	377.2 5	400.6 5	400.6 5	402.1 5	389.2 5	392.8 5	400.7 5	401.3 5	400.1 5
Re-boiler duty (MW)	0.130 6	0.101	0.155 5	0.045 9	0.111 1	0.125 3	0.112 7	0.105 6	0.141 3	0.079	0.099 8	0.134 6	0.129	0.114 5
Rich solvent Temp (°C)	320.5	316.9	319.9	310.2	314.6	315.4	316.9	314.1	320.5	314.6	314	317.8	315.7	311.9
CO <sub>2</sub> rate from stripper (kg/h)	118.8	93.6	129.6	39.6	100.8	111.6	93.6	82.8	64.8	115.2	79.2	115.2	111.6	93.6



Condenser rate (kg/s)	0.02	0.008	0.019	0.002	0.011	0.012	0.005	0.004	0.011	0.013	0.004	0.011	0.010	0.009
CO <sub>2</sub> rich Loading (mol /mol)	0.3	0.37	0.33	0.4	0.358	0.36	0.364	0.369	0.338	0.381	0.382	0.362	0.360	0.382
PZ concentration (%wt.)	37.25	39.35	45.9	40.9	39.1	41.05	40.3	39.4	39.2	38.35	24.05	24.75	24.5	23.2

### 4.3.2 Model validation of PCC using PZ at pilot scale

The rate-based model validation was conducted for case (5). The model predictions ( $\text{CO}_2$  lean Loading,  $\text{CO}_2$  rich loading, and re-boiler duty) were in agreement with pilot plant data as shown in Table 4.7. The rate-based model is reliable and accurate because it satisfactorily predicted the pilot plant data with a small deviation around 5%.

**Table 4.7: model predictions for rate-based model against pilot plant data**

Parameter	Rate-based model	Experimental data	Relative percentage error (%)
$\text{CO}_2$ capture level (%)	82.2	85.9	4.31
$\text{CO}_2$ Lean Loading (mol $\text{CO}_2$ /mol PZ)	0.29	0.28	3.57
$\text{CO}_2$ rich loading (mol $\text{CO}_2$ /mol PZ)	0.35	0.358	2.23
Re-boiler duty (kW)	110	111.1	0.99

Figure 4.2 depicts the temperature profile of absorber column validation against the pilot plant data. It is noted from the trend that there is satisfactory agreement with pilot plant data. Moreover, it is clear that the temperature bulge is located at the bottom with a L/G ratio of 5.5 kg/kg. The heat generated by the chemical reactions provided causes a discrepancy between pilot plant data and the rate-based model, where the provided temperature profile of rate-based model is higher than experimental data.

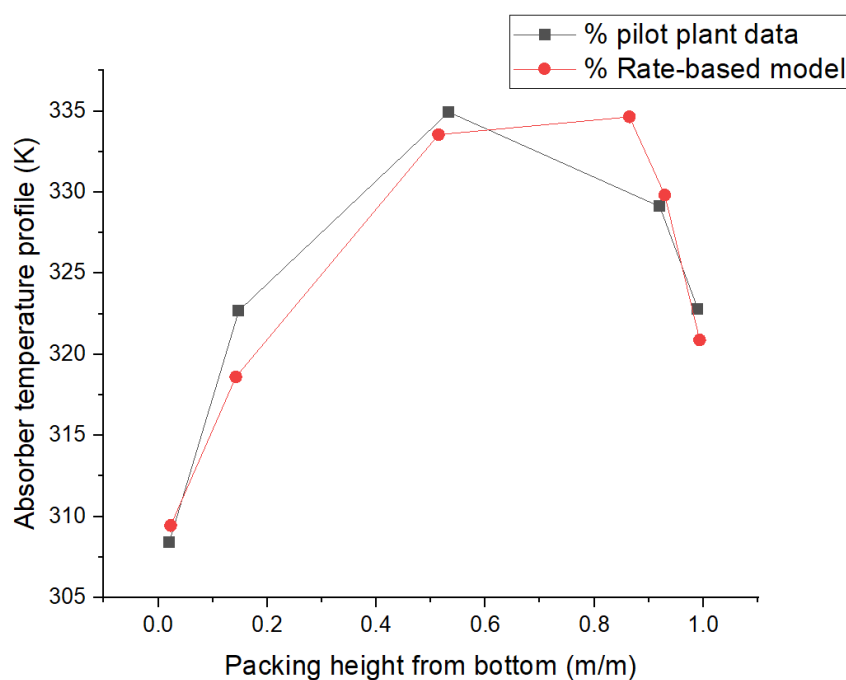


Figure 4.2: Absorber temperature profile for PCC model using PZ

#### 4.4 Scale-up of solvent-based PCC using PZ to commercial scale

The scale-up is aimed at estimating the main columns' size so they can handle the flue gas flow rate from a CCGT power plant. The scale-up process was performed using 40 and 30 %wt. PZ solvent, respectively. These concentrations are considered because PZ should be compared with 30%wt. the benchmark MEA. Also, 40% wt. PZ was investigated to analyse its impact at a higher weight percentage than the benchmark solvent. The operating conditions, i.e., flue gas, lean amine temperature, absorber pressure, and stripper pressure were taken from the rate-based model at pilot scale. The scale-up procedure can be summarised as follows: (i) Calculation of flue gas flowrate and composition; (ii) calculation of lean solvent flowrate; and (iii) estimation of absorber and stripper diameter. The PZ model was scaled up to capture 90% CO<sub>2</sub> from flue gas from 250 MWe CCGT power plants, with CO<sub>2</sub> purity of 99% coming out of the stripper. The assumptions of scale-up were summarised to achieve the process targets as follows:

- PZ weight is 40, 30% to have similar comparison basis with the benchmark solvent (MEA).
- The capture level is 90%

- Absorber and stripper pressure was the same as in the pilot plant
- Lean amine and flue gas temperature was similar to the pilot plant
- Negligible oxygen content in flue gas content.

#### 4.4.1 Flue gas specifications

The flue gas specifications from a 250 MWe CCGT power plant, which includes flowrate and compositions are shown in Table 4.8.

**Table 4.8: Flue gas specifications and its composition(Canepa et al., 2013)**

Input	Flue gas specification from CCGT power plant			
Flue gas flowrate (kg/s)	356 after cooling and pre-treatment			
Composition (mol fraction)	CO <sub>2</sub>	N <sub>2</sub>	H <sub>2</sub> O	Ar
	0.0486	0.867	0.0735	0.0105

The flue gas specifications were similar to the MEA model, where flue gas flowrate is considered after gas pre-treatment, where acid gases, i.e., NO<sub>x</sub> and SO<sub>x</sub>, were removed to prevent the formation of heat-stable salts, impacting the solvent regeneration process. Moreover, oxygen content was removed before entering the absorber because oxygen can enhance the equipment's corrosion and solvent degradation.

#### 4.4.2 Lean solvent flowrate estimation

After flue gas flowrate specification, lean solvent flowrate required to capture 90 % CO<sub>2</sub> capture level should be estimated using equation provided Agbonghae *et al.*, (2014)

#### 4.4.3 Packed column sizing

To ensure a similar basis for energy consumption, the packing material type is similar to that used for MEA solvent. Some physical properties are required for column sizing, such as density for the liquid and gas phases and kinematic viscosity for the liquid phase, which are considered in the model at the pilot plant. To calculate the flow parameter for packed column size, the L/G ratio is required after estimation of the first guess of lean solvent flowrate, which is similar to the scale-up method in Section 3.4

In general, for gas absorption and distillation, packing or plating is considered. However, it is indicated that for small diameters, packing material is better than plate due to its difficulty in installation and being more expensive than packing material. Moreover, liquid hold-up in packing material is lower than that in plate, which is essential when handling

flammable liquids (Towler and Sinnott, 1969). Thus, packing materials were used in the entire process and the inputs of scale-up calculation for packed columns absorber and stripper are given in Table 4.9, where gas and liquid densities and viscosity were obtained from the rate-based model at pilot scale. Also, the packing materials were similar as in MEA model at commercial scale. This calculations are considered at default value of 42 mm H<sub>2</sub>O pressure drop per meter of packing height(Sinnott, 2005).

**Table 4.9: Scale-up calculation for packed columns (absorber and stripper)**

Inputs		
	Absorber	Stripper
$\rho_v$ (kg/m <sup>3</sup> )	0.9838	1.151
$L_w / V_w$	1.03	2.32
$\rho_L$ (kg/m <sup>3</sup> )	1063.26	1037.820
Pressure drop (mm H <sub>2</sub> O/ m Packing)	42	42
$\mu_L$ (Pa.s)	0.00059	0.000348
$F_p$ (m <sup>-1</sup> )	78.74	168.2
Results		
$F_{LV}$	0.031558	0.077
$K_4$	1.5	1.3
Cross sectional area (m <sup>2</sup> )	119.5	35

For this input specification, the scale-up results are provided in Table 4.10, where pressure were considered from the experimental data. On the other hand, packed column diameter was calculated from the scale-up calculations, while packed column height was auto estimated from Aspen Plus<sup>®</sup> based on the calculated lean solvent flowrate, where it was lower than that of MEA solvent.

**Table 4.10: Scale-up results for packed columns**

Specification	Absorber	Stripper
Number of Column	1	1
Packing of Column	IMTP#40	FLEXIPAK 1Y
Pressure (bar)	1	1.36
Diameter (m)	12.3	6.67

Packing height (m)	22	22
--------------------	----	----

It is clear that packed column in case of using PZ is lower than using the benchmark MEA solvent. As a consequence, lower height and diameter was provided because PZ solvent requires lower solvent flowrate to provide 90% CO<sub>2</sub> capture level.

The operating conditions of scaled-up validated model are given in Table 4.11

**Table 4.11: Operating conditions of PCC scaled model**

Scaled model Operating Conditions	
CO <sub>2</sub> lean Loading (mol/mol)	0.28
CO <sub>2</sub> rich Loading (mol/mol)	0.734
Re-boiler temperature (°C)	115
Re-boiler duty (MW)	89.9424
Condenser temperature (°C)	70
Capture Level (%)	90
L/G ratio (kg/kg)	0.692
Solvent flowrate (kg/s)	246.46
Specific re-boiler duty (GJ/tonne CO <sub>2</sub> )	3.67

## 4.5 Technical evaluation of commercial solvent-based PCC using PZ

### 4.5.1 Technical evaluation of solvent-based PCC process of 30 and 40% wt. PZ

The technical evaluation of the PCC commercial model was conducted in Aspen Plus<sup>®</sup> V.11. The first procedure was implemented using the commercial PCC model at 40 %wt.PZ. The independent variable was CO<sub>2</sub> lean loading (mol CO<sub>2</sub>/mol PZ), on the other hand, the dependent variables were L/G ratio (kg/kg) and specific re-boiler duty (GJ/tonne CO<sub>2</sub>). The range of CO<sub>2</sub> lean loading was 0.14–0.306 (mol CO<sub>2</sub>/mol PZ), where the model was converged using PZ solvent. The technical evaluation findings are shown in Table 4.12. These results are depicted in Figure 4.3, expressing the impact of increasing CO<sub>2</sub> lean loading on dependent variables. Hence, increasing the solvent flow rate on the L/G ratio and specific re-boiler duty It is noted that an increase in CO<sub>2</sub> lean loading increases the L/G ratio. The trend gradually increases linearly until it becomes exponential. Specific re-boiler duty is decreasing in contract as CO<sub>2</sub> lean loading increases.

**Table 4.12: Technical evaluation results of PCC model using 40%wt. PZ**

Lean solvent flowrate (kg/s)	L/G ratio (kg/kg)	CO <sub>2</sub> lean loading	Re-boiler duty (MW)	Specific re-boiler duty (GJ/tonne CO <sub>2</sub> )
201.99	0.56	0.140	160.85	6.57
205.42	0.57	0.150	152.13	6.21
208.98	0.58	0.160	144.41	5.90
212.68	0.597	0.170	137.55	5.62
216.52	0.60	0.180	131.45	5.37
220.51	0.62	0.19	126.01	5.15
224.66	0.63	0.20	121.15	4.95
228.99	0.64	0.21	116.82	4.77
233.50	0.66	0.22	112.95	4.62
238.22	0.67	0.23	109.51	4.48
243.16	0.68	0.24	106.46	4.35
248.34	0.70	0.25	103.76	4.24
253.78	0.71	0.26	101.38	4.14
259.50	0.73	0.27	99.28	4.06
265.86	0.75	0.28	97.55	3.98
269.38	0.76	0.29	96.45	3.94
270.88	0.76	0.29	96.21	3.93
272.16	0.76	0.29	95.90	3.92
278.78	0.78	0.30	94.38	3.86
280.43	0.79	0.30	94.20	3.85
283.46	0.80	0.31	93.74	3.83

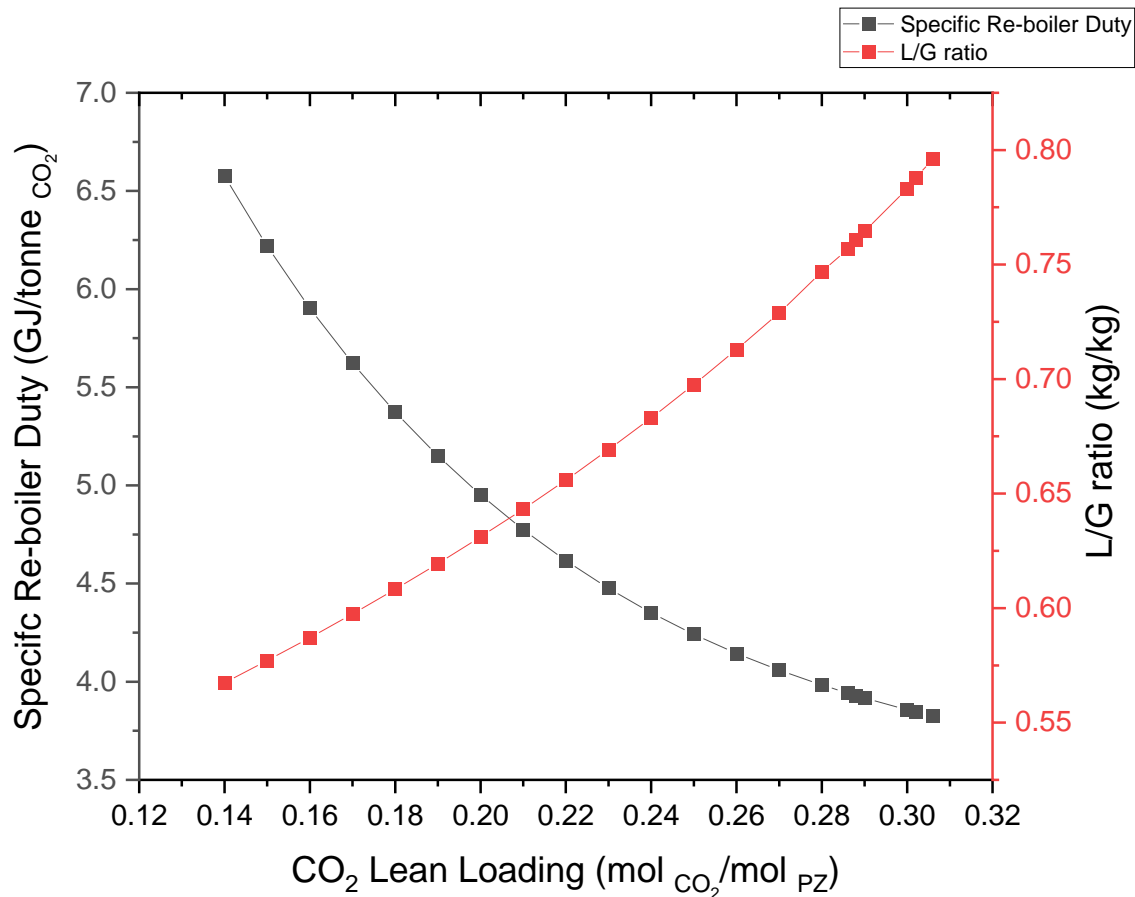


**Figure 4.3: Technical evaluation results of PCC model using 40%wt. PZ**

The commercial PCC model with 30% PZ was also used because the weight percentage of the solvents used in the whole process should be the same for both PZ and MEA solvents. The technical evaluation finding for commercial PCC using 30% wt. PZ is shown in at 0.2 CO<sub>2</sub> lean loading for PCC using 30% wt. PZ, the specific re-boiler duty was 3.2 GJ/tonne CO<sub>2</sub> with 0.88 L/G ratio kg/kg. The solvent flow rate was 313.28 kg/s at 0.2 CO<sub>2</sub> lean loading mol CO<sub>2</sub>/mol PZ, while the solvent flow rate was 296.2 kg/s in this study.

Table 4.13. The trend follows the same behaviour in case of 40% wt. PZ as depicted in Figure 4.4. However, it is noted that using 30 % wt. PZ is more efficient than 40% wt. PZ regarding the re-boiler duty required to regenerate the PZ solvent. In terms of L/G ratio, 40% wt. PZ has a lower L/G ratio to obtain a 90% CO<sub>2</sub> capture level. The range of solvent flowrate for 40% wt. PZ was between 201.9 and 283.4 kg/s. In contract; the range of solvent flowrate for 30% wt. PZ was between 265.9 and 405 kg/s. The specific re-boiler duty range for 40% wt. PZ. On the other hand, was between 6.57 and 3.82 GJ/tonne CO<sub>2</sub>. In the case of 30% wt. PZ, the range was between 6.33 and 3.51 GJ/tonne CO<sub>2</sub>.



Compared to the previous study (Otitoju *et al.*, 2021), at 0.2 CO<sub>2</sub> lean loading for PCC using 30% wt. PZ, the specific re-boiler duty was 3.2 GJ/tonne CO<sub>2</sub> with 0.88 L/G ratio kg/kg. The solvent flow rate was 313.28 kg/s at 0.2 CO<sub>2</sub> lean loading mol CO<sub>2</sub>/mol PZ, while the solvent flow rate was 296.2 kg/s in this study.

**Table 4.13: Technical evaluation results of PCC model using 30%wt. PZ**

Solvent flowrate (kg/s)	L/G ratio (kg/kg)	CO <sub>2</sub> lean loading	Re-boiler duty (MW)	Specific re-boiler duty (GJ/tonne CO <sub>2</sub> )
265.91	0.75	0.14	154.92	6.33
270.50	0.76	0.15	146.45	5.99
275.40	0.77	0.16	139.07	5.68
280.21	0.79	0.17	132.41	5.41
285.36	0.80	0.18	126.56	5.17
290.72	0.82	0.19	121.37	4.96
296.20	0.83	0.20	116.66	4.77
302.36	0.85	0.21	112.69	4.61
308.10	0.87	0.22	108.92	4.46
315.10	0.89	0.23	105.84	4.32
321.86	0.90	0.24	102.94	4.20
329.01	0.92	0.25	100.31	4.10
336.21	0.94	0.26	97.94	4.00
344.40	0.97	0.27	95.94	3.92
352.99	0.99	0.28	94.03	3.84
362.03	1.02	0.29	92.26	3.77
371.71	1.04	0.30	90.58	3.70
382.13	1.07	0.31	88.97	3.63
393.41	1.11	0.32	87.39	3.57
405.71	1.14	0.33	85.81	3.51

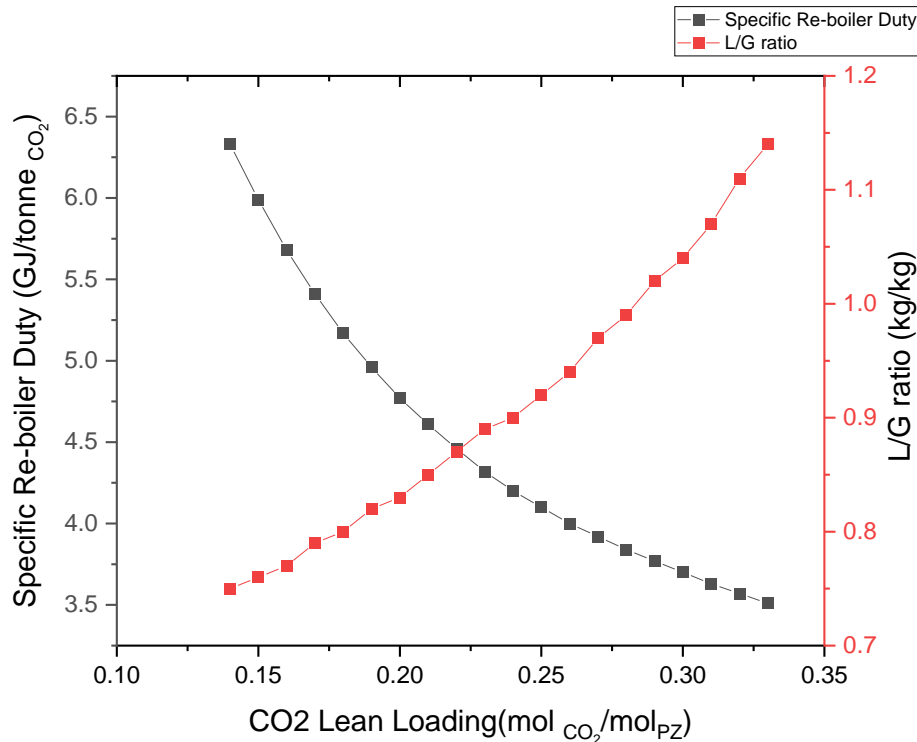


Figure 4.4: Technical evaluation results of commercial PCC model using 30%wt. PZ

#### 4.5.2 PCC process comparison of 30%wt. MEA versus 30,40%wt.PZ

Through chemical absorption, the PCC process using 30% wt. MEA is defined as the benchmark among other solvents in the PCC process. The key parameters compared are absorber diameter, stripper diameter, absorber height, stripper height, specific re-boiler duty, and L/G ratio. These are the essential parameters required for comparison. The fundamental comparisons were performed at a 90% CO<sub>2</sub> capture level with similar packing materials for both packed columns. The flue gas flowrate and composition were similar for both solvents. The key parameters are shown in Figure 4.5. It is noted from Figure 4.5 that PZ is 40% wt lighter and has smaller columns (diameter and stripper). It also has a lower L/G ratio than 30% wt. MEA and 30% wt. PZ. However, have a higher specific re-boiler duty than 30% wt. PZ because it has higher solvent flowrate with increasing CO<sub>2</sub> lean loading than 30%wt.PZ This result was compared with the previous study (Otitoju et al., 2021).The result of this study was in agreement with the result in the previous study provided by Otitoju et al. (2021).

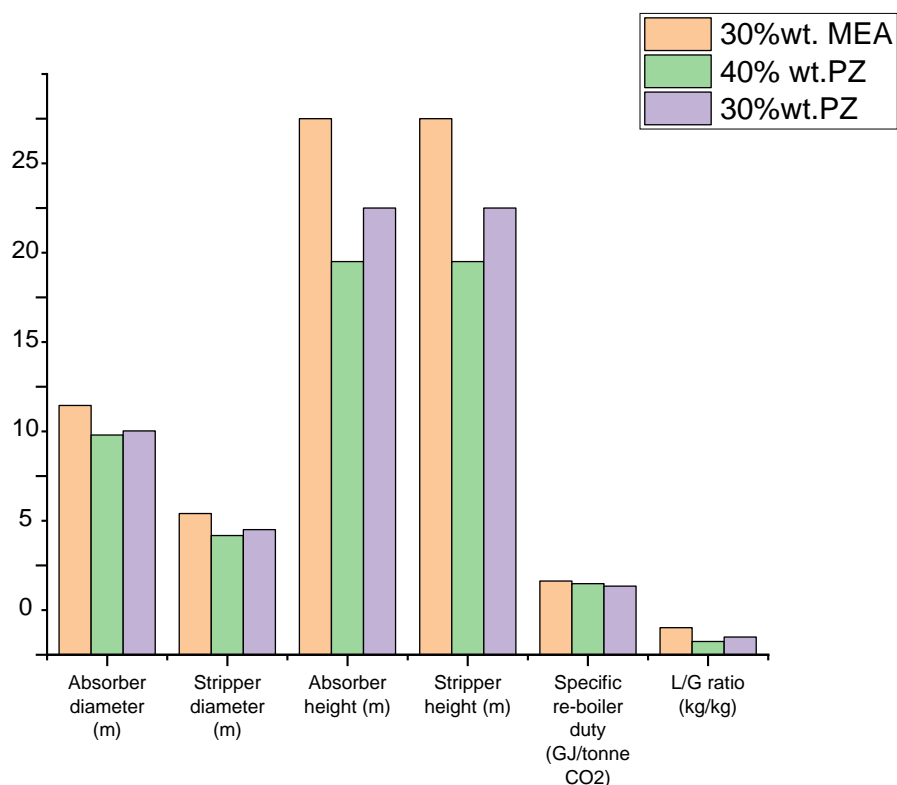


Figure 4.5: The Key parameters of PCC model using MEA, PZ solvents

#### 4.6 Economic evaluation of commercial PCC model

Economic evaluation of commercial scale The PCC model was implemented in Aspen Process Economic Analyser<sup>®</sup> followed the same procedure as in Section 3.6. However, the solvent basis price is different because the solvent used was piperazine. The price is assumed to be £5/kg of solvent, which is similar to the previous study (Otitoju *et al.*, 2021).

The total cost breakdown was similar to total cost breakdown in Table 3.13. The project lifetime is 20 years with a 10% interest rate. The economic evaluation was carried out for the specific PZ concentrations of 30 wt.% and 40 wt.% to analyse the effect of using different concentrations on operating and capital costs for the entire process.

It was observed that using PZ at CO<sub>2</sub> lean loadings lower than 0.16 mol (CO<sub>2</sub>/mol PZ) provided solid precipitation due to its high viscosity, which is higher than at higher CO<sub>2</sub> lean loadings. Figure 4.8 shows that the trend wasn't smooth because the condenser duty was increased at certain CO<sub>2</sub> lean loads to help the model converge.

Figures 4.6, 4.6, 4.7, 4.8 depict the relationship between annualised capital cost (ACC), annualised total cost (ATC), and annualised total cost per tonne CO<sub>2</sub> and CO<sub>2</sub> lean loading change using 30% PZ. It is clear that the trends are decreasing steeply until the change is negligible (when the CO<sub>2</sub> lean loading is above 0.25 molCO<sub>2</sub>/molPZ). The maximum annualised capital cost is 1.38 million pounds per year, whereas the maximum annualised total cost per tonne CO<sub>2</sub> is 31.5 million pounds per year in the case of ATC. The annual operating cost was 21.1 million pounds at 0.19 CO<sub>2</sub> lean loading and 18.9 million pounds at 0.29 CO<sub>2</sub> lean loading. It was observed that using PZ at CO<sub>2</sub> lean loadings lower than 0.16 mol (CO<sub>2</sub>/mol PZ) provided solid precipitation due to its high viscosity, which is higher than at higher CO<sub>2</sub> lean loadings. Figure 4.8 shows that the trend wasn't smooth because the condenser duty was increased at certain CO<sub>2</sub> lean loads to help the model converge.

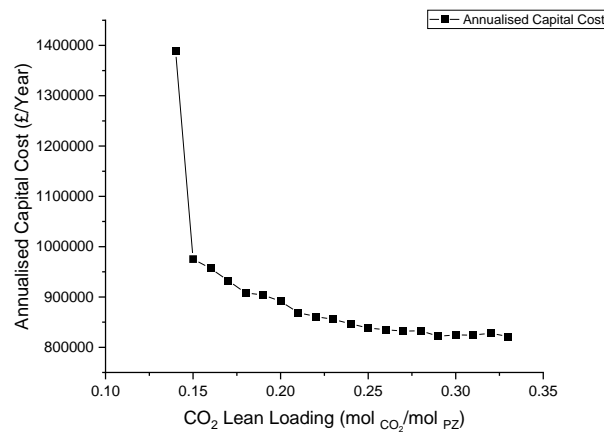


**Figure 4.6: Annualised capital cost correlation using 30%wt. PZ with changing CO<sub>2</sub> lean loading**

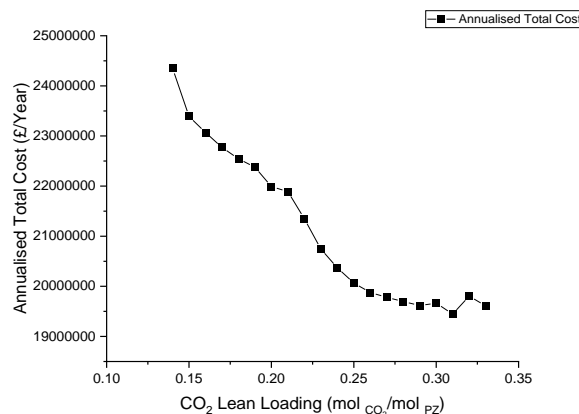


**Figure 4.7: Annualised total cost per tonne CO<sub>2</sub> correlation using 30%wt. PZ with changing CO<sub>2</sub> lean loading**

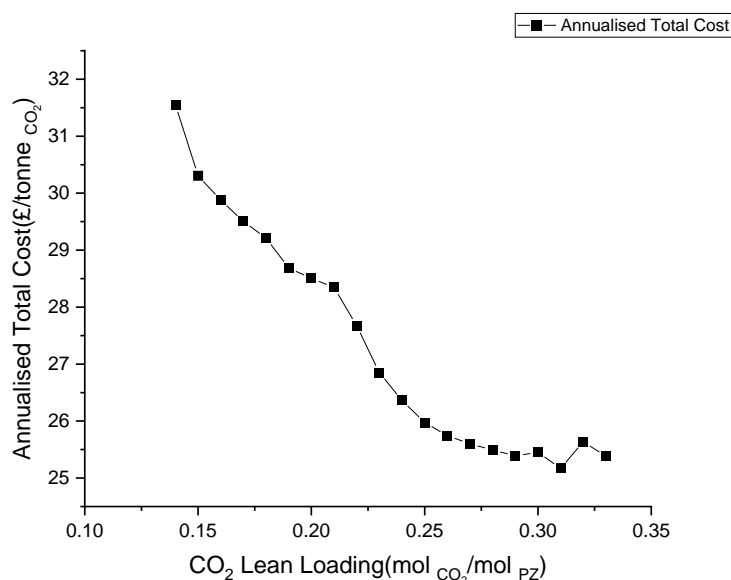


**Figure 4.8: Annualised total cost correlation using 30%wt. PZ with changing CO<sub>2</sub> lean loading**

Figure 4.9-Figure 4.11 depict the relationship between annualised capital cost (ACC), annualised total cost (ATC), and annualised total cost per tonne CO<sub>2</sub> and CO<sub>2</sub> lean loading change using 40% PZ. It is clear that the trends are decreasing steeply until the difference is negligible when the CO<sub>2</sub> lean loading is greater than 0.28 mol CO<sub>2</sub>/mol PZ), which has a similar trend when the PZ concentration is 30%. The maximum annualised capital cost is 1.38 million pounds per year, whereas ATC's maximum annualised capital cost is 22.1 million pounds per year, resulting in a max of 28.7 annualised total costs per tonne CO<sub>2</sub>. Furthermore, at 0.19 CO<sub>2</sub> lean loading, the operating cost for 40% wt. PZ was 18.4 million pounds per year, while it was 15.2 million pounds per year at 0.29 CO<sub>2</sub> lean loading. From this finding, it is confirmed that using 40 wt.% PZ has a lower annualised total cost compared to 30 wt.% PZ. It was observed that using PZ at CO<sub>2</sub> lean loadings lower than 0.16 mol (CO<sub>2</sub>/mol PZ) provided solid precipitation due to its high viscosity, which is higher than at higher CO<sub>2</sub> lean loadings. Figure 4.8 shows that the trend wasn't smooth because the condenser duty was increased at certain CO<sub>2</sub> lean loads to help the model converge.

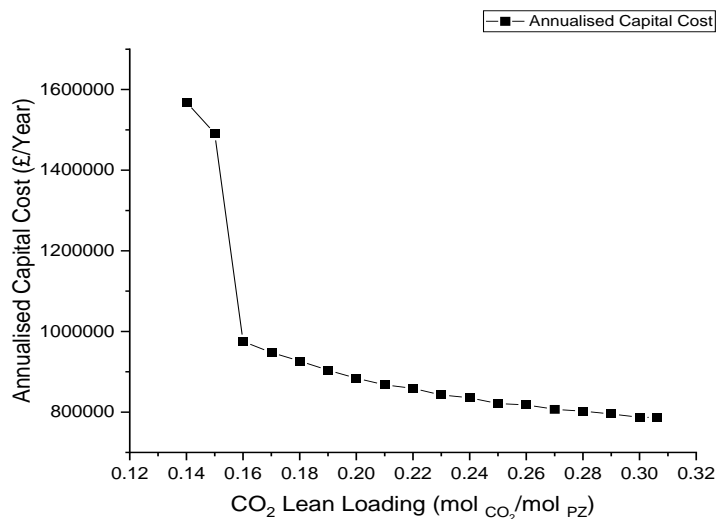


Figure 4.9: Annualised capital cost correlation using 40wt.% PZ with changing CO<sub>2</sub> lean loading

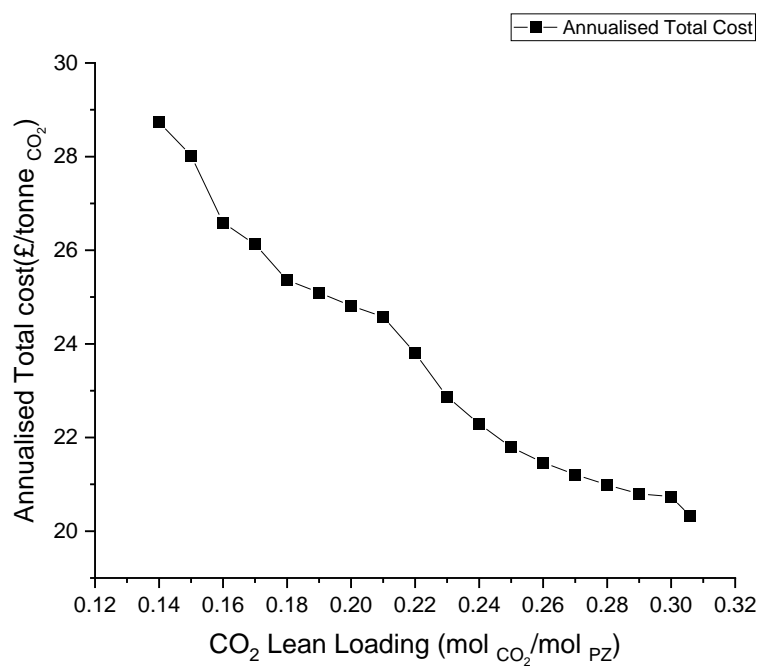


Figure 4.10: Annualised total cost per tonne CO<sub>2</sub> using 40wt.% PZ with changing CO<sub>2</sub> lean loading

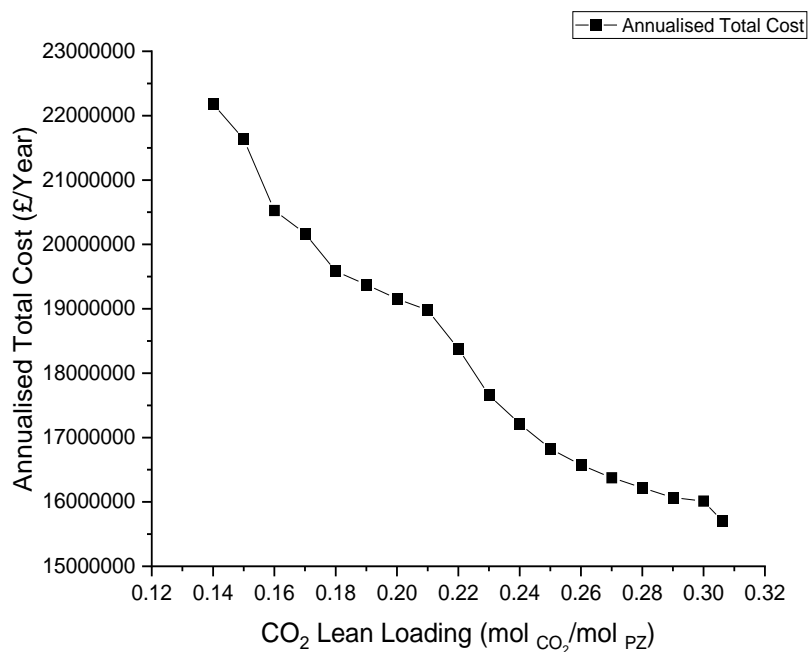


Figure 4.11: Annualised total cost correlation using 40wt.% PZ with changing CO<sub>2</sub> lean loading

## 4.7 Dynamic performance analysis of PCC using PZ

This section explains the dynamic analysis of the entire process using PZ as a solvent. The base case operating condition for the PCC model is presented, and control structure and design are performed in a similar manner as in Section 3.7.3

### 4.7.1 Base case operating conditions

The base case model is selected based on the economic evaluation in Section 4.6. This case study has the lowest annual total capital and operating costs. It is the commercial scale of the validated PCC model compared to the experimental data.

A variety of equipment is added to Aspen Plus<sup>®</sup> to stabilise the transient behaviour to run a dynamic model of commercial PCC, including an absorber sump, a stripper sump, an external condenser, a heat exchanger, a reflux drum, and a buffer tank for water and solvent make-up to compensate for the loss in the entire process.

For the sump, reflux drum, and buffer tank, the size should be estimated before exporting the steady-state model to Aspen Dynamics<sup>®</sup>. The calculations are conducted based on the flow rate in a steady-state. Table 4.14 shows the base operating conditions for the

commercial PCC model, which are used as the setpoint for the transient behavior. Some specifications were obtained from the pilot plant, such as operating pressure and pressure drop. The flue gas flowrate was provided by Canepa et al. (2013). The sump level was estimated as in MEA model. Also, sump diameter was similar to packed column diameter.

**Table 4.14: Base case operating conditions of absorber for commercial PCC model using PZ**

Parameter	Value
Absorber	
Flue gas flowrate (kg/s)	356
Lean solvent flowrate (kg/s)	352.9
Absorber diameter (m)	12.3
Packing height(m)	22
Operating pressure(N/m <sup>2</sup> )	97000
Absorber pressure drop(bar)	0.1
Packing material	IMTP#40
Number of stages	20
Sump level(m)	0.3
Sump diameter(m)	12.3
CO <sub>2</sub> capture level (%)	90
Model type	Equilibrium-based model

The stripper specification with external condenser including heat exchanger with reflux drum and buffer tank is given in Table 4.15, where buffer tank level and diameter were estimated by providing 10 min hold-up time residence to fill the tank.

**Table 4.15: Base case operating conditions of stripper for commercial PCC model using PZ**

Parameter	Value
Packing height(m)	22
Stripper diameter(m)	6.67
Operating pressure(N/m <sup>2</sup> )	162090
Stripper pressure drop	0.1
Number of stages	20
Model type	Equilibrium-based model
Packing material	FLEXIPAC 1Y
Re-boiler duty (MW)	96.2
Re-boiler temperature(K)	389.3



Condenser Temperature(K)	350.05
Reflux drum level(m)	0.4
Sump level(m)	0.2
Sump diameter(m)	6.67
Buffer tank level(m)	7
Buffer tank diameter(m)	3

### 4.7.2 Control structure and design

Control structures are selected based on open loop analysis, which is represented in Figure 4.12. For CO<sub>2</sub> capture, it was controlled by comparing the CO<sub>2</sub> mass flow in the flue gas stream entering the bottom of the absorber with the CO<sub>2</sub> mass flow in the vented gas stream leaving the top of the absorber and then adjusting the lean solvent flow rate. Condenser temperature was controlled by manipulating condenser heat duty. Also, the re-boiler temperature was controlled by adjusting the re-boiler heat duty in the stripper. Water makeup was paired with water mass fraction in lean solvent flowrate, which was treated as a variable to be manipulated.

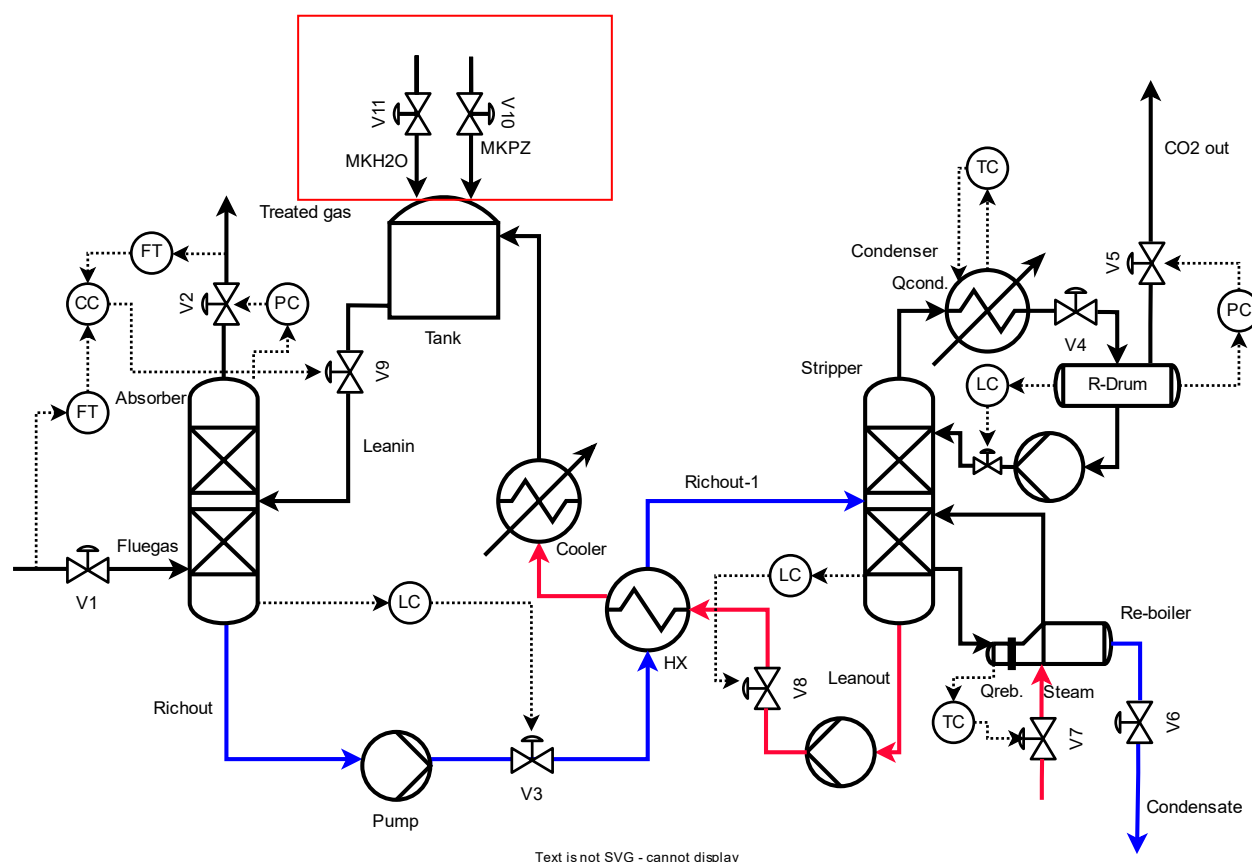


Figure 4.12: A schematic of PCC using PZ solvent with control structure

In a packed column sump, the absorber sump level was controlled by manipulating the valve (3). By adjusting the valve (8), the stripper sump level can be tightly controlled. The drum level is controlled by manipulating the valve located after the reflux drum. Liquid levels in the whole process should be tightly controlled to enhance the controllability of the CO<sub>2</sub> capture level and re-boiler temperature. The controller type used in this process is conventional control. P controllers were selected for the liquid level controller. On the other hand, CO<sub>2</sub> capture level, re-boiler temperature, and condenser temperature were controlled using a PI controller. The controller tuning is given in Table 4.16. In this study, CO<sub>2</sub> capture level and re-boiler temperature were assessed dynamically against setpoint tracking and disturbance change, which are discussed in Section 4.7.3.

**Table 4.16: Tuning parameter of controller in PCC model using PZ**

Manipulated variables	Controlled variables	Controller type	$\tau_i$ (min) time integral	K <sub>c</sub> Gain	setpoint
Valve 3	Absorber sump Level (m)	Proportional	-	60	0.15
Valve 8	Stripper sump Level (m)	Proportional	-	60	0.15
Valve 12	Drum level (m)	Proportional	-	120	1.5
Lean solvent flowrate	CO <sub>2</sub> capture level (%)	Proportional/Integral	30	20	90
Re-boiler duty	Re-boiler temperature (K)	Proportional/Integral	65	13	389.2
Condenser duty	Condenser temperature(K)	Proportional/Integral	20	10	350.05

### 4.7.3 Process control evaluation

PCC process control evaluation was assessed using two criteria: disturbance rejection, which is expressed by flue gas flowrate change, which illustrates the fluctuation in the operation of power demand, and its response to reject the effect of flue gas flowrate fluctuation. The second evaluation is the CO<sub>2</sub> capture level setpoint step change.

#### 4.7.3.1 Flue gas step change

This scenario is expressed by a 10% step change increase in flue gas flowrate where the setpoint is 356 kg/s to analyse its effect on CO<sub>2</sub> capture level and re-boiler

temperature. Figure 4.14, Figure 4.15 show that a +10 flue gas step change reduces CO<sub>2</sub> capture level and re-boiler temperature. However, re-boiler temperature had a spike due to valve opening for lean solvent flowrate to compensate the reduction in the CO<sub>2</sub> capture level. The reduction in re-boiler temperature was achieved by increasing the re-boiler duty required in the re-boiler. This dynamic performance has a similar trend as previous studies. (Lawal, 2011; Nittaya, 2014) Additionally, it is observed that the dynamic performance at the commercial scale has similar behaviour at the pilot scale. The settling times for CO<sub>2</sub> capture level and re-boiler temperature are 6 and 5.5 hours, respectively. Figures 4.15, 4.16 confirmed that the correlation was different from MEA solvent model due to precipitation of PZ solvent. Also there is fluctuation because it is difficult to monitor what is happening when there are setpoint tracking and disturbance rejection. This issue is part of the result limitation. Moreover, this process is integrated which means decoupling should be performed to enhance its controllability.

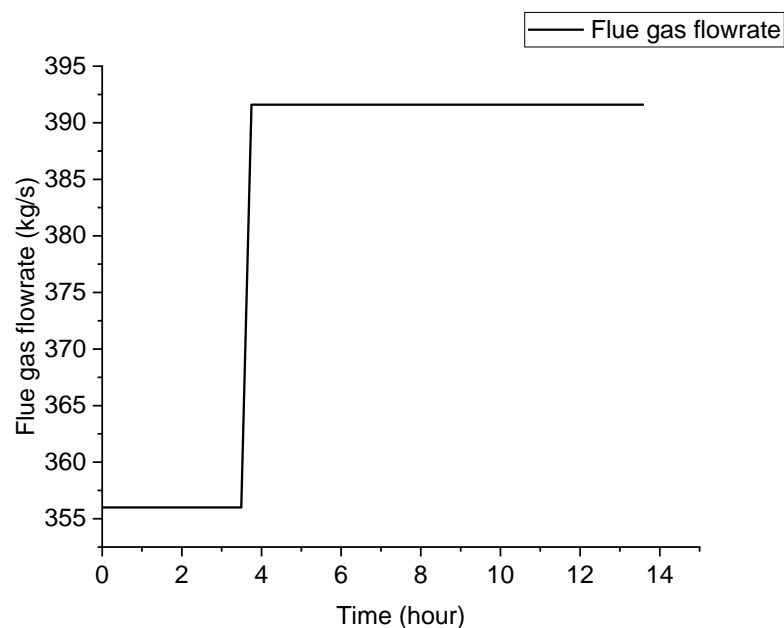


**Figure 4.13: Flue gas 10% step change using 40%wt.PZ**

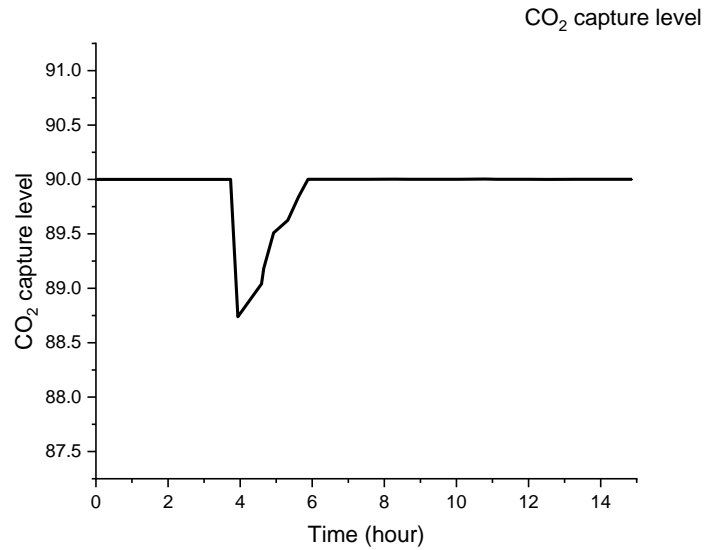


Figure 4.14: CO<sub>2</sub> capture level performance with 10% flue gas step change using 40%wt.PZ

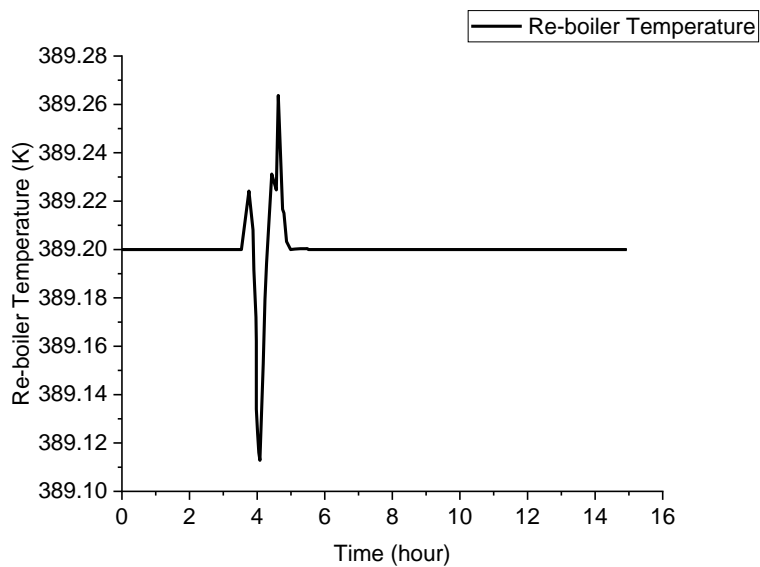


Figure 4.15: Re-boiler temperature performance with 10% flue gas step change

#### 4.7.3.2 CO<sub>2</sub> capture level step change

This scenario was evaluated by increasing setpoint CO<sub>2</sub> capture level from 90 to 85% to investigate its impact on re-boiler duty in the stripper. Figure 4.17 represents the trend of re-boiler duty with decreasing CO<sub>2</sub> capture level. Where it is decreased because of the decrease in lean solvent flowrate. Consequently, low vapor flowrate provided in the stripper. Moreover, the settling time is high which is 5.5 hour to reach the first steady-state. It is clear that there is fluctuation because it is difficult to monitor what is happening

when there are setpoint tracking and disturbance rejection. This issue is part of the result limitation. Moreover, this process is integrated which means decoupling should be performed to enhance its controllability.

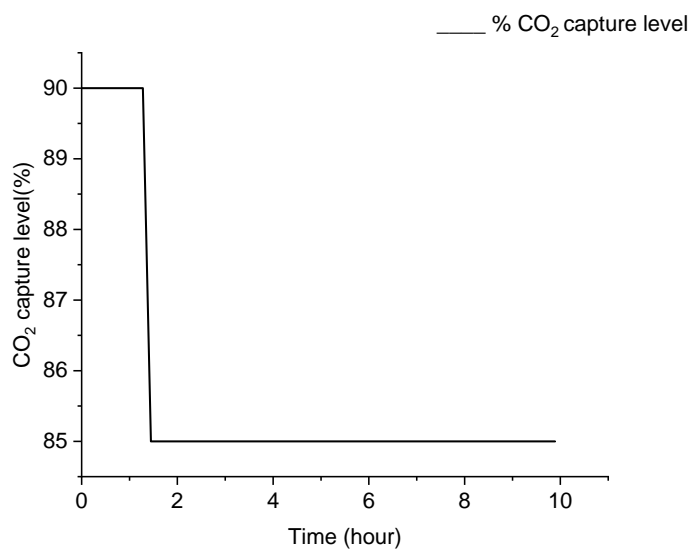


Figure 4.16: CO<sub>2</sub> capture level setpoint step change -5.5% using PZ

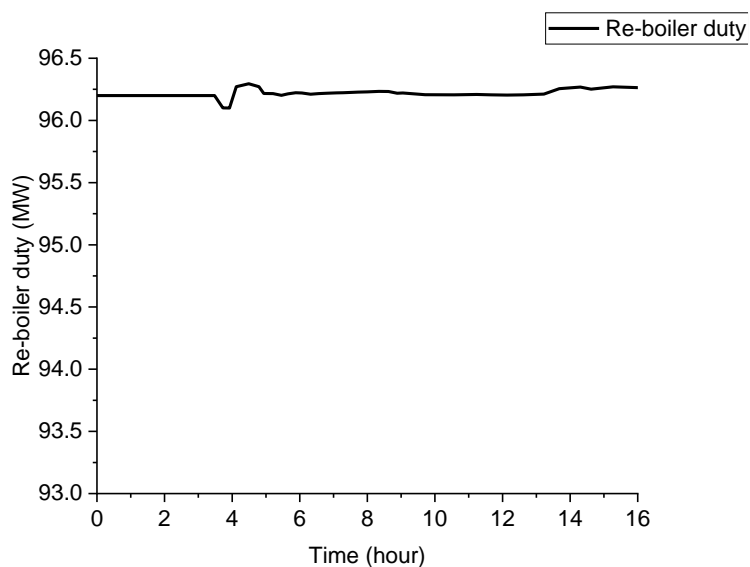


Figure 4.17: Re-boiler duty performance with CO<sub>2</sub> capture level step -5.5% change

## 4.8 Conclusion

In this chapter, steady-state modelling of the solvent-based PCC process with 30% and 40% wt. PZ was done with Aspen Plus<sup>®</sup>. Model validation was performed at a pilot scale against the experimental data. The model validation findings confirmed the rate-based model is in agreement with the experimental data from previous studies( Plaza and Rochelle, 2011; Van Wagener, 2011). To meet the needs of a 250 MWe CCGT power plant, a scale-up procedure was carried out using the same method as in the previous study (Canepa et al., 2013). A technical evaluation was implemented to obtain the optimal value for the operating conditions. Additionally, economic evaluation was investigated. Finally, control structure and design were analysed in Aspen Dynamics<sup>®</sup>. The following key findings are presented in this chapter:

- The rate-based model was validated against the experimental data with a lower than 5% deviation. Furthermore, the temperature profile for packed column (absorber) accurately predicts the temperature profile in the experimental data, demonstrating that the temperature bulge is located at the bottom or top of the packed columns.
- The scale-up procedure was performed from the pilot scale to the 250 MWe CCGT power plant to obtain the packed column sizes. The absorber diameter was 12.3 m, while the stripper diameter was 6.67 m. The packed columns' height was auto estimated in Aspen Plus<sup>®</sup>, which equals 22 m. The scale-up method accurately predicts absorber and stripper performance at pilot scale.
- Technical analysis revealed that CO<sub>2</sub> lean loading affects the L/G ratio and specific re-boiler duty, with 0.3 mol CO<sub>2</sub>/mol PZ being the optimal CO<sub>2</sub> lean loading. A technical evaluation was performed using 40%wt. PZ and 30%wt. PZ, and it was observed that using 40% wt. PZ has lower energy consumption and a lower L/G ratio compared to 30% wt. PZ.
- The annualised total cost of the solvent-based PCC using 30% wt. PZ is 22.5 M£/year at 0.19 CO<sub>2</sub> lean loading, according to economic analysis. It was 20 M£/year at a CO<sub>2</sub> lean loading of 0.28. At 0.306 CO<sub>2</sub> lean loading, it was 19.7M£/year. On the other hand, using 40%wt.PZ provides a 19.3 M£/year annualised total cost. It was 16.2 M£/year at a CO<sub>2</sub> lean loading of 0.28, implying a lower total cost than the 30% wt. PZ.

- 
- Dynamic analysis of solvent-based PCC indicates that the settling times for CO<sub>2</sub> capture level and re-boiler temperature in the case of a 10% flue gas step change were 6 and 5.5 hours, respectively. On the other hand, the re-boiler duty settling time was 5.5 hours. Furthermore, the control structure tightly adjusts the performance of the controlled variables while performing disturbance rejection and setpoint tracking. and setpoint tracking.

# Chapter 5: Process simulation using a blend of PZ with AMP

## 5.1 Overview

This chapter presents the PCC model using mixed solvents (PZ with AMP), which provide better characteristics than single solvents (e.g., MEA, PZ). This mixing of solvents has higher mass transfer because it has a higher reaction rate and can reduce the energy consumption compared to single solvents (MEA, PZ). Sections 5.2.5.3 present steady-state model development and validation of solvent-based PCC process at pilot scale in Aspen Plus® v.11. The scale-up of the validated model to 250 MW CCGT power plant is presented in Section 5.4. In Section 5.5, technical evaluation is carried out in detail. Section 5.6 evaluates the economic assessments of commercial PCC model in Aspen Process Economic Analyser® v.11.

Section 5.7 demonstrates the dynamic analysis of commercial model using mixed solvents in Aspen Dynamics® v.11, Followed by control structure, design, and process dynamics evaluation, these were discussed in Section 5.8.1.

## 5.2 Steady-state model development of PCC at pilot scale using PZ with AMP solvent

This section provides the details of the steady-state model development of PCC using mixed solvents (28% wt. AMP with 17% wt. PZ), which were provided by experimental data (Zhang et al., 2017). This development was performed in Aspen Plus® v.11. The rate-based model was selected because of its reliability over the equilibrium-based model. Model development evolves thermodynamic properties, kinetics, and equilibrium reactions. Equilibrium reactions were illustrated in chemistry to calculate the mass and heat transfer. Moreover, the correlations for heat transfer, mass transfer, and interfacial area were used.

Some assumptions were used to develop this model:

- It is steady-state modelling where there is no change of dependant variables with time



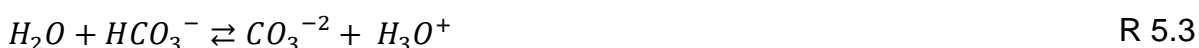
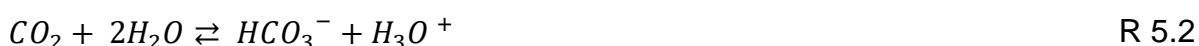
- All the reactions occur and mass transfer in liquid phase.
- The flow of liquid and gas phase is counter-current
- No reactions occur in liquid and gas film.
- Liquid phase contains these ions:  $H_3O^+$ ,  $OH^-$ ,  $HCO_3^-$ ,  $CO_3^{2-}$ ,  $PZH^+$ ,  $PZCOO^-$ ,  $HPZCOO^-$ ,  $PZ(COO^-)_2$ ,  $AMPH^+$ ,  $AMPCOO^-$ . Also, the molecule of  $CO_2$ ,  $N_2$ ,  $H_2O$ , AMP, and PZ.

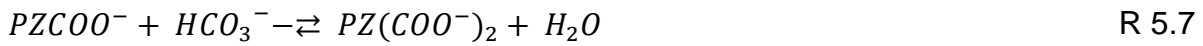
### 5.2.1 Thermodynamic properties

In Aspen Plus<sup>®</sup>, a thermodynamic property, a kinetic reaction, and equilibrium reactions were used to simulate the PCC process. To calculate the thermodynamic properties, use the electrolyte non-random two liquid activity coefficient (ENRTL) with the equation of state Redlich-Kwong (RK). These equations were implemented to calculate the thermodynamic properties for the liquid phase and the gas phase, respectively. Vapour-liquid equilibrium data (VLE) was regressed using the previous study (Li et al., 2014) to obtain the integrated parameter for molecule-electrolyte binaries. Also, some properties for protonated amine are obtained from pKa data. VLE and heat capacity data for the interaction of PZ-AMP-H<sub>2</sub>O were used with the VLE data for PZ-AMP-CO<sub>2</sub>-H<sub>2</sub>O to provide the thermodynamic properties for PZ-AMP-CO<sub>2</sub>-H<sub>2</sub>O.

### 5.2.2 Chemical reactions used in this model

For the chemistry of this model, it was assumed that AMP reacts with  $H_3O^+$  to generate  $AMPH^+$ , which then reacts with  $CO_2$  to produce unstable carbamate, which then easily reacts with other species in the electrolyte to regenerate  $AMPH^+$ . In the case of the PZ molecule, it associates with the  $H_3O^+$  ion to form  $PZH^+$  which reacts with  $CO_2$  to generate  $PZCOO^-$  carbamate, and di-carbamate  $PZ(COO^-)_2$ . The following equilibrium reactions were assumed to be global electrolytes:





For reactions (R 5.1-R 5.8), the equilibrium constant was estimated from standard Gibbs free energy change, where it can be calculated by the ion's properties available in the electrolyte. Equation 5.1 were used for equilibrium constants:

$$K_j = \exp\left(-\frac{\Delta G_j^0}{RT}\right) \quad 5.1$$

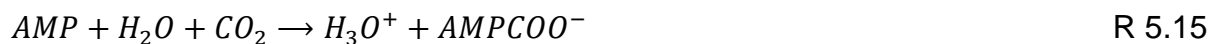
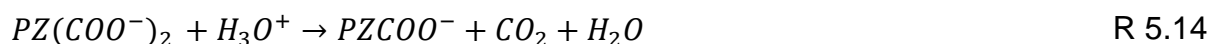
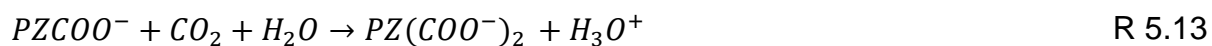
Where  $K_j$  is defined as the equilibrium constant of reaction  $j$ ,  $\Delta G_j$  is known as the change of reference state free energies for reaction  $j$ ,  $T$  is defined as the temperature while  $R$  is universal gas constant.

Rate-based model were implemented which kinetics reactions were required. Therefore, kinetic reactions were added by Equation 5.2:

$$k_j = k_j^0 \exp\left(\frac{-E_j}{RT}\right) \prod_{i=1}^{i=N} C_i^{a_{ij}} \quad 5.2$$

Where the parameters in this equation are expressed as follows:  $k_j^0$  represents the pre-exponential factor,  $E_j$  expresses the activation energy,  $T$  is the environment working temperature,  $R$  is the universal gas constant,  $C_i$  represents the concentration of species  $i$ ,  $a_{ij}$  is the reaction order for species  $i$  in the reaction  $j$ .





The kinetic parameters for the reactions (R 5.9-R 5.16) are shown in Table 5.1: Kinetics parameters for kinetic-rate reactions Table 5.1.

**Table 5.1: Kinetics parameters for kinetic-rate reactions**

Reaction number	k°	E Activation Energy (kJ/mol)	Reference
R 5.9	4.24e13	55.41	Dash <i>et al.</i> (2014)
R 5.10	5.8e4	146.44	Dash <i>et al.</i> (2014)
R 5.11	2.38e+17	123.22	Zhang <i>et al.</i> (2017)
R 5.12	3.62e+10	33.63	Zhang <i>et al.</i> (2017)
R 5.13	5.95e+4	148.53	Samanta and Bandyopadhyay (2009)
R 5.14	5.56e+25	76.86	Samanta and Bandyopadhyay(2009)
R 5.15	1e+9	34.31	Zhang <i>et al.</i> (2017)
R 5.16	1.52e+20	53.10	Zhang <i>et al.</i> (2017)

### 5.2.3 Model development of PCC using PZ with AMP

The simulation of PCC using a blend of PZ and AMP was carried out in Aspen Plus® v. 11. The process is mainly an absorber, stripper, and heat exchanger. Both columns were represented as RadFrac blocks, which represented mass transfer and chemical reactions. The heat exchanger is modelled as a shortcut for specifying a temperature approach of 10 °C. The heat exchanger is used to improve heat transfer between the lean solvent pumped from the stripper and the rich solvent pumped from the absorber. The flue gas flow rate was 80 kg/h. Lean solvent flowrate was 152 kg/h to provide 90% CO<sub>2</sub> capture level (Mangalapally and Hasse, 2011). A rate-based model approach was deployed in

both columns because of its reliability over an equilibrium-based model. The flue gas and lean solvent specifications are given in Table 5.2, where these specification were taken from (Zhang et al., 2017)

**Table 5.2: Flue gas and lean solvent specifications (Zhang et al., 2017)**

Specification	Lean solvent		Flue gas	
Flowrate (kg/h)	152		80	
CO <sub>2</sub> partial pressure in flue gas (mbar)	-		102	
Composition	Weight %		Mol%	
	CO <sub>2</sub>	0.5	CO <sub>2</sub>	8.8
	AMP	28	H <sub>2</sub> O	8
	PZ	17	N <sub>2</sub>	83.2
	H <sub>2</sub> O	54.5	-	-
Pressure (bar)	1.62		1.15	
Temperature (°C)	40		46	
CO <sub>2</sub> lean loading (mol/kg PZ+AMP)	0.8			
CO <sub>2</sub> rich loading (mol/kg PZ+AMP)	2.4			

Absorber and stripper were modelled as RadFrac block. The specifications are illustrated in Table 5.3.

**Table 5.3: Absorber and stripper specifications for PCC model development (Zhang et al., 2017)**

Specification	Absorber	Stripper
Model flow	mixed	mixed
Number of stages	11	9
Condenser type	-	Partial vapour
Re-boiler type	-	Kettle
Packing material	Sulzer (BX 500)	Sulzer (BX 500)
Column diameter (m)	0.125	0.125
Packing height (m)	4.25	2.55
Hold-up correlation	(Stichlmair et al. (1989))	(Stichlmair et al. (1989))
Interfacial area and mass transfer correlations	(Hanley et al. (2012))	(Hanley et al. (2012))
Heat transfer coefficient correlation	(Chilton et al., 1934)	(Chilton and Colburn (1934))
Pressure (bar)	1	1.62

### 5.3 Steady-state Model validation of PCC at pilot scale using PZ with AMP

#### 5.3.1 Pilot Plant data

To assure that the rate-based PCC model using PZ with AMP is reliable, CESAR 1 (28 wt.% AMP, 17 wt.% PZ, and 55 wt.% H<sub>2</sub>O) was used to validate this model (Mangalapally and Hasse, 2011). The flue gas source is extracted from a natural gas burner with a flow rate ranging from 30-100 kg/h. The flue gas temperature is between 40 and 50 °C, which enters the bottom of the absorber, while lean solvent flows from the top of the absorber at a temperature of 40 °C. The range of its flow rate is between 20 and 350 kg/h, depending on the L/G ratio required to provide 90% CO<sub>2</sub> capture level. A washing section is located at the top of the absorber to reduce solvent loss in the absorber to reduce solvent degradation. The packing material used in the absorber is BX 500, which is known as structured packing from Sulzer. The packing section is divided into 5 sections of 0.85 m, resulting in a 4.25 m total packing height.

The stripper is fed by rich solvent coming from the absorber through a heat exchanger. The stripper's packing material is similar to the absorber's in terms of type; however, it has different packing sections. The sections divide into three sections, resulting in a total packing height of 2.55 m. The two packed column diameters are the same, which is 0.125 m. The main pilot plant data is shown in Table.5.4.

**Table 5.4: Pilot plant data specifications Mangalapally and Hasse, 2011)**

Specification	CESAR1 pilot plant data
CO <sub>2</sub> partial pressure in flue gas (mbar)	102
Flue gas flowrate (kg/h)	80
Solvent flowrate (kg/h)	75-275
L/G ratio (kg/kg)	0.94-3.5
CO <sub>2</sub> flowrate in flue gas (kg/h)	11.6
The captured CO <sub>2</sub> flowrate (kg/h)	10.5

#### 5.3.2 Model validation of PCC at pilot scale using PZ with AMP

To assure that the model is reliable. It should be validated against specific pilot plant data. The model predictions (CO<sub>2</sub> capture level, CO<sub>2</sub> rich loading, specific re-boiler duty, CO<sub>2</sub>

captured mass flowrate, and temperature profile for both columns) were evaluated against the CESAR1 pilot plant data. The validation results show that the model is in agreement with the pilot plant data, as is clear in Table 5.5.

**Table 5.5: Model predictions validation of PCC against CESAR 1 pilot plant data**

Specification	Rate-based model	CESAR 1 pilot plant data	Relative percentage error (%)
CO <sub>2</sub> capture level (%)	91.3	90	1.4
CO <sub>2</sub> lean loading (mol/kg AMP+PZ)	0.8	0.8	0
CO <sub>2</sub> rich loading (mol/kg AMP+PZ)	2.3	2.4	4.2
Specific re-boiler duty (GJ/tonne CO <sub>2</sub> )	3.4	3.62	6.1
Captured CO <sub>2</sub> mass flowrate (kg/h)	9.9	10.5	5.7
L/G ratio (kg/kg)	1.9	1.9	0

The absorber temperature profile is depicted in Figure 5.1. It is clear that the temperature bulge is near the bottom of the absorber, in which L/G ratio is 1.9 (kg/kg), as shown in Figure 5.1. In contrast to the stripper, where temperature bulge is located at the top of stripper, as shown in Figure 5.2. Furthermore, the trends confirm that rate-based model for both packed columns is in agreement with the CESAR 1 pilot plant data. From Figure.5.1, it was observed that there is discrepancy at the bottom of the absorber, where heat generated from the chemical reactions causes lower temperature profile in rate-based model compared to experimental data.

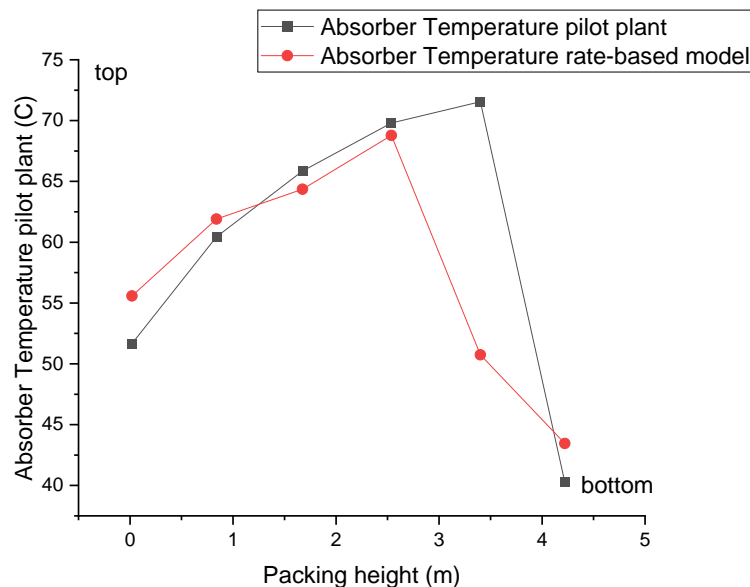


Figure 5.1: Absorber temperature profile of rate-based model against CESAR 1 pilot plant data

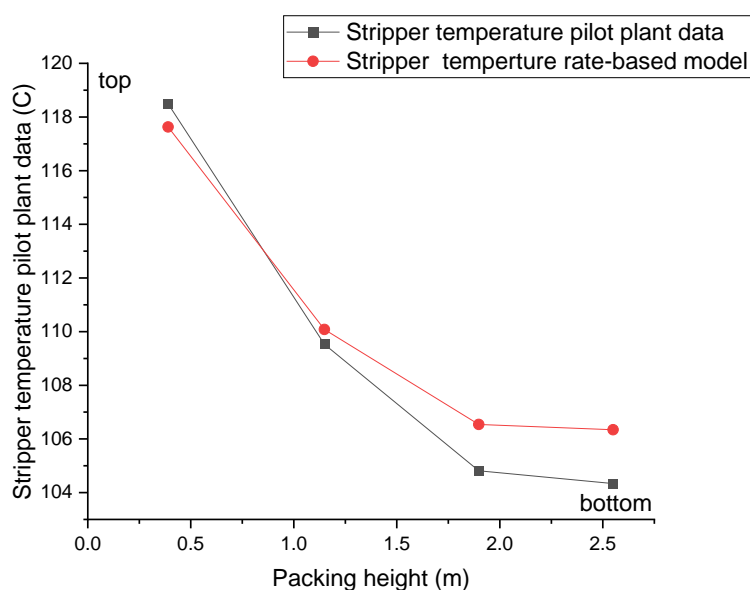


Figure 5.2: Stripper temperature profile of rate-based model against CESAR1 pilot plant data

## 5.4 Scale-up of solvent-based PCC to commercial scale

Scale-up procedure for a blend of PZ and AMP was performed using similar method as in Sections 3.4 and 4.4. The flue gas flowrate and its composition were obtained from the same literature (Canepa et al., 2013). The initial inputs used to estimate the packed

column size are presented in Table 5.6, where liquid and gas densities, and viscosity were obtained from the rate-based model at pilot scale, while flow parameter,  $K_4$ , and packed column diameters were calculated using scale-up procedure.

**Table 5.6: Initial inputs for scale-up calculations for absorber and stripper**

Inputs		
	Absorber	Stripper
$\rho_v$ (kg/m <sup>3</sup> )	1.020	1.145
$L_w / V_w$	1.34	2.72
$\rho_L$ (kg/m <sup>3</sup> )	948.26	916.56
Pressure drop (mm H <sub>2</sub> O/ m Packing)	42	42
$\mu_L$ (Pa.s)	0.000744	0.000314
$F_p$ (m <sup>-1</sup> )	78.74	168.2
Results		
$F_{LV}$	0.043938	0.096136
$K_4$	1.6	1.4
Packed column Diameter (m)	13.34	11
Packed column height (m)	30	30

The specifications for absorber and stripper after the above estimations were conducted in Aspen Plus<sup>®</sup>, as given in Table 5.7. The actual lean solvent flowrate required to capture 90% of CO<sub>2</sub>. These values were performed at a similar concentration for the blend on the pilot scale. It was observed that this scaled-up operating condition has a higher re-boiler duty and L/G ratio compared to PZ solvent. This blend was 17 wt.% PZ and 28 wt.% AMP. Hence, different concentrations were selected based on literature in order to figure out which blend concentration has the lowest re-boiler duty and L/G ratio.

**Table 5.7: The operating condition for scaled model using 17wt.% PZ and 28 wt.% AMP**

Scaled model Operating Conditions	
CO <sub>2</sub> lean Loading (mol/mol)	0.154
CO <sub>2</sub> rich Loading (mol/mol)	0.248
Re-boiler temperature (°C)	118
Re-boiler duty (MW)	142
Condenser temperature (°C)	60



Capture Level (%)	90
L/G ratio (kg/kg)	1.76
Solvent flowrate (kg/s)	626.5
Specific re-boiler duty (GJ/tonne CO <sub>2</sub> )	3.3

## 5.5 Technical evaluation of commercial scale PCC using PZ with AMP

The technical evaluation of PCC process using the blend of PZ and AMP was conducted at different ratios based on the previous study (Zhang *et al.*, 2017). A Similar ratio was selected to compare it with what was provided in Zhang *et al.*, (2017). Table 5.8 represents the optimal value of specific re-boiler duty (GJ/ tonne CO<sub>2</sub>) where it has the lowest specific re-boiler duty. Specific re-boiler duty obtained in the study is in agreement with the previous study (Zhang *et al.*, 2017). It is indicated that increasing AMP weight in the blend reduces the energy consumption which is related to re-boiler duty.

**Table 5.8: blend solvents composition ratios**

Blend ratio	Specific re-boiler duty (GJ/ tonne CO <sub>2</sub> )
7wt. %PZ & 38wt. %AMP	2.95
17wt.%PZ & 28wt.%AMP	3.3
12wt.%PZ & 33wt.%AMP	3.10
22wt.%PZ & 23wt.%AMP	3.45

The L/G ratio was evaluated based on different blend ratios to assess the lean solvent flowrate required to provide 90% CO<sub>2</sub> capture level, as shown in Figure 5.3 where it is observed that 7 wt.%PZ with 38 wt.% AMP has lower specific re-boiler duty compared to other ratios and the previous study (Zhang *et al.*, 2017), where specific re-boiler duty was 2.84 GJ/tonne CO<sub>2</sub> which is 3.87% lower than this study due to assumption differences for correlations in the simulation. Economically, it will be costly to perform higher concentration of PZ with AMP because they are more expensive than MEA. Nevertheless, they have higher absorption rate as a blend than single solvent such as MEA, PZ. Moreover, more blend ratio weight means lower re-boiler duty than single solvents.

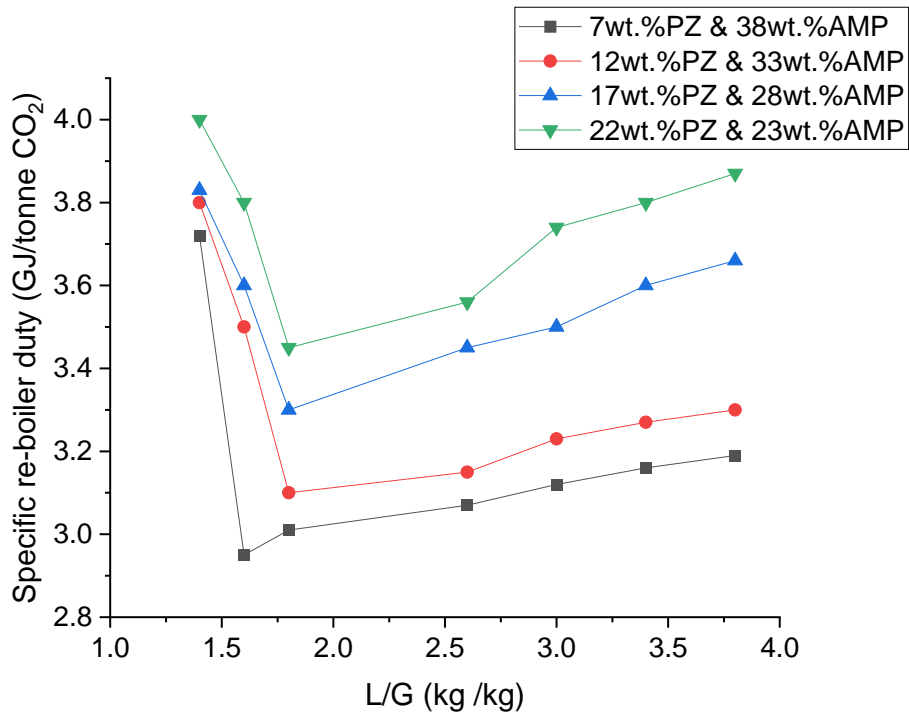


Figure 5.3: Specific re-boiler duty correlation with changing L/G ratio at different blend ratios

## 5.6 Economic evaluation of commercial scale solvent-based PCC

The economic evaluation of the scaled-up PCC model was conducted for the 7 wt.% PZ and 38 wt.% AMP because it provides the lowest specific re-boiler duty compared to other blend ratios. The same procedure was performed to calculate the annualised total cost and capital cost. The AMP price was obtained from Alibaba, which is 4.3 £ per kilo. Figure 5.4, Figure 5.5 show the annualised total cost for the selected blend ratio. It has been confirmed that the annualised total cost will range between 23 and 16 million pounds. The optimal CO<sub>2</sub> lean loading with AMP is 0.28 mol CO<sub>2</sub>/mol PZ. It was observed that the annualised total cost is higher after the optimal CO<sub>2</sub> lean loading.

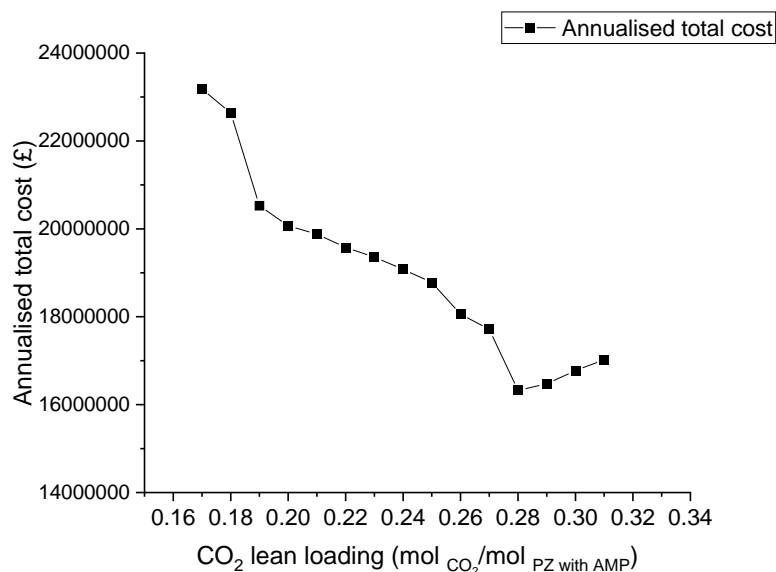


Figure 5.4: Annualised total cost with changing CO<sub>2</sub> lean loading using 7 wt.% PZ and 38 wt.% AMP

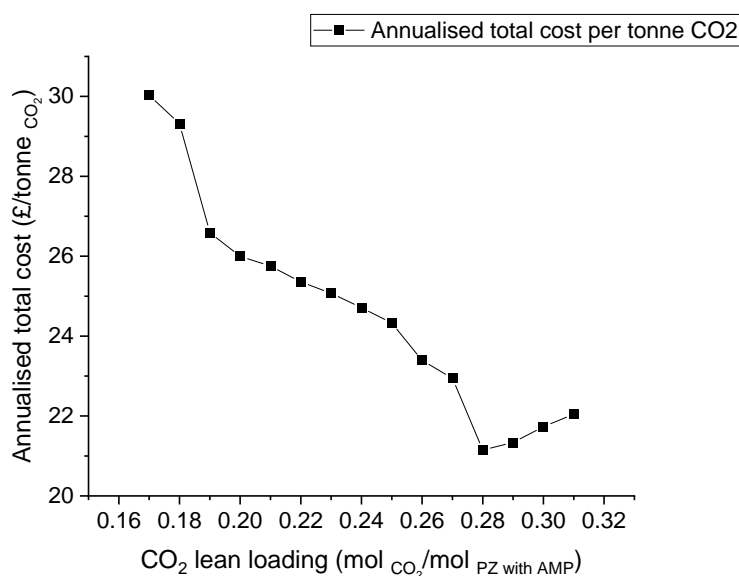


Figure 5.5: Annualised total cost per tonne CO<sub>2</sub> with changing CO<sub>2</sub> lean loading using 7 wt.% PZ and 38 wt.% AMP

## 5.7 Dynamic performance analysis of PCC using PZ with AMP

This section explains the dynamic analysis of the entire process using PZ with AMP as mixed solvent. Furthermore, control structure and design are discussed in detail.

## 5.8 Base case operating condition for PCC model

The base case model is selected based on the economic evaluation in Section 5.6. This case study has the lowest annual total capital and operating costs, as shown in Table 5.9, where operating pressure for both packed columns was considered from the rate-based model at pilot scale. Aspen Plus<sup>®</sup> was used to estimate packing heights. The packed columns' diameter was calculated from scale-up calculations. The sump level and buffer tank size were calculated based on a 10-minute hold-up time for the residence to fill. It is the commercial scale of the validated PCC model compared to the experimental data. To conduct a dynamic model of commercial PCC, some equipment is added to stabilise the the transient behaviour in order to run a dynamic model of commercial PC behaviour, such as an absorber sump, a stripper sump, an external condenser, including a heat exchanger and a reflux drum, and a buffer tank for water and solvent make-up to compensate for the loss in the whole process. For the sump, reflux drum, and buffer tank, the size should be estimated before exporting the steady-state model to Aspen Dynamics<sup>®</sup>. The calculations are conducted based on the flow rate at steady-state.

**Table 5.9: Base case operating conditions of absorber for commercial PCC model using PZ with AMP**

Parameter	Value
Absorber	
Flue gas flowrate (kg/s)	356
Lean solvent flowrate (kg/s)	551.8
Absorber diameter (m)	13.34
Packing height(m)	30
Operating pressure(N/m <sup>2</sup> )	97000
Absorber pressure drop(bar)	0.1
Packing material	IMTP#40
Number of stages	20
Sump level(m)	0.3
Sump diameter(m)	13.34
CO <sub>2</sub> capture level (%)	90
Model type	Equilibrium-based model

The stripper specifications with external condenser, including heat exchanger, reflux drum, and buffer tank are given in Table 5.10

**Table 5.10: Base case operating conditions of stripper for commercial PCC model using PZ with AMP**

Parameter	Value
Packing height(m)	30
Stripper diameter(m)	8
Operating pressure(N/m <sup>2</sup> )	162090
Stripper pressure drop	0.1
Number of stages	20
Model type	Equilibrium-based model
Packing material	FLEXIPAC 1Y
Re-boiler duty (MW)	77
Re-boiler temperature(K)	389.39
Condenser Temperature(K)	355
Reflux drum level(m)	0.7
Sump level(m)	0.3
Sump diameter(m)	8
Buffer tank level(m)	10
Buffer tank diameter(m)	6

- Operating pressure was taken from rate-based model, where absorber is operated at atmospheric pressure to reduce the solvent degradation.
- Number of stages: It is estimated based on the CO<sub>2</sub> composition profile in liquid phase. It is specified when there is equilibrium transfer in its composition.
- CO<sub>2</sub> capture level: it was specified to be 90 % to have tradeoff between profit and efficiency.
- Sump diameter: It was included in the packed column, where it assumed to be the same absorber diameter.
- Sump level: It was assumed by taken the flowrate of the packed column last stage and assume 10 min hold up time residence to fill the whole packed column.
- Model type: it is an equilibrium-based model to be prepared for Aspen Dynamics because this software does not support kinetic reactions.

### 5.8.1 Control structure and design

Control structures are selected based on open loop analysis where it is represented in Figure 5.6 . For CO<sub>2</sub> capture, it was controlled by comparing the CO<sub>2</sub> mass flow in the flue gas stream entering the bottom of the absorber with the CO<sub>2</sub> mass flow in the vented gas stream leaving the top of the absorber and then adjusting the lean solvent flow rate. Condenser temperature was controlled by manipulating condenser heat duty. Also, the re-boiler temperature was controlled by adjusting the re-boiler heat duty in the stripper. Water makeup was paired with water mass fraction in lean solvent flowrate, which was treated as a variable to be manipulated.

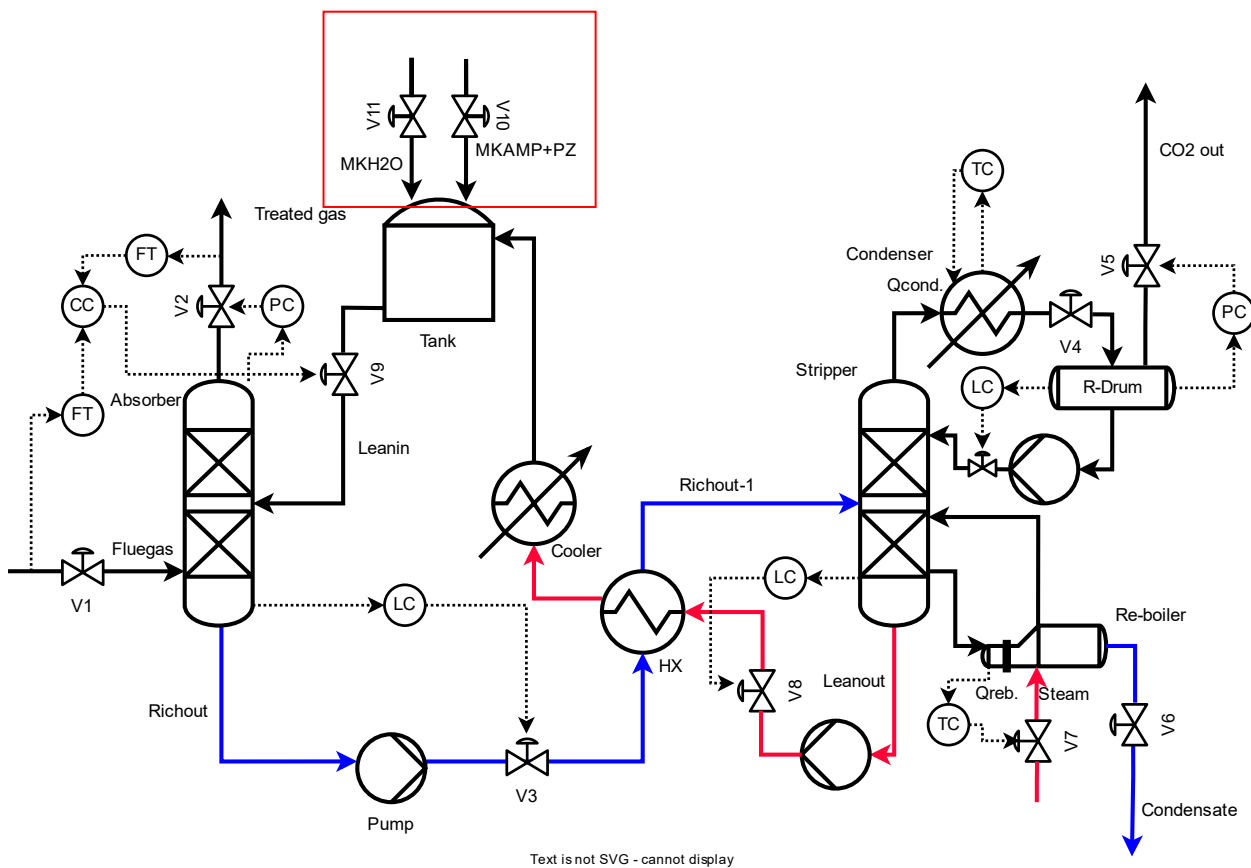


**Figure 5.6: A schematic of PCC model with control structure using PZ with AMP**

In a packed column sump, the absorber sump level was controlled by manipulating the valve (3). By adjusting the valve (8), the stripper sump level can be tightly controlled. The drum level is controlled by manipulating the valve after the reflux drum. Liquid levels in the whole process should be tightly controlled to enhance the controllability of the CO<sub>2</sub> capture level and re-boiler temperature. The controller type used in this process is conventional control. P controllers were selected for the liquid level controller. On the other hand, CO<sub>2</sub> capture level, re-boiler temperature, and condenser temperature were

controlled using a PI controller. The tuning parameters are shown in Table 5.11. In this study, CO<sub>2</sub> capture level and re-boiler temperature were assessed dynamically against setpoint tracking and disturbance change, which are discussed in Section 5.8.1.

**Table 5.11: Tuning parameter for control structure**

Manipulated variables	Controlled variables	Controller type	$\tau_i$ (min)	$K_c$ gain	setpoint
Valve 3	Absorber sump Level (m)	Proportional	-	42	0.45
Valve 8	Stripper sump Level (m)	Proportional	-	82	0.56
Valve 12	Drum level (m)	Proportional	-	145	3
Lean solvent flowrate	CO <sub>2</sub> capture level (%)	Proportional /Integral	25	17	90
Re-boiler duty	Re-boiler temperature (K)	Proportional /Integral	40	7	388.229
Condenser duty	Condenser temperature(K)	Proportional /Integral	9	4	355

## 5.8.2 Process control evaluation

PCC process control evaluation was assessed using two criteria: disturbance rejection, which is expressed by flue gas flowrate change, which illustrates the fluctuation in the operation of power demand, and its response to reject the effect of flue gas flowrate fluctuation. The second evaluation is the CO<sub>2</sub> capture level setpoint step change.

### 5.8.2.1 Flue gas step change

This scenario is expressed by a 10% step change increase in flue gas flowrate where the setpoint is 356 kg/s to analyse its effect on CO<sub>2</sub> capture level and re-boiler temperature.

Figure 5.7, Figure 5.8 show that a +10 flue gas step change reduces CO<sub>2</sub> capture level and re-boiler temperature. However, re-boiler temperature had a spike due to valve opening for lean solvent flowrate to compensate the reduction in the CO<sub>2</sub> capture level.

There is a fluctuation because the stability issue in controllability as this process is classified as an integrated process.

The reduction in re-boiler temperature was achieved by increasing the re-boiler duty required in the re-boiler. This dynamic performance has a similar trend as previous studies (Lawal, 2011; Nittaya, 2014). Additionally, it is observed that the dynamic performance at the commercial scale has similar behaviour at the pilot scale. Both variables have settling times of 8, 9, and 2 hours for CO<sub>2</sub> capture level and re-boiler temperature.

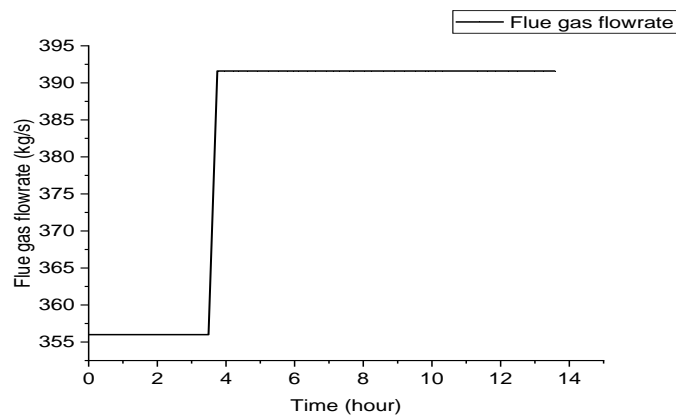


**Figure 5.7: 10% flue gas step change using PZ with AMP**



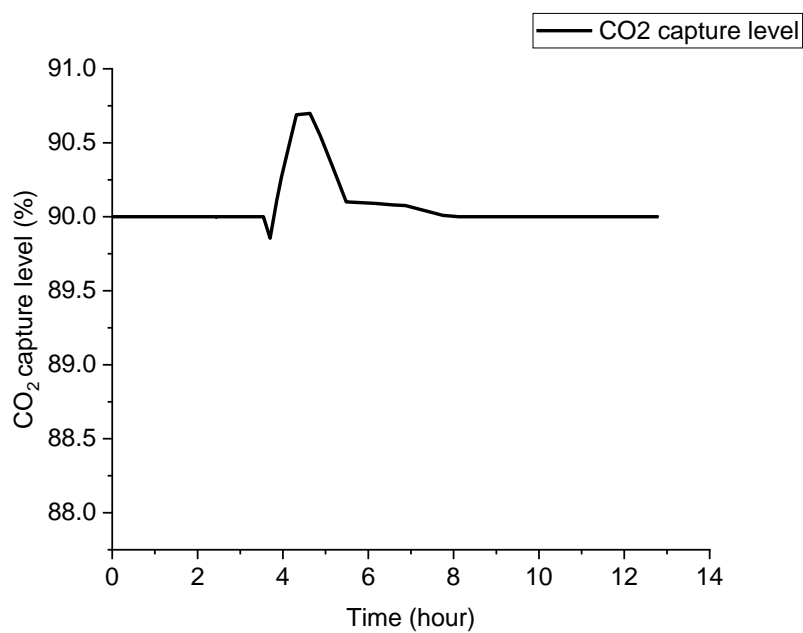


Figure 5.8: CO<sub>2</sub> capture level performance with flue gas step change using PZ with AMP

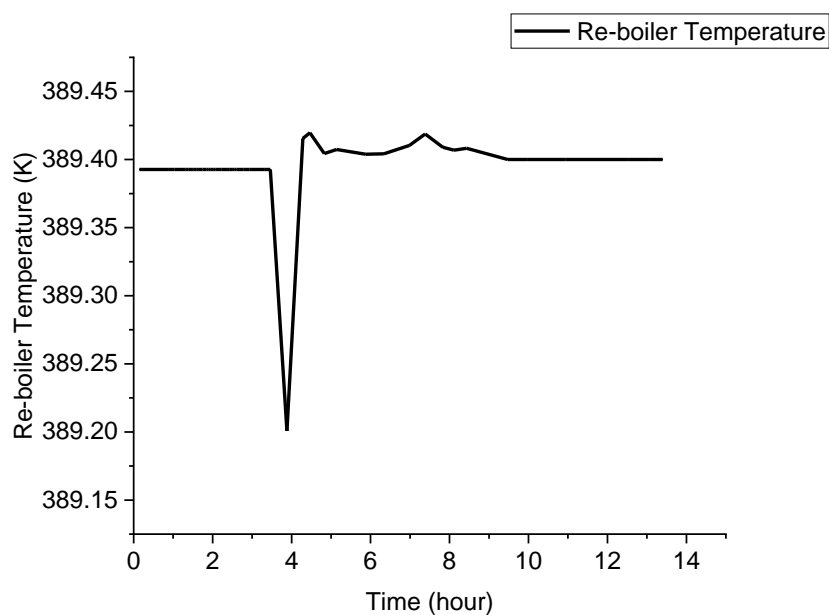


Figure 5.9: Re-boiler temperature performance with flue gas step change using PZ with AMP

### 5.8.2.2 CO<sub>2</sub> capture level step change

This scenario was evaluated by increasing the setpoint CO<sub>2</sub> capture level from 90 to 85% to investigate its impact on re-boiler duty in the stripper, as shown in Figure 5.10. Figure

5.11 depicts the trend of re-boiler duty as CO<sub>2</sub> capture level decreases. where it has decreased because of the decrease in lean solvent flow rate. Consequently, a low vapour flow rate is provided in the stripper. Moreover, the settling time is high, at 9.9 hours to reach the first steady-state. In the case of step change in CO<sub>2</sub> capture level from 90% to 85% , re-boiler duty was reduced at 4 hours. However, there is a small spike, showing that re-boiler duty is increased due to the steam flowrate supplied to the re-boiler at 4.5 hours, which may vary rapidly. Hence, it affects the stability of and transient performance of the process to meet the reduction in the amount of CO<sub>2</sub> captured.

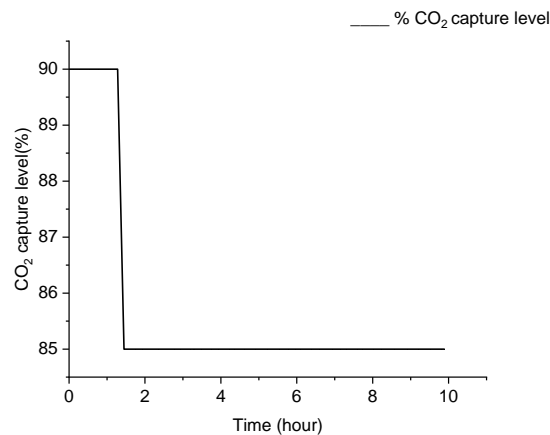


Figure 5.10: CO<sub>2</sub> capture level change -5.5% using PZ with AMP

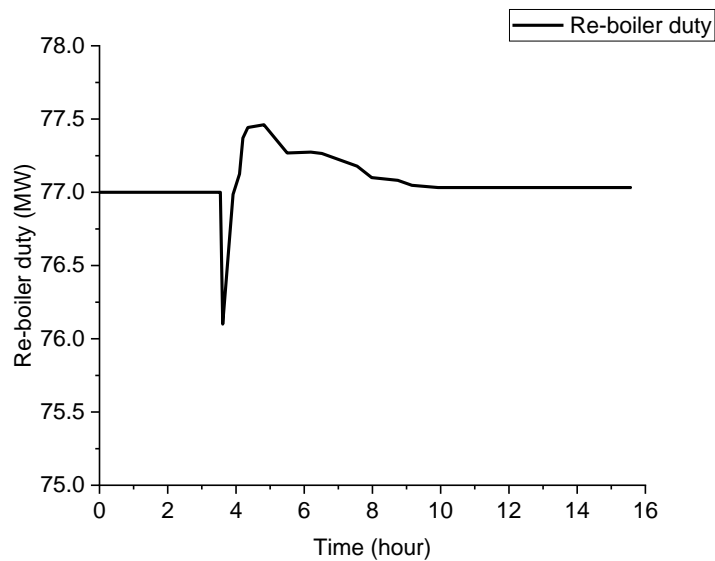


Figure 5.11: Re-boiler duty performance with -5.5% CO<sub>2</sub> capture level

## 5.9 Conclusion

In this chapter, Aspen Plus<sup>®</sup> was used to develop steady-state modelling of a solvent-based PCC process using a blend of PZ and AMP. Model validation was performed at pilot scale against the CESAR 1 pilot plant (Zhang *et al.*, 2017). The model validation findings confirmed the rate-based model is in agreement with the experimental data from previous studies. A scale-up procedure was conducted using the same method as in the previous study (Canepa *et al.*, 2013) to meet the needs of a 250 MWe CCGT power plant. A technical evaluation was implemented to obtain the optimal value for the operating conditions. Additionally, economic evaluation was investigated. Finally, control structure and design were analysed in Aspen Dynamics<sup>®</sup>. The following key findings are presented in this chapter:

- The rate-based model was validated against the experimental data with a lower than 6.2% deviation. Furthermore, the temperature profile for both packed columns accurately predicts the temperature profile in the experimental data, demonstrating that the temperature bulge is located at the bottom or top of the packed columns.
- The The scale-up procedure was performed from the pilot scale to the 250 MWe CCGT power plant to obtain the packed column sizes. The absorber diameter was 13.34 m, while the stripper diameter was 11 m. The packed columns' height was assumed to be 30 m. The scale-up method accurately predicts absorber and stripper performance at pilot scale.
- Technical analysis revealed that CO<sub>2</sub> lean loading affects the L/G ratio and specific re-boiler duty, with 0.3 mol CO<sub>2</sub>/mol PZ being the optimal CO<sub>2</sub> lean loading. A technical evaluation was performed using different blend ratios, and it was observed that using 7% wt. PZ with 38% wt. AMP has lower energy consumption and a lower L/G ratio compared to other blend ratios.
- Dynamic analysis of solvent-based PCC indicates that the settling times for CO<sub>2</sub> capture level and re-boiler temperature in the case of a +10% flue gas step change were 8 and 9.1 hours, respectively. On the other hand, the re-boiler duty settling time was 10 hours.

## Chapter 6: Comparative analysis of PCC using MEA, PZ, and (PZ with AMP)

This chapter presents the comparative results between the three solvents; MEA, PZ, and PZ with AMP in terms of scale-up calculation including the packed column sizes (diameter and height), technical evaluation results, Economic evaluation, and dynamic performance.

### 6.1 Comparative analysis of scale-up

Scale-up results for the three models show that using PZ has the lowest packed bed column sizes including diameter and height as shown in Table 6.1. Hence, it is indicated that using PZ solvent has lower capital cost than MEA and mixed solvents. Moreover, the best appropriate solvent selection will enhance the trade-off procedure between efficiency and low operating and capital costs. In Table 6.1, it is clear that the packed column sizes for absorber and stripper are different for each solvent. In the case of absorber size, including the diameter and height, the diameter was 13.95 m for MEA solvent, which exhibits the largest diameter solvent has the smallest absorber diameter, which equals 12.3. Hence, Lower L/G ratio. On the other hand, mixed solvents (PZ with AMP) has 13.34 m, which is close to the benchmark solvent MEA. Absorber heights were auto estimated in Aspen Plus<sup>®</sup>, by considering the calculated required lean solvent flowrate needed to provide 90% CO<sub>2</sub> capture level. The finding presents that the benchmark solvent MEA and mixed solvents have higher absorber heights compared to PZ solvent, which has 22 m.

In terms of stripper column, the similar results were obtained, which follow the absorber sizes. The lowest stripper diameter was clear when PZ solvent was used. It has the lowest L/G ratio at commercial scale. It exhibits 6.67m for stripper diameter. On the other hand, MEA solvent had the highest stripper diameter, which equals 7.9m, while mixed solvents shows that the stripper diameter was 7m. The stripper heights for the three solvents were the same as in absorber columns.

**Table 6.1: Packed bed column sizes resulting from scale-up calculations**

Packed bed size (m)	MEA	PZ	PZ with AMP
Absorber diameter	13.95	12.3	13.34
Absorber height	30	22	30
Stripper diameter	7.9	6.67	7
Stripper height	30	22	30

## 6.2 Comparative results of technical and economic evaluations

The results of the technical evaluation, which are efficient in terms of energy consumption and have low operating and capital costs throughout the process, show that the L/G ratio and specific re-boiler duty must be optimised with changing CO<sub>2</sub> lean loading. The three scaled-up models were optimised using three solvents as given in Figure 6.1 , which illustrates that in terms of specific re-boiler duty, PZ with AMP had the lowest value, which is equal to 2.95 GJ/tonne CO<sub>2</sub>. However, it has the highest L/G ratio among other solvents because it has a lower value in terms of absorption capacity while having a lower regeneration duty. To conclude based on energy consumption and L/G ratio, mixed solvent utilisation illustrates the lowest energy consumption for solvent-based PCC because its specific re-boiler duty was 2.95 GJ/tonne CO<sub>2</sub>. In the case of MEA and PZ, specific re-boiler duty was 4.17 GJ/tonne CO<sub>2</sub>, and 3.83 GJ/tonne CO<sub>2</sub>, respectively. The lowest L/G ratio was obtained when 40% wt. PZ was performed, which equals 0.76 kg/kg.

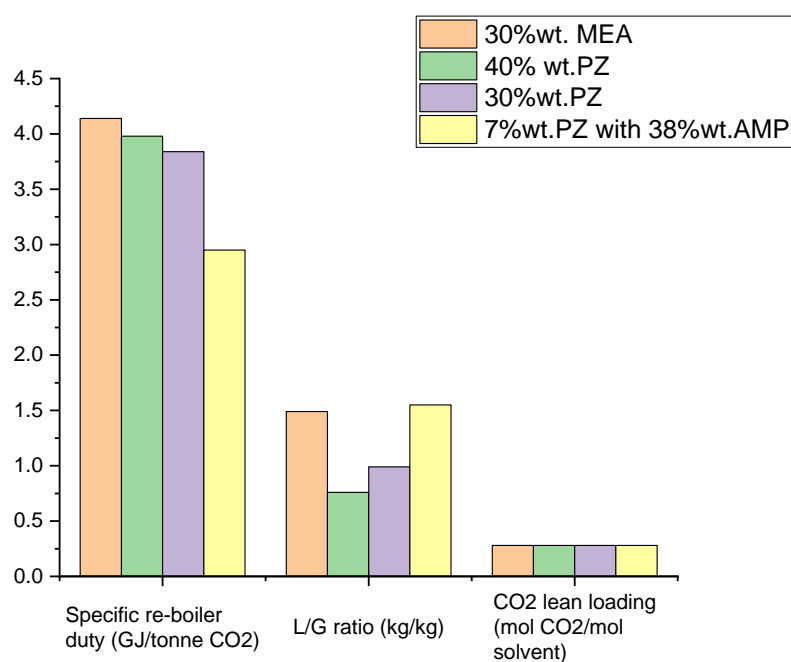


**Figure 6.1: Comparative results of technical evaluation for the three solvents**

Based on economic evaluation, it was estimated that the lowest total annualised total cost was obtained when using 40%wt. PZ, followed by mixed solvent PZ with AMP, as shown in Table 6.2. Consequently, single solvents (PZ) and mixed solvents (PZ with AMP) show lower energy consumption in terms of re-boiler duty and lower operating costs compared to the benchmark solvent (MEA). Annualized total costs for MEA solvent were 16.53 million pounds per year and 21.9 pounds per tonne CO<sub>2</sub>, respectively. On the other hand, PZ solvent at different concentrations, such as 30 and 40%wt. exhibits 19.7 and 16.2 M£/year, and the costs per tonne CO<sub>2</sub> were 25.5 and 21 M£/tonne CO<sub>2</sub>, respectively. In mixed solvents, the costs were 16.5 M£/year and 21.1 M£/tonne CO<sub>2</sub>, respectively.

**Table 6.2: Economic evaluation comparison for three solvents**

Solvent	Annualised total cost (M£/year)	Annualised total cost (£/tonne CO <sub>2</sub> )
30% wt. MEA	16.53	21.9
30% wt. PZ	19.7	25.5
40% wt. PZ	16.2	21
7%wt. PZ with 38% wt. AMP	16.5	21.1

### 6.3 Dynamic performance comparison

Dynamic performance assessment was performed based on settling time to steady-state and integral square error. For example Integral square error of CO<sub>2</sub> capture level was calculated using the equation 6.1:

$$ISE (CO_{2\text{CAPTURE LEVEL}})\% = \sum_{t=0}^{tf} (CO_{2\text{CAPTURE SP}} - CO_2(t))^2 \quad 6.1$$

The ISE was calculated for all solvent-based PCC models using three different solvents: MEA, PZ, PZ with AMP. The ISE measurements were conducted based on two cases : +10% flue gas step change (disturbance rejection) and CO<sub>2</sub> capture level step change (setpoint tracking) from 90 to 85%, which equal -5.5%. The results are provided by Table 6.3.

**Table 6.3: Integral square error results for solvent-based PCC using the three solvents**

Specification	+10% Flue gas step change (ISE%)	-5.5% CO <sub>2</sub> capture level step change (ISE%)
30 wt.% MEA		
CO <sub>2</sub> capture level (%)	38.157	-
Re-boiler temperature(K)	0.01298	
Re-boiler duty (MW)		0.1712
40wt.% PZ		
CO <sub>2</sub> capture level (%)	3.588	-
Re-boiler temperature(K)	0.000539	-
Re-boiler duty (MW)	-	0.077
7wt.% PZ with 38wt.% AMP		

CO <sub>2</sub> capture level (%)	1.515	-
Re-boiler temperature(K)	0.040	-
Re-boiler duty (MW)	-	1.722

According to the ISE results, the ISE of the CO<sub>2</sub> capture level for PZ solvent in the case of disturbance rejection (flue gas step change) was the lowest value among MEA, PZ with AMP, indicating that the deviation from the CO<sub>2</sub> capture level setpoint is negligible. Also, the ISE of the re-boiler temperature showed a lower value for PZ solvent as well. In terms of setpoint tracking (CO<sub>2</sub> capture level). The ISE of re-boiler duty showed the lowest value among other solvents. It was observed that 40% wt. PZ has the shortest settling time among MEA and mixed solvents (PZ with AMP), as given in Table 6.4. This chapter analyses the dynamic performance of PCC process through chemical absorption at commercial scale. The methodology was to develop three models using different solvents, such as MEA, PZ, and a blend of PZ and AMP. Using three solvents, it provides discrepancies in their chemical and physical characteristics, which has impact on L/G ratio and specific re-boiler duty. The dynamic performance of a solvent-based PCC process at commercial scale shows similar correlations as the process at pilot scale. Hence, it was confirmed that scaling up the rate-based model does not affect the behaviour of transient analysis but affects the time constant variable and settling time for the three models. Consequently, the residence time is different for the three solvents.

**Table 6.4: Settling time of dynamic performance for the three solvents**

Specification	+10% Flue gas step change (Settling time -hour)	-5.5% CO <sub>2</sub> capture level step change (settling time-hour)
30 wt.% MEA		
CO <sub>2</sub> capture level (%)	8	
Re-boiler temperature(K)	9.2	
Re-boiler duty (MW)	-	10



40wt.% PZ		
CO <sub>2</sub> capture level (%)	6	
Re-boiler temperature(K)	5.5	
Re-boiler duty (MW)	-	5.5
7wt.% PZ with 38wt.% AMP		
CO <sub>2</sub> capture level (%)	8	
Re-boiler temperature(K)	9.1	
Re-boiler duty (MW)	-	10

## 6.4 Conclusion

- Rate-based PCC models were developed via Aspen Plus<sup>®</sup> at pilot scale for three solvents: MEA, PZ, and PZ with AMP. Model validations were implemented against experimental data to assure the reliability of the three models. Validation results confirmed that the three models accurately predict the experimental data with less than 10% error, as represented by temperature profile plots for both packed bed columns.
- Scale-up of the validated rate-based model to a 250 MWe CCGT power plant shows the packed column sizes for 40% PZ have the lowest value compared to MEA and PZ with AMP due to the smallest lean solvent flowrate required to provide 90% CO<sub>2</sub> capture.
- The technical evaluation results for three solvents demonstrate that PZ with AMP has the lowest specific re-boiler duty, which was 2.95 GJ/tonne CO<sub>2</sub>, compared to 30% and 40% wt.PZ which were 3.84 and 3.92 GJ/tonne CO<sub>2</sub>, respectively. However, a larger L/G ratio is estimated in mixed solvents. For MEA, in terms of energy consumption, the specific re-boiler duty was 4.14 GJ/tonne CO<sub>2</sub>.
- An economic analysis was carried out to determine which of the three solvents had the lowest total annualised cost per tonne CO<sub>2</sub>. It cost 21£ per tonne CO<sub>2</sub>, 21.1£ per tonne CO<sub>2</sub>, and 21.9£ per tonne CO<sub>2</sub> for 40% wt. PZ, 7% wt. PZ, 38%wt. AMP, and 30%wt.MEA, respectively.

- A dynamic performance assessment was performed based on the settling time to steady-state and the ISE calculation. It was observed that 40%wt. PZ has the shortest settling time among MEA and mixed solvents (PZ with AMP) and the lowest value in terms of ISE.

## Chapter 7: Conclusion and recommendation for future research

This research studies the dynamic performance of PCC process through chemical absorption at commercial scale. The methodology was to develop three models using different solvents, such as MEA, PZ, and a blend of PZ and AMP. Using three solvents, it provides discrepancies in their chemical and physical characteristics, which has impact on L/G ratio and specific re-boiler duty. The dynamic performance of a solvent-based PCC process at commercial scale shows similar correlations as the process at pilot scale. Hence, it was confirmed that scaling up the rate-based model does not affect the behaviour of transient analysis but affects the time constant variable and settling time for the three models. Consequently, the residence time is different for the three solvents. The limitation of this study is discussed as follows:

- The reliability of Aspen dynamics<sup>®</sup> is lower because this software does not support kinetic reactions, which means lower reliability in providing the 90% CO<sub>2</sub> capture level, but it was solved by providing the temperature profile of a rate-based model to the theoretical tray efficiency of an equilibrium-based model to obtain the 90% CO<sub>2</sub> capture level.
- Piperazine has a low viscosity at low CO<sub>2</sub> lean loading as a physical property. This issue increases the divergence of the model in the case of PZ solvent.
- Aspen Dynamics<sup>®</sup> is classified as an integrated process, so using it as a Blackbox model might weaken the understanding of dynamic performance of the entire process.

In this chapter, conclusion and recommendations are discussed.

### 7.1 Conclusion

- Rate-based PCC models were developed via Aspen Plus<sup>®</sup> at pilot scale for three solvent MEA, PZ, and PZ with AMP. Models validations were implemented against experimental data to assure reliability of the three models. Validation results confirmed that the three models predict well the experimental data with

lower than 10% deviation, representing the temperature bulge location by temperature profile plots for both packed bed columns.

- Scale-up of validated rate-based model to 250 MWe CCGT power plant shows the packed column sizes for 40% PZ have lowest value compared to MEA, PZ with AMP due to the smallest lean solvent flowrate required to provide 90% CO<sub>2</sub> capture level.
- Technical evaluation results for three solvents demonstrate PZ with AMP has lowest specific re-boiler duty which was 2.95 GJ/tonne CO<sub>2</sub> compared to 30, 40% wt.PZ which were 3.84, 3.92 GJ/tonne CO<sub>2</sub>, respectively. However, Larger L/G ratio is estimated in mixed solvents. For MEA, in term of energy consumption, specific re-boiler duty was 4.14 GJ/tonne CO<sub>2</sub>.
- Economic evaluation was performed to assess the lowest total annualised cost per tonne CO<sub>2</sub> for the three solvents. The total annualised cost equals 21£ per tonne CO<sub>2</sub>, 21.1 £ per tonne CO<sub>2</sub>, 21.9 £ per tonne CO<sub>2</sub>, for 40% wt. PZ, 7% wt.PZ with 38%wt. AMP, 30%wt.MEA, respectively.
- Dynamic performance assessment was performed based on settling time to steady-state and ISE calculation. It was observed that 40%wt. PZ has the shortest settling time among MEA and mixed solvents (PZ with AMP) and the lowest value in term of ISE. The aim of dynamic modelling is to analyse the effect of setpoints tracking and disturbance rejection on the entire process for three solvents. The difference between three solvent is the time residence, where it is affected by lean solvent flowrate. In reality, it is important to gain knowledge about the process in case of shortage in lean solvent flowrate, low flue gas flowrate, low steam provided to re-boiler. Consequently, this process is integrated with power load. The control action should be faster in a sufficient way to provide stable dynamic behaviour

## 7.2 Recommendation for future research

- Due to the high energy consumption and high operating and capital costs connected to MEA as a benchmark solvent, using a tertiary blend such as MEA, PZ, or AMP should be investigated to analyse its effect on energy consumption and operating and capital costs.
- an investigation study on process modifications such as rich solvent split, intercooling, or mixed process modifications to assess their impact on reducing energy consumption related to solvent regeneration.
- Analytical assessments of solvent physical properties should be investigated to provide a thorough understanding of solvent mixed selection.
- The multiple input, multiple output control structure should be considered in the PCC process because it is classified as an integrating process.

## References

- Abu-Zahra, Mohammad R.M., Schneiders, Léon H.J., Niederer, John P.M., Feron, Paul H.M. and Versteeg, Geert F. (2007), CO<sub>2</sub> Capture from Power Plants. Part I. A Parametric Study of the Technical Performance Based on Monoethanolamine. *International Journal of Greenhouse Gas Control*, 1(1): 37–46.
- Abu-Zahra, Mohammad R M, Niederer, John P M, Feron, Paul H M and Versteeg, Geert F (2007), CO<sub>2</sub> Capture from Power Plants: Part II. A Parametric Study of the Economical Performance Based on Mono-Ethanolamine. *International journal of greenhouse gas control*, 1(2): 135–142.
- Adeosun, Adewale, Hadri, Nabil El, Goetheer, Earl and Abu-Zahra, Mohammad R M (2013), Absorption of CO<sub>2</sub> by Amine Blends Solution: An Experimental Evaluation. *Research Inventy: International Journal Of Engineering And Science Issn Www.Researchinventy.Com*, 3(9p): 12–23.
- Agbonghae, E. O., Hughes, K. J., Ingham, D. B., Ma, L. and Pourkashanian, M. (2014), Optimal Process Design of Commercial-Scale Amine-Based CO<sub>2</sub> Capture Plants. *Industrial and Engineering Chemistry Research*, 53(38): 14815–14829.
- Åkesson, Johan, Laird, Carl D, Lavedan, Geoffry, Prölliß, Katrin, Tummescheit, Hubertus, Velut, Stephane and Zhu, Yu (2012), Nonlinear Model Predictive Control of a CO<sub>2</sub> Post-combustion Absorption Unit. *Chemical Engineering & Technology*, 35(3): 445–454.
- Akinola, Toluleke Emmanuel, Oko, Eni and Wang, Meihong (2019), Study of CO<sub>2</sub> Removal in Natural Gas Process Using Mixture of Ionic Liquid and MEA through Process Simulation. *Fuel*, 236(July 2018): 135–146.
- Al-malah, Kamal i.m. (2017), *Aspen Plus (Chemical Engineering Applications)*.
- Alatiqi, I., Sabri, M. F., Bouhamra, W. and Alper, E. (1994), Steady-State Rate-Based Modelling for CO<sub>2</sub>/Amine Absorption-Desorption Systems. *Gas Separation and Purification*, 8(1): 3–11.
- Artanto, Yuli, Jansen, James, Pearson, Pauline, Puxty, Graeme, Cottrell, Aaron, Meuleman, Erik and Feron, Paul (2014), Pilot-Scale Evaluation of AMP/PZ to Capture

- CO<sub>2</sub> from Flue Gas of an Australian Brown Coal-Fired Power Station. *International Journal of Greenhouse Gas Control*, 20: 189–195.
- AspenTech (2010), Aspen Plus: Rate-Based Model of the CO<sub>2</sub> Capture Process by MEA Using Aspen Plus (ENRTL-RK). : 1–25.
- Athanasios I. Papadopoulos (2017), *Process Systems and Materials for CO<sub>2</sub> Capture*.
- Baumann, Hans D (2009), *Control Valve Primer: A User's Guide*. ISA.
- Biliyok, Chechet, Lawal, Adekola, Wang, Meihong and Seibert, Frank (2012), Dynamic Modelling, Validation and Analysis of Post-Combustion Chemical Absorption CO<sub>2</sub> Capture Plant. *International Journal of Greenhouse Gas Control*, 9(2012): 428–445.
- Bishnoi, Sanjay and Rochelle, Gary T (2000), Absorption of Carbon Dioxide into Aqueous Piperazine: Reaction Kinetics, Mass Transfer and Solubility. *Chemical engineering science*, 55(22): 5531–5543.
- Bravo, Jose L (1985), Mass Transfer in Gauze Packings. *Hydrocarbon processing*, 64(1): 91–95.
- Bravo, Jose L, Rocha, J Antonio and Fair, J R (1992), A Comprehensive Model for the Performance of Columns Containing Structured Packings, A489–A489, in: *Institution of Chemical Engineers Symposium Series*. HEMISPHERE PUBLISHING CORPORATION.
- Canepa, Roberto, Wang, Meihong, Biliyok, Chechet and Satta, Antonio (2013), Thermodynamic Analysis of Combined Cycle Gas Turbine Power Plant with Postcombustion CO<sub>2</sub> Capture and Exhaust Gas Recirculation. *Proceedings of the Institution of Mechanical Engineers, Part E: Journal of Process Mechanical Engineering*, 227(2): 89–105.
- Chen, Chau-Chyun and Evans, Lawrence B (1986), A Local Composition Model for the Excess Gibbs Energy of Aqueous Electrolyte Systems. *AIChE journal*, 32(3): 444–454.
- Chilton, Thomas H and Colburn, Allan Philip (1934), Mass Transfer (Absorption) Coefficients Prediction from Data on Heat Transfer and Fluid Friction. *Industrial & engineering chemistry*, 26(11): 1183–1187.
- Closmann, Fred, Nguyen, Thu and Rochelle, Gary T (2009), MDEA/Piperazine as a Solvent for CO<sub>2</sub> Capture. *Energy Procedia*, 1(1): 1351–1357.

- Dash, Sukanta Kumar, Samanta, Amar Nath and Bandyopadhyay, Syamalendu S. (2014), Simulation and Parametric Study of Post Combustion CO<sub>2</sub> Capture Process Using (AMP+PZ) Blended Solvent. *International Journal of Greenhouse Gas Control*, 21: 130–139.
- Davis, Jason and Rochelle, Gary (2009), Thermal Degradation of Monoethanolamine at Stripper Conditions. *Energy Procedia*, 1(1): 327–333.
- Deiana, Paolo, Bassano, Claudia, Calì, Gabriele, Miraglia, Paolo and Maggio, Enrico (2017), CO<sub>2</sub> Capture and Amine Solvent Regeneration in Sotacarbo Pilot Plant. *Fuel*, 207: 663–670. available at <http://dx.doi.org/10.1016/j.fuel.2017.05.066>
- Dietl, Karin, Joos, Andreas and Schmitz, Gerhard (2012), Dynamic Analysis of the Absorption/Desorption Loop of a Carbon Capture Plant Using an Object-Oriented Approach. *Chemical Engineering and Processing: Process Intensification*, 52: 132–139.
- Mac Dowell, N., Samsatli, N. J. and Shah, N. (2013), Dynamic Modelling and Analysis of an Amine-Based Post-Combustion CO<sub>2</sub> Capture Absorption Column. *International Journal of Greenhouse Gas Control*, 12: 247–258.
- Dugas, Ross E (2006), Pilot Plant Study of Carbon Dioxide Capture by Aqueous Monoethanolamine. *MSE Thesis, University of Texas at Austin*.
- Dugas, Ross E and Rochelle, Gary T (2011), CO<sub>2</sub> Absorption Rate into Concentrated Aqueous Monoethanolamine and Piperazine. *Journal of Chemical & Engineering Data*, 56(5): 2187–2195.
- Enaasen, Nina, Zangrilli, Luigi, Mangiaracina, Angela, Mejdell, Thor, Kvamsdal, Hanne M. and Hillestad, Magne (2014), Validation of a Dynamic Model of the Brindisi Pilot Plant. *Energy Procedia*, 63(1876): 1040–1054.
- Engineering world (2018), Flow Calculation for Gases. *East Grand Folks*, (Cv): 1.
- Ermatchkov, Viktor, Pérez-Salado Kamps, Álvaro, Speyer, Dirk and Maurer, Gerd (2006), Solubility of Carbon Dioxide in Aqueous Solutions of Piperazine in the Low Gas Loading Region. *Journal of Chemical & Engineering Data*, 51(5): 1788–1796.
- Feron, Paul H.M., Cousins, Ashleigh, Jiang, Kaiqi, Zhai, Rongrong and Garcia, Monica (2020), An Update of the Benchmark Post-Combustion CO<sub>2</sub>-Capture Technology.



*Fuel*, 273(April): 117776.

Flø, Nina Enaasen, Knuutila, Hanna, Kvamsdal, Hanne Marie and Hillestad, Magne (2015), Dynamic Model Validation of the Post-Combustion CO<sub>2</sub> Absorption Process. *International Journal of Greenhouse Gas Control*, 41: 127–141.

Fredriksen, S. B. and Jens, Klaus J. (2013), Oxidative Degradation of Aqueous Amine Solutions of MEA, AMP, MDEA, Pz: A Review. *Energy Procedia*, 37(1876): 1770–1777.

Freeman, Stephanie Anne and Rochelle, Gary Thomas (2012), Thermal Degradation of Aqueous Piperazine for CO<sub>2</sub> Capture: 2. Product Types and Generation Rates. *Industrial and Engineering Chemistry Research*, 51(22): 7726–7735.

Freguia, Stefano and Rochelle, Gary T. (2003), Modeling of CO<sub>2</sub> Capture by Aqueous Monoethanolamine. *AIChE Journal*, 49(7): 1676–1686.

Gabrielsen, Jostein (2005), CO<sub>2</sub> Capture from Coal Fired Power Plants. *PhD thesis*: 61.

Gáspár, Jozsef and Cormoş, Ana-Maria (2011), Dynamic Modeling and Validation of Absorber and Desorber Columns for Post-Combustion CO<sub>2</sub> Capture. *Computers & Chemical Engineering*, 35(10): 2044–2052.

Gaspar, Jozsef, Gladis, Arne, Jørgensen, John Bagterp, Thomsen, Kaj, von Solms, Nicolas and Fosbøl, Philip Loldrup (2016), Dynamic Operation and Simulation of Post-Combustion CO<sub>2</sub> Capture. *Energy Procedia*, 86: 205–214.

Gaspar, Jozsef, Jørgensen, John Bagterp and Fosbøl, Philip Loldrup (2015), Control of a Post-Combustion CO<sub>2</sub> Capture Plant during Process Start-up and Load Variations. *IFAC-PapersOnLine*, 28(8): 580–585.

Global, B. (2020), Statistical Review of World Energy - Global. *British Petroleum*: 6–9. available at [www.bp.com](http://www.bp.com)

Greer, T, Bedelbayev, A, Igreja, José M, Gomes, J F and Lie, B (2010), A Simulation Study on the Abatement of CO<sub>2</sub> Emissions by De-absorption with Monoethanolamine. *Environmental technology*, 31(1): 107–115.

Gupta, Neeraj, Paul, Darrell, Cumming, Lydia, Place, Matt and Mannes, Robert G (2014), Testing for Large-Scale CO<sub>2</sub>-Enhanced Oil Recovery and Geologic Storage in the Midwestern USA. *Energy Procedia*, 63: 6393–6403.

Van De Haar, Adam, Trapp, Carsten, Wellner, Kai, De Kler, Robert, Schmitz, Gerhard

- and Colonna, Piero (2017), Dynamics of Postcombustion CO<sub>2</sub> Capture Plants: Modeling, Validation, and Case Study. *Industrial and Engineering Chemistry Research*, 56(7): 1810–1822.
- Hanley, Brian and Chen, Chau-Chyun (2012), New Mass-transfer Correlations for Packed Towers. *AIChE Journal*, 58(1): 132–152.
- von Harbou, Inga, Mangalapally, Hari Prasad and Hasse, Hans (2013), Pilot Plant Experiments for Two New Amine Solvents for Post-Combustion Carbon Dioxide Capture. *International Journal of Greenhouse Gas Control*, 18: 305–314.
- Harun, Noorlisa, Nittaya, Thanita, Douglas, Peter L, Croiset, Eric and Ricardez-Sandoval, Luis A (2012), Dynamic Simulation of MEA Absorption Process for CO<sub>2</sub> Capture from Power Plants. *International Journal of Greenhouse Gas Control*, 10: 295–309.
- Hasanuzzaman, M, Zubir, Ummu Salamah, Ilham, Nur Iqtiyani and Che, Hang Seng (2017), Global Electricity Demand , Generation , Grid System , and Renewable Energy Polices : A Review . , 6(June): 1–18.
- Hetzer, Hannah B, Robinson, R A and Bates, Roger G (1968), Dissociation Constants of Piperazinium Ion and Related Thermodynamic Quantities from 0 to 50. Deg. *The Journal of Physical Chemistry*, 72(6): 2081–2086.
- Hill, L Bruce, Li, XiaoChun and Wei, Ning (2020), CO<sub>2</sub>-EOR in China: A Comparative Review. *International Journal of Greenhouse Gas Control*, 103: 103173.
- Huertas, José I, Gomez, Martin D, Giraldo, Nicolas and Garzón, Jessica (2015), CO<sub>2</sub> Absorbing Capacity of MEA. , 2015(2).
- Hüser, Nicole, Schmitz, Oliver and Kenig, Eugeny Y. (2017), A Comparative Study of Different Amine-Based Solvents for CO<sub>2</sub>-Capture Using the Rate-Based Approach. *Chemical Engineering Science*, 157: 221–231.
- Idem, Raphael, Wilson, Malcolm, Tontiwachwuthikul, Paitoon, Chakma, Amit, Veawab, Amornvadee, Aroonwilas, Adisorn and Gelowitz, Don (2006), Pilot Plant Studies of the CO<sub>2</sub> Capture Performance of Aqueous MEA and Mixed MEA/MDEA Solvents at the University of Regina CO<sub>2</sub> Capture Technology Development Plant and the Boundary Dam CO<sub>2</sub> Capture Demonstration Plant. *Industrial and Engineering Chemistry Research*, 45(8): 2414–2420.

- Incropera, Frank P, DeWitt, David P, Bergman, Theodore L and Lavine, Adrienne S (1996), *Fundamentals of Heat and Mass Transfer*. Wiley New York.
- Ingram, Geoffrey M (2007), Site Selection And Characterisation For Storage Of CO<sub>2</sub>—The Callide 'Oxy-Fuel' project Experience & Key Characterisation Work.
- Jassim, Majeed S., Rochelle, Gary, Eimer, Dag and Ramshaw, Colin (2007), Carbon Dioxide Absorption and Desorption in Aqueous Monoethanolamine Solutions in a Rotating Packed Bed. *Industrial and Engineering Chemistry Research*, 46(9): 2823–2833.
- Jayarathna, Sanoja A, Lie, Bernt and Melaaen, Morten C (2013), Dynamic Modelling of the Absorber of a Post-Combustion CO<sub>2</sub> Capture Plant: Modelling and Simulations. *Computers & Chemical Engineering*, 53: 178–189.
- Jin, Lu, Pekot, Lawrence J, Hawthorne, Steven B, Gobran, Brian, Greeves, Allan, Bosshart, Nicholas W, Jiang, Tao, Hamling, John A and Gorecki, Charles D (2017), Impact of CO<sub>2</sub> Impurity on MMP and Oil Recovery Performance of the Bell Creek Oil Field. *Energy Procedia*, 114: 6997–7008.
- Karimi, Mehdi, Hillestad, Magne and Svendsen, Hallvard F (2011), Capital Costs and Energy Considerations of Different Alternative Stripper Configurations for Post Combustion CO<sub>2</sub> Capture. *Chemical engineering research and design*, 89(8): 1229–1236.
- Karunaratne, Sumudu S., Eimer, Dag A. and Øi, Lars E. (2020), Physical Properties of MEA + Water + CO<sub>2</sub> Mixtures in Postcombustion CO<sub>2</sub> Capture: A Review of Correlations and Experimental Studies. *Journal of Engineering (United Kingdom)*, 2020.
- Kittel, J., Idem, R., Gelowitz, D., Tontiwachwuthikul, P., Parrain, G. and Bonneau, A. (2009), Corrosion in MEA Units for CO<sub>2</sub> Capture: Pilot Plant Studies. *Energy Procedia*, 1(1): 791–797.
- Knudsen, Jacob Nygaard, Andersen, Jimmy, Jensen, Jørgen Nørklit and Biede, Ole (2011), Results from Test Campaigns at the 1 t/h CO<sub>2</sub> Post-Combustion Capture Pilot-Plant in Esbjerg under the EU FP7 CESAR Project. *1st Post Combustion Capture Conference*: 2–3.
- Krótki, Aleksander, Tatarczuk, Adam, Stec, Marcin, Spietz, Tomasz, Więclaw-Solny, Lucyna, Wilk, Andrzej and Cousins, Ashleigh (2017), Experimental Results of Split

- Flow Process Using AMP/PZ Solution for Post-Combustion CO<sub>2</sub> Capture. *Greenhouse Gases: Science and Technology*, 7(3): 550–561.
- Kvamsdal, H. M., Jakobsen, J. P. and Hoff, K. A. (2009), Dynamic Modeling and Simulation of a CO<sub>2</sub> Absorber Column for Post-Combustion CO<sub>2</sub> Capture. *Chemical Engineering and Processing: Process Intensification*, 48(1): 135–144.
- Kvamsdal, H M, Jakobsen, J P and Hoff, K A (2009), Dynamic Modeling and Simulation of a CO<sub>2</sub> Absorber Column for Post-Combustion CO<sub>2</sub> Capture. *Chemical Engineering and Processing: Process Intensification*, 48(1): 135–144.
- Kvamsdal, Hanne M., Chikukwa, Actor, Hillestad, Magne, Zakeri, Ali and Einbu, Aslak (2011), A Comparison of Different Parameter Correlation Models and the Validation of an MEA-Based Absorber Model. *Energy Procedia*, 4: 1526–1533.
- Lawal, A., Wang, M., Stephenson, P., Koumpouras, G. and Yeung, H. (2010), Dynamic Modelling and Analysis of Post-Combustion CO<sub>2</sub> Chemical Absorption Process for Coal-Fired Power Plants. *Fuel*, 89(10): 2791–2801.
- Lawal, A., Wang, M., Stephenson, P. and Yeung, H. (2009), Dynamic Modelling of CO<sub>2</sub> Absorption for Post Combustion Capture in Coal-Fired Power Plants. *Fuel*, 88(12): 2455–2462.
- Lawal, Adekola (2011), Study Of Post-Combustion CO<sub>2</sub> Capture For Coal-Fired Power Plant Through modelling And Simulation. *Phd Thesis*: 264–267.
- Lawal, Adekola, Wang, Meihong, Stephenson, Peter and Obi, Okwose (2012), Demonstrating Full-Scale Post-Combustion CO<sub>2</sub> Capture for Coal-Fired Power Plants through Dynamic Modelling and Simulation. *Fuel*, 101: 115–128.
- Lawal, Adekola, Wang, Meihong, Stephenson, Peter and Yeung, Hoi (2009), Dynamic Modeling and Simulation of CO<sub>2</sub> Chemical Absorption Process for Coal-Fired Power Plants, 1725–1730, in: *Computer Aided Chemical Engineering*. Elsevier.
- Li, Fei, Zhang, Jie, Oko, Eni and Wang, Meihong (2015), Modelling of a Post-Combustion CO<sub>2</sub> Capture Process Using Neural Networks. *Fuel*, 151: 156–163.
- Li, Han, Frailie, Peter T., Rochelle, Gary T. and Chen, Jian (2014), Thermodynamic Modeling of Piperazine/2-Aminomethylpropanol/CO<sub>2</sub>/Water. *Chemical Engineering Science*, 117: 331–341.

- Li, Kangkang, Leigh, Wardhaugh, Feron, Paul, Yu, Hai and Tade, Moses (2016), Systematic Study of Aqueous Monoethanolamine (MEA)-Based CO<sub>2</sub> Capture Process: Techno-Economic Assessment of the MEA Process and Its Improvements. *Applied Energy*, 165: 648–659.
- Lin, Yu Jeng, Pan, Tian Hong, Wong, David Shan Hill, Jang, Shi Shang, Chi, Yu Wen and Yeh, Chia Hao (2011), Plantwide Control of CO<sub>2</sub> Capture by Absorption and Stripping Using Monoethanolamine Solution. *Industrial and Engineering Chemistry Research*, 50(3): 1338–1345.
- Liu, Helei, Idem, Raphael and Tontiwachwuthikul, Paitoon (2019), *Post-Combustion CO<sub>2</sub> Capture Technology By Using the Amine Based Solvents*.
- Liu, Ji, Li, Xiaoshan, Zhang, Zewu, Li, Liwei, Bi, Yajun and Zhang, Liqi (2019), Promotion of CO<sub>2</sub> Capture Performance Using Piperazine (PZ) and Diethylenetriamine (DETA) Bi-Solvent Blends. *Greenhouse Gases: Science and Technology*, 9(2): 349–359.
- Luo, Xiaoyan and Wang, Congmin (2017), The Development of Carbon Capture by Functionalized Ionic Liquids. *Current Opinion in Green and Sustainable Chemistry*, 3: 33–38.
- Luo, Yong, Chu, Guang Wen, Zou, Hai Kui, Xiang, Yang, Shao, Lei and Chen, Jian Feng (2012), Characteristics of a Two-Stage Counter-Current Rotating Packed Bed for Continuous Distillation. *Chemical Engineering and Processing: Process Intensification*, 52: 55–62.
- Luyben, Michael L. and Luyben, William L. (1997), Essentials of Process Control McGraw-Hill Chemical Engineering Series Emeritus Advisory Board Building the Literature of a Profession. *Essentials of Process Control*: 584.
- Luyben, William L. (2016), *Distillation Systems for Separating Design and Control of Distillation Systems for Separating*.
- Madeddu, Claudio, Errico, Massimiliano and Baratti, Roberto (2019), *CO<sub>2</sub> Capture by Reactive Absorption-Stripping. a*
- Mahajani, Vaidya (2005), Kinetics of the Reaction of CO<sub>2</sub> with Aqueous Formulated Solution Containing Monoethanolamine,. *Industrial & Engineering Chemistry Research*: 1868–1873.
- Mangalapally, Hari Prasad. and Hasse, Hans (2011a), Pilot Plant Study of Two New Solvents for Post Combustion Carbon Dioxide Capture by Reactive Absorption and

- Comparison to Monoethanolamine. *Chemical Engineering Science*, 66(22): 5512–5522.
- Mangalapally, Hari Prasad and Hasse, Hans (2011b), Pilot Plant Experiments for Post Combustion Carbon Dioxide Capture by Reactive Absorption with Novel Solvents. *Energy Procedia*, 4: 1–8
- Mangalapally, Hari Prasad, Notz, Ralf, Asprion, Norbert, Sieder, Georg, Garcia, Hugo and Hasse, Hans (2012), Pilot Plant Study of Four New Solvents for Post Combustion Carbon Dioxide Capture by Reactive Absorption and Comparison to MEA. *International Journal of Greenhouse Gas Control*, 8(22): 205–216.
- Maroto-Valer, M. Mercedes (2010), *Developments and Innovation in Carbon Dioxide Capture and Storage Technology. Volume 1: Carbon Dioxide Capture, Transport and Industrial Applications*.
- Mechleri, Evgenia, Lawal, Adekola, Ramos, Alfredo, Davison, John and Dowell, Niall Mac (2017), Process Control Strategies for Flexible Operation of Post-Combustion CO<sub>2</sub> Capture Plants. *International Journal of Greenhouse Gas Control*, 57: 14–25.
- MR Rahimi, S Mosleh (2015), CO<sub>2</sub> Removal from Air in a Countercurrent Rotating Packed Bed, Experimental Determination of Height of Transfer Unit. *Advances in environmental technology*, 1(1): 25–30.
- Nittaya, Thanita (2014), Dynamic Modelling and Control of MEA Absorption Processes for CO<sub>2</sub> Capture from Power Plants. *PhD thesis*.
- Nittaya, Thanita, Douglas, Peter L., Croiset, Eric and Ricardez-Sandoval, Luis A. (2014a), Dynamic Modelling and Control of MEA Absorption Processes for CO<sub>2</sub> Capture from Power Plants. *Fuel*, 116: 672–691.
- Nittaya, Thanita, Douglas, Peter L., Croiset, Eric and Ricardez-Sandoval, Luis A. (2014b), Dynamic Modeling and Evaluation of an Industrial-Scale CO<sub>2</sub> Capture Plant Using Monoethanolamine Absorption Processes. *Industrial and Engineering Chemistry Research*, 53(28): 11411–11426.
- Nittaya, Thanita, Douglas, Peter L, Croiset, Eric and Ricardez-Sandoval, Luis A (2014), Dynamic Modelling and Controllability Studies of a Commercial-Scale MEA Absorption Processes for CO<sub>2</sub> Capture from Coal-Fired Power Plants. *Energy*

*Procedia*, 63: 1595–1600.

Oexmann, Jochen, Hensel, Christian and Kather, Alfons (2008), Post-Combustion CO<sub>2</sub>-Capture from Coal-Fired Power Plants: Preliminary Evaluation of an Integrated Chemical Absorption Process with Piperazine-Promoted Potassium Carbonate. *International journal of greenhouse gas control*, 2(4): 539–552.

Oh, Hyun Taek, Ju, Youngsan, Chung, Kyounghee and Lee, Chang Ha (2020), Techno-Economic Analysis of Advanced Stripper Configurations for Post-Combustion CO<sub>2</sub> Capture Amine Processes. *Energy*, 206: 118164

Onda, Kakusaburo, Sada, Eizo and Takeuchi, Hiroshi (1968), Gas Absorption with Chemical Reaction in Packed Columns. *Journal of Chemical Engineering of Japan*, 1(1): 62–66.

Otitoju, Olajide, Oko, Eni and Wang, Meihong (2020), A New Method for Scale-up of Solvent-Based Post-Combustion Carbon Capture Process with Packed Columns. *International Journal of Greenhouse Gas Control*, 93.

Otitoju, Olajide, Oko, Eni and Wang, Meihong (2021), Technical and Economic Performance Assessment of Post-Combustion Carbon Capture Using Piperazine for Large Scale Natural Gas Combined Cycle Power Plants through Process Simulation. *Applied Energy*, 292(March): 116893.

Oyenekan, Babatunde Adegboyega (2007), Modeling of Strippers for CO<sub>2</sub> Capture by Aqueous Amines. *Doctoral thesis at Technical University of Texas at Austin*, (May): 317.

Papadopoulos, Athanasios I (2017), *Process Systems and Materials for CO<sub>2</sub> Capture*.

Peng, Jianjun, Edgar, Thomas F and Eldridge, R Bruce (2003), Dynamic Rate-Based and Equilibrium Models for a Packed Reactive Distillation Column. *Chemical Engineering Science*, 58(12): 2671–2680.

Perumal, Muthumari, Jayaraman, Dhanalakshmi and Balraj, Ambedkar (2021), Experimental Studies on CO<sub>2</sub> Absorption and Solvent Recovery in Aqueous Blends of Monoethanolamine and Tetrabutylammonium Hydroxide. *Chemosphere*, 276: 130159.

Pinsent, B. R.W., Pearson, L. and Roughton, F. J.W. (1956), The Kinetics of Combination of Carbon Dioxide with Hydroxide Ions. *Transactions of the Faraday Society*, 52: 1512–1520.

- Pintola, Thorat, Tontiwachwuthikul, Paitoon and Meisen, Axel (1993), Simulation of Pilot Plant and Industrial CO<sub>2</sub>-MEA Absorbers. *Gas Separation and Purification*, 7(1): 47–52.
- Posch, Sebastian and Haider, Markus (2013), Dynamic Modeling of CO<sub>2</sub> Absorption from Coal-Fired Power Plants into an Aqueous Monoethanolamine Solution. *Chemical engineering research and design*, 91(6): 977–987.
- Razi, Neda, Svendsen, Hallvard F. and Bolland, Olav (2013), Validation of Mass Transfer Correlations for CO<sub>2</sub> Absorption with MEA Using Pilot Data. *International Journal of Greenhouse Gas Control*, 19: 478–491.
- Rodriguez, Javier, Andrade, Artur, Lawal, Adekola, Samsatli, N, Calado, Mário, Ramos, Alfredo, Lafitte, T, Fuentes, J and Pantelides, C C (2014), An Integrated Framework for the Dynamic Modelling of Solvent-Based CO<sub>2</sub> Capture Processes. *Energy Procedia*, 63: 1206–1217.
- Romeo, Luis M., Minguell, Diego, Shirmohammadi, Reza and Andrés, José M. (2020), Comparative Analysis of the Efficiency Penalty in Power Plants of Different Amine-Based Solvents for CO<sub>2</sub> Capture. *Industrial and Engineering Chemistry Research*, 59(21): 10082–10092.
- Samanta, Arunkumar and Bandyopadhyay, S S (2009), Absorption of Carbon Dioxide into Aqueous Solutions of Piperazine Activated 2-Amino-2-Methyl-1-Propanol. *Chemical Engineering Science*, 64(6): 1185–1194.
- Sinnott, R.K. (2005) *Chemical Engineering*. Amsterdam: Elsevier.
- Smith, Steven A, Sorensen, James A, Steadman, Edward N, Harju, John A and Ryan, David (2011), Zama Acid Gas EOR, CO<sub>2</sub> Sequestration, and Monitoring Project. *Energy procedia*, 4: 3957–3964.
- van der Spek, Mijndert, Arendsen, Richard, Ramirez, Andrea and Faaij, André (2016), Model Development and Process Simulation of Postcombustion Carbon Capture Technology with Aqueous AMP/PZ Solvent. *International Journal of Greenhouse Gas Control*, 47: 176–199.
- Stec, M., Tatarczuk, A., Więclaw-Solny, L., Krótki, A., Spietz, T. and Wilk, A. (2017), Process Development Unit Experimental Studies of a Split-Flow Modification for the



- Post-Combustion CO<sub>2</sub> Capture Process. *Asia-Pacific Journal of Chemical Engineering*, 12(2): 283–291.
- Stec, Marcin, Tatarczuk, Adam, Więclaw-Solny, Lucyna, Krótki, Aleksander, Źięzko, Marek and Tokarski, Stanisław (2015), Pilot Plant Results for Advanced CO<sub>2</sub> Capture Process Using Amine Scrubbing at the Jaworzno II Power Plant in Poland. *Fuel*, 151: 50–56.
- Stichlmair, J, Bravo, J L and Fair, J R (1989), General Model for Prediction of Pressure Drop and Capacity of Countercurrent Gas/Liquid Packed Columns. *Gas Separation & Purification*, 3(1): 19–28.
- Tontiwachwuthikul, Paitoon, Meisen, Axel and Lim, C. Jim (1992), CO<sub>2</sub> Absorption by NaOH, Monoethanolamine and 2-Amino-2-Methyl-1-Propanol Solutions in a Packed Column. *Chemical Engineering Science*, 47(2): 381–390.
- Towler and Ray Sinnott (1969), *Chemical Engineering Design Principles, Practice and Economics of Plant and Process Design*.
- Van Wagener, David Hamilton (2011), Stripper Modeling for CO<sub>2</sub> Removal Using Monoethanolamine and Piperazine Solvents.
- Walters, Matthew S., Edgar, Thomas F. and Rochelle, Gary T. (2016), Dynamic Modeling and Control of an Intercooled Absorber for Post-Combustion CO<sub>2</sub> Capture. *Chemical Engineering and Processing: Process Intensification*, 107: 1–10.
- Wang, M., Lawal, A., Stephenson, P., Sidders, J. and Ramshaw, C. (2011), Post-Combustion CO<sub>2</sub> Capture with Chemical Absorption: A State-of-the-Art Review. *Chemical Engineering Research and Design*, 89(9): 1609–1624. available at <http://dx.doi.org/10.1016/j.cherd.2010.11.005>
- Yu, Cheng Hsiu, Cheng, Hsu Hsiang and Tan, Chung Sung (2012), CO<sub>2</sub> Capture by Alkanolamine Solutions Containing Diethylenetriamine and Piperazine in a Rotating Packed Bed. *International Journal of Greenhouse Gas Control*, 9: 136–147.
- Zhang, Weiyu, Chen, Jian, Luo, Xiaobo and Wang, Meihong (2017), Modelling and Process Analysis of Post-Combustion Carbon Capture with the Blend of 2-Amino-2-Methyl-1-Propanol and Piperazine. *International Journal of Greenhouse Gas Control*, 63(May): 37–46.
- Zhang, Xiaowen, Zhang, Rui, Liu, Helei, Gao, Hongxia and Liang, Zhiwu (2018), Evaluating CO<sub>2</sub> Desorption Performance in CO<sub>2</sub>-Loaded Aqueous Tri-Solvent Blend

- Amines with and without Solid Acid Catalysts. *Applied energy*, 218: 417–429.
- Zheng, Chong, Guo, Kai, Feng, Yuanding, Yang, Cun and Gardner, Nelson C. (2000), Pressure Drop of Centripetal Gas Flow through Rotating Beds. *Industrial and Engineering Chemistry Research*, 39(3): 829–834.
- Ziaii, Sepideh, Rochelle, Gary T. and Edgar, Thomas F. (2009), Dynamic Modeling to Minimize Energy Use for CO<sub>2</sub> Capture in Power Plants by Aqueous Monoethanolamine. *Industrial and Engineering Chemistry Research*, 48(13): 6105–6111.